



3 1176 00168 5198

NASA CR-165,212

NASA-CR-165212
19810015645

NASA CR-165212
R81AEG208



National Aeronautics and
Space Administration

DEVELOPMENT OF ADVANCED LIGHTWEIGHT CONTAINMENT SYSTEMS FINAL REPORT

MAY 1981

by

C.L. Stotler

GENERAL ELECTRIC COMPANY

LIBRARY COPY

JUN 15 1981

LANGLEY RESEARCH CENTER
LIBRARY, NASA
HAMPTON, VIRGINIA

Prepared For

National Aeronautics and Space Administration

NASA Lewis Research Center
Contract NAS3-21823



NF02441

**All Blank Pages
Intentionally Left Blank
To Keep Document Continuity**

TABLE OF CONTENTS

<u>Section</u>		<u>Page</u>
1.0	SUMMARY	1
2.0	INTRODUCTION	3
3.0	TECHNICAL DISCUSSION	8
	3.1 Design and Testing	8
	3.1.1 Test Method Used to Evaluate Containment Process	8
	3.1.2 Test Plan	13
	3.1.3 Containment Design and Test Results	13
	3.1.3.1 Phase I Testing	17
	3.1.3.2 Phase II Testing	33
	3.2 Data Analysis	64
	3.3 Full Scale Containment System Design	72
4.0	CONCLUSIONS	79
5.0	REFERENCES	80
	DISTRIBUTION LIST	81

LIST OF ILLUSTRATIONS

<u>Figure</u>		<u>Page</u>
1.	Typical State-of-the-Art Containment Case.	4
2.	Rotating Rig for Containment Tests.	5
3.	Steel/Kevlar Containment Concepts.	6
4.	Basic Whirligig Test Setup.	11
5.	Containment Test Setup.	12
6.	TF34 Titanium Blade.	14
7.	TF34 Superhybird Titanium Composite T1Com Blade.	15
8.	Test Setup - Test 1.	18
9.	Test 1 - Overall View.	19
10.	Typical Damage - Flowpath Side - Test 1.	20
11.	Exterior View - 12-Ply Side - Test 1.	21
12.	Exterior View - Eight-Ply Side - Test 1.	22
13.	Interior View - 12-Ply Side - Test 2.	24
14.	Test 3 - Overall View.	25
15.	Exterior View - 12-Ply Side - Test 3.	26
16.	Exterior View - Eight-Ply Side Test 3.	28
17.	Exterior View - 12-Ply Side - Kevlar Removed - Test 3.	29
18.	Exterior View - Eight-Ply Side - Kevlar Removed - Test 3.	30
19.	Witness Plate Dent - Test 4.	31
20.	Exterior View - 12-Ply Side - Test 4.	32
21.	Exterior View - Eight-Ply Side - Test 4.	33
22.	Kevlar Felt Concepts.	35

LIST OF ILLUSTRATIONS (Continued)

<u>Figure</u>		<u>Page</u>
23.	Exterior View - Test 5.	36
24.	Exterior View - Test 5 - Cloth Removed - Concept B.	37
25.	Exterior View - Test 5 - Cloth Removed - Concept A.	38
26.	Test 6 Configurations.	40
27.	Exterior View - 10 Plies of 328-Weave Kevlar - Test 6.	41
28.	Exterior View - 10 Plies of 143-Weave Kevlar - Test 6.	42
29.	Aluminum Face Sheet - Test 6.	44
30.	Test 6 - Overall View.	45
31.	Exterior View - Test 7 - No Felt.	46
32.	Exterior View - Test 7 - Kevlar Felt.	47
33.	Exterior View - Test 8 - 143-Weave Cloth Plus Felt.	49
34.	Witness Plate Damage - Test 8.	50
35.	Exterior View - Test 8 - 328 Weave Cloth Plus Felt.	51
36.	Exterior View - Test 9 - Six-Ply Side.	53
37.	Exterior View - Test 9 - Six-Ply Side Aluminum Cover Removed.	54
38.	Interior View - Test 9 - Composite Debris.	55
39.	Exterior View - Test 9 - Eight-Ply Side.	56
40.	Broken Circumferential Restraint - Test 9.	57
41.	Test Setup - Test 10.	59

LIST OF ILLUSTRATIONS (Concluded)

<u>Figure</u>		<u>Page</u>
42.	Interior View - Impact Area - Test 10.	61
43.	Exterior View - Impact Area - Test 11.	62
44.	Blade Platform Penetration - Test 11.	63
45.	Edge Attachment Failure - Test 11.	64
46.	Impact Area - Test 11.	66
47.	Test 11 - Overall View.	66
48.	Closeup of Rub Area - Test 11.	68
49.	Test Data - Free Edges.	70
50.	Test Data - Restrained Edges.	71
51.	Baseline Containment Design.	73
52.	Lightweight Containment Design.	75
53.	Superhybrid - CF6 TiCom Prototype Blade.	77

1.0 SUMMARY

This report presents the results of the testing performed under Contract NAS3-21823. The objective of the program was to obtain parametric-type data on advanced lightweight containment systems. These data were used to generate design methods and procedures necessary for the successful development of such systems. The methods developed were then demonstrated through the design of a lightweight containment system for a CF6 size engine.

All testing conducted under this program was done in a rotating rig using TF34 fan blades. Both titanium and superhybrid versions of this blade were used. The superhybrid version consisted of a titanium spar, a graphite/glass/epoxy shell, and titanium foil outer covering. The containment concept evaluated was that developed under NASA Contract NAS3-20118 and consists basically of a lightweight structural sandwich shell wrapped with dry Kevlar cloth. The initial testing was directed towards the determination of the amount of Kevlar required to result in threshold containment for a specific set of test conditions. A relationship was then developed between the thickness required and the energy of the released blade so that the data could be used to design for conditions other than those tested.

The remainder of the testing was directed towards the evaluation of a number of variations in the basic concept. These variations included changing the weave from a bidirectional weave to a unidirectional weave, incorporating several densities of Kevlar felt as part of the containment material, changing the thickness and material of the flowpath facing of the sandwich shell, and restraining the fore and aft edges of the Kevlar. The most significant change proved to be providing restrained to the fore and aft edges. This greatly improved the system's ability to absorb subsequent secondary impacts by keeping the Kevlar in place. When the edges were left free, the primary impact caused large displacements of the Kevlar, thus leaving extensive areas of the containment case vulnerable to penetration by secondary impacts. The unidirectional woven material did not contain as well as the bidirectional material while the addition of Kevlar felt had no appreciable effect on the containment process.

Based on the data generated by this program, a design curve was developed which can be used to determine the amount of dry Kevlar 328 weave cloth that would be required for a given impact energy. This design curve was based on an amount of damage that could be acceptable in commercial practice and not on threshold containment which produces more damage than was considered safe design practice. Using this design curve, a lightweight containment design was made for a large turbofan engine using the General Electric CF6-50 as the baseline. Based on this design, a weight saving in the range of 20% to 25% over the current system was projected.

2.0 INTRODUCTION

One of the primary requirements of modern, high bypass turbofan engine installations in commercial service is that they must be able to contain any fan blade or pieces of blades should a failure occur, thus precluding any damage to the rest of the aircraft. The size of the objects to be contained ranges from a single complete blade to pieces of blades such as would result from bird impact.

Current containment practice is to install heavy steel rings around the nacelle fan area. A typical containment ring is shown in Figure 1. In large turbofan engines, this can amount to almost 227 kg (500 lb). Except for the rare occasion when debris must be contained, this heavy structure serves little purpose yet adds significantly to engine weight and fuel consumption.

In order to evaluate other containment concepts which offered the potential of reducing the weight of containment systems, NASA sponsored a program (NAS3-20118) which investigated a number of different concepts and materials that could be used in place of a steel ring. The different concepts were initially evaluated by impacting small 180° targets using a gas gun as the means of accelerating the impacting projectile. As a result of these tests, the best concept/material combination, based on energy absorbed per unit containment weight, was selected for evaluation in a rotating rig such as shown in Figure 2. The containment system selected for this evaluation consisted of a thin steel facing backed up by layers of unimpregnated Kevlar cloth. Two versions of this basic concept, as shown in Figure 3, were evaluated. Those specimens which included a section of honeycomb material between the steel facing and the dry kevlar cloth exhibited much better containment characteristics than those in which the Kevlar was immediately behind the steel sheet. The honeycomb not only kept the Kevlar cloth from falling into the rotor path, which can cause extensive secondary damage to the rotor, but also provided a place for the blade fragments to nest so they did not bounce around in the the rotor path damaging other blades. In addition, this honeycomb area, if properly designed, can provide considerable casing stiffness at a very low weight. The results of this program are reported in Reference (1).

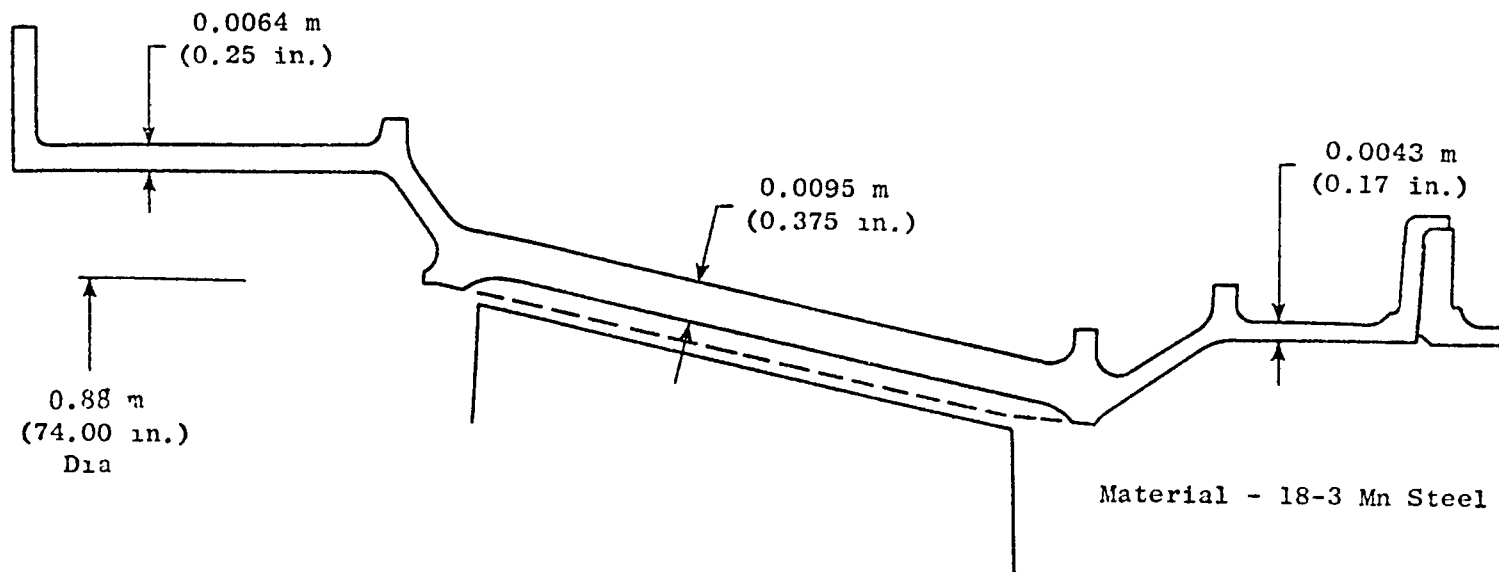


Figure 1. Typical State-of-the-Art Containment Case.

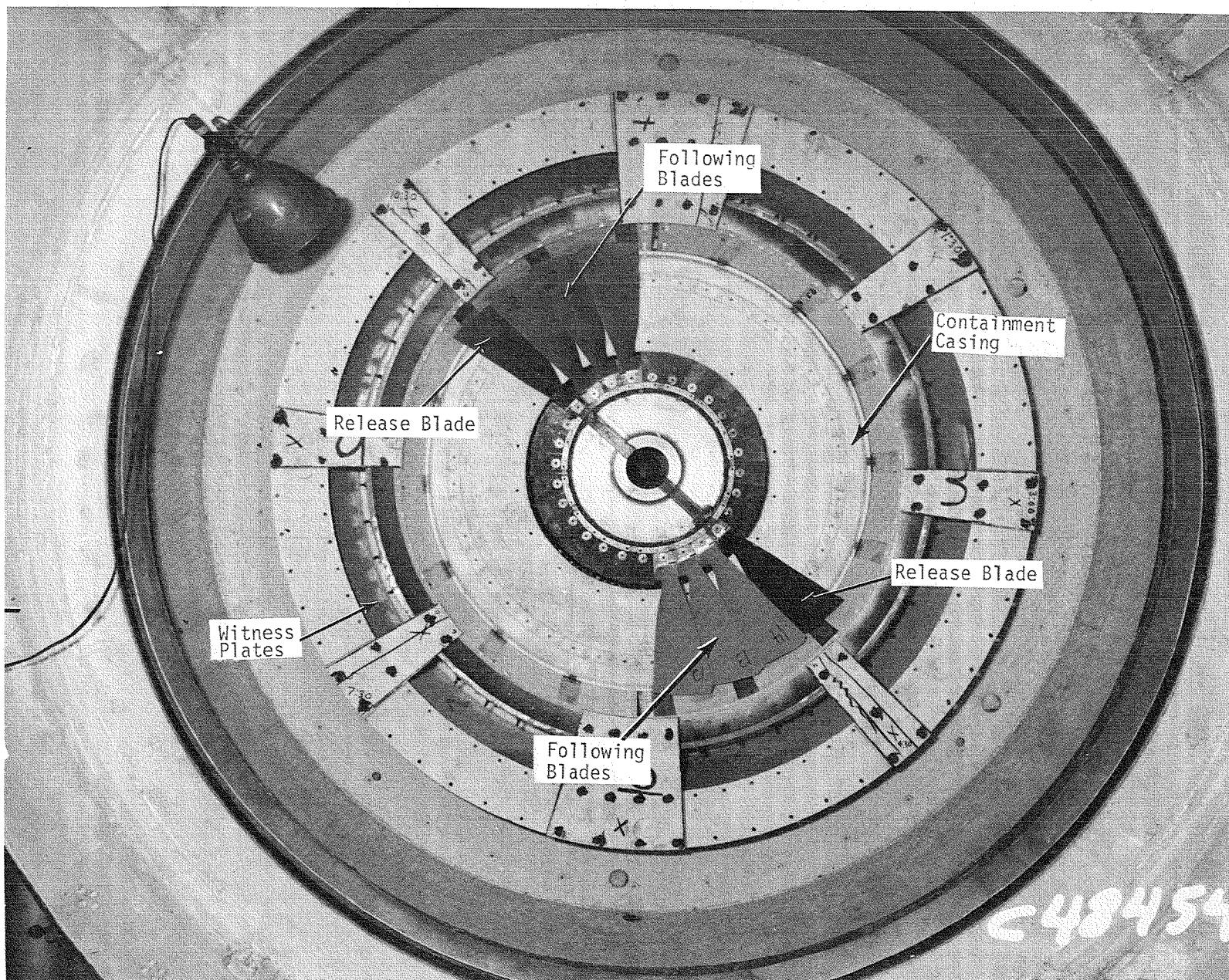


Figure 2. Rotating Rig for Containment Tests.

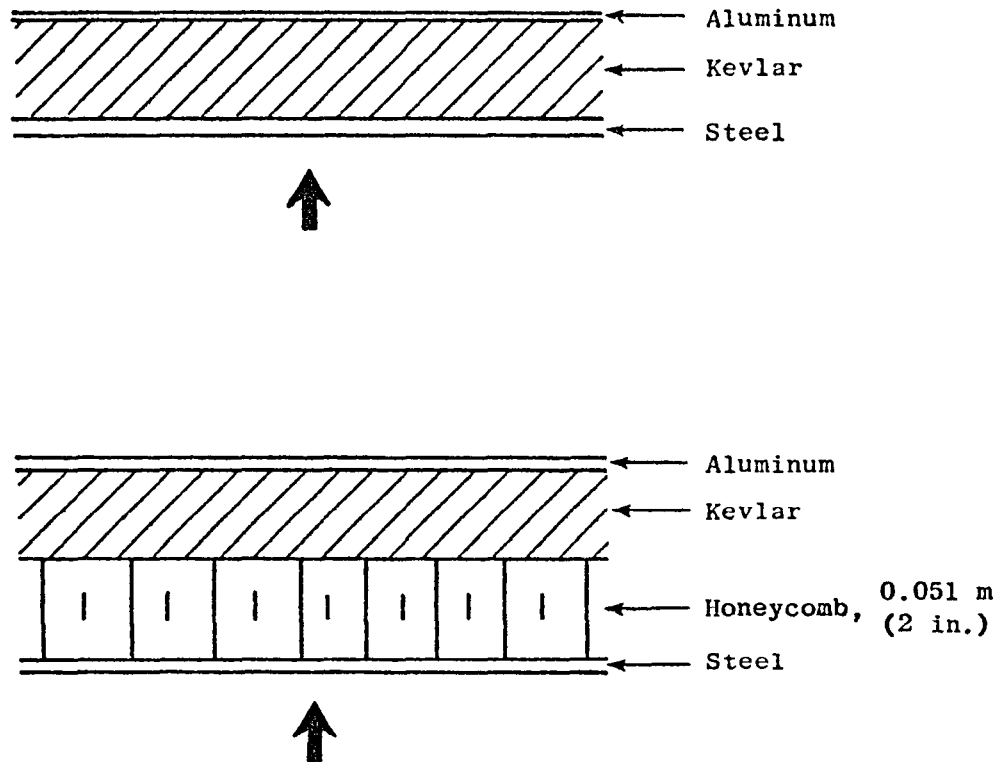


Figure 3. Steel/Kevlar Containment Concepts.

In order for the concepts developed under Contract NAS3-20118 to be applied to production hardware, it was necessary to generate enough parametric data to permit an optimum design with respect to the amount and configuration of the Kevlar material. The objective of this program was therefore to obtain the required data and to apply the results to the design of an advanced, light-weight containment system for a large modern turbofan engine.

3.0 TECHNICAL DISCUSSION

This section presents the results of the technical effort performed under this program. This work was divided into four tasks for the purposes of reporting. However, the first three tasks - selection of Containment Concepts and Design of Spin Test Specimens; Hardware Fabrication and Procurement; and Subscale Spin Impact Testing - are so interrelated that, for the sake of coherency, they will be discussed without reference to task. The last task, Data Analysis and Full Scale Containment System Design, will be discussed as a separate item.

3.1 DESIGN AND TESTING

The objective of the design and testing portion of the program was to determine the amount of Kevlar cloth required for threshold containment for several types and sizes of impacting objects and to investigate methods of potential improvement in both the ability of the system to contain and to control the motion of the impacting object.

3.1.1 Test Method Used to Evaluate Containment Process

In order to evaluate the ability of the containment method to contain typical engine fan blades and blade fragments, a test method must be employed which, as closely as possible, duplicates actual engine conditions.

To do this requires the simulation of the low pressure system of a typical turbofan engine. The ability to rotate the first stage fan at typical engine speeds must also be provided so that an actual blade may be released into the containment system with the proper motion. This motion must also include any potential interaction with the other blades in the rotor in addition to the rotational motion. In order to provide a meaningful evaluation of the containment systems to be tested, it is necessary to choose a specific blade/rotor design so that the containment system can be designed for the proper energy levels. To choose a very large fan design, such as the CF6, would be very expensive in terms of containment structure costs, blade cost,

and test cost. However, it was feasible to conduct the testing using a similar, but somewhat smaller, blade/rotor configuration which has characteristics similar to the large fan but is more convenient to test. The blade/rotor configuration which was selected for the rotating evaluation of the containment designs was the TF34 first-stage fan. Its 1.1 m (44 in.) tip diameter makes this choice particularly convenient, for the fan is large enough to permit meaningful testing yet can be operated without requiring extensive modification to existing facilities.

An existing whirligig test facility consisting of a basic TF39 fan package, described below, and a constant speed 4000-hp electric motor with a dynamic variable speed output magnetic clutch was modified to adapt to a TF34 fan disk and to allow mounting of the containment systems to be tested.

The TF39 fan package consists of a TF39 fan frame with the No. 1 and 2 bearings and sump systems and slave Stage 1 shrouding. With the exception of the slave Stage 1 shroud, the entire vehicle is soft-mounted.

The slave shroud with an inside diameter of 2.3 m (92 in.) is mounted to the ground. It is constructed of steel and serves as the mounting fixture for the containment systems being tested.

A TF34 fan disk is mounted on a drive shaft adapter which then provides for mounting up to a full stage (28 blades) of TF34 first stage fan blades.

An environment chamber, or bell jar, is attached to the fan case. This provides the capability of operating in a helium atmosphere in order to reduce horsepower requirements and temperature buildup. The chamber also provides high speed photographic capability and additional debris containment.

Witness plates are incorporated into the test facility to allow estimation of the residual energy of any fragments that defeat the containment system. The blade impact condition is established three ways: (1) by monitoring the rotor speed, (2) by determining the blade impacting weight by measuring blade specimen weight before and after test (subtracting the weight of the posttest retained blade root from the weight of the total blade specimen), and (3) by studying high speed motion picture records of the impact. An

automatic trip system is used to permit a continuous rapid acceleration. This eliminates the need to stabilized speed at the release point. This rapid acceleration reduces the time at speed and the heat/temperature buildup. The trip system consists simply of a revolution counter with two built-in relay "trips". The first trip is set such that, with the drive at maximum acceleration rate, the blade is released at a point established by prior checkout. The second trip is set to shut the drive system down to prevent excessive damage and/or overspeed. To achieve the maximum acceleration rate, the drive is operated at maximum-rated motor current.

The basic test setup and assembly of the soft-mounted test vehicle are shown in Figures 4 and 5.

The blades or parts of blades, are released by an explosive charge. By precise timing, two blades 180° apart can be released together. Rotor imbalance is thus minimized, and two containment tests can be accomplished in a single whirligig test operation. Most of the testing conducted during the program was performed in this manner. The last two tests of the program, however, involved single releases out of a fully bladed rotor into continuous 360° containment systems. This test procedure results in a net rotor unbalance subsequent to releasing the test projectile, and this condition raised the possibility of the remaining blades in the rotor rubbing on the casing. The bearing system employed for these tests proved sufficiently rugged to withstand the unbalance forces without damage.

In order to control the impact point of the blade specimen relative to the containment system, the explosive charge is detonated with the rotor at at circumferential position that permits the blade to impact in the containment system at a preselected target location. In addition, the camera and lights are activated to catch the event. An electronic "black box" called the whirligig triggering system, designed and built to satisfy these requirements, is utilized. It uses a very precise "clock" to permit timing the detonation of the explosive charge. This timing can be varied and is set to allow time for the flashbulbs to reach full brilliance and account for the angular position of the blade relative to a 1/rev indicator on the rotor.

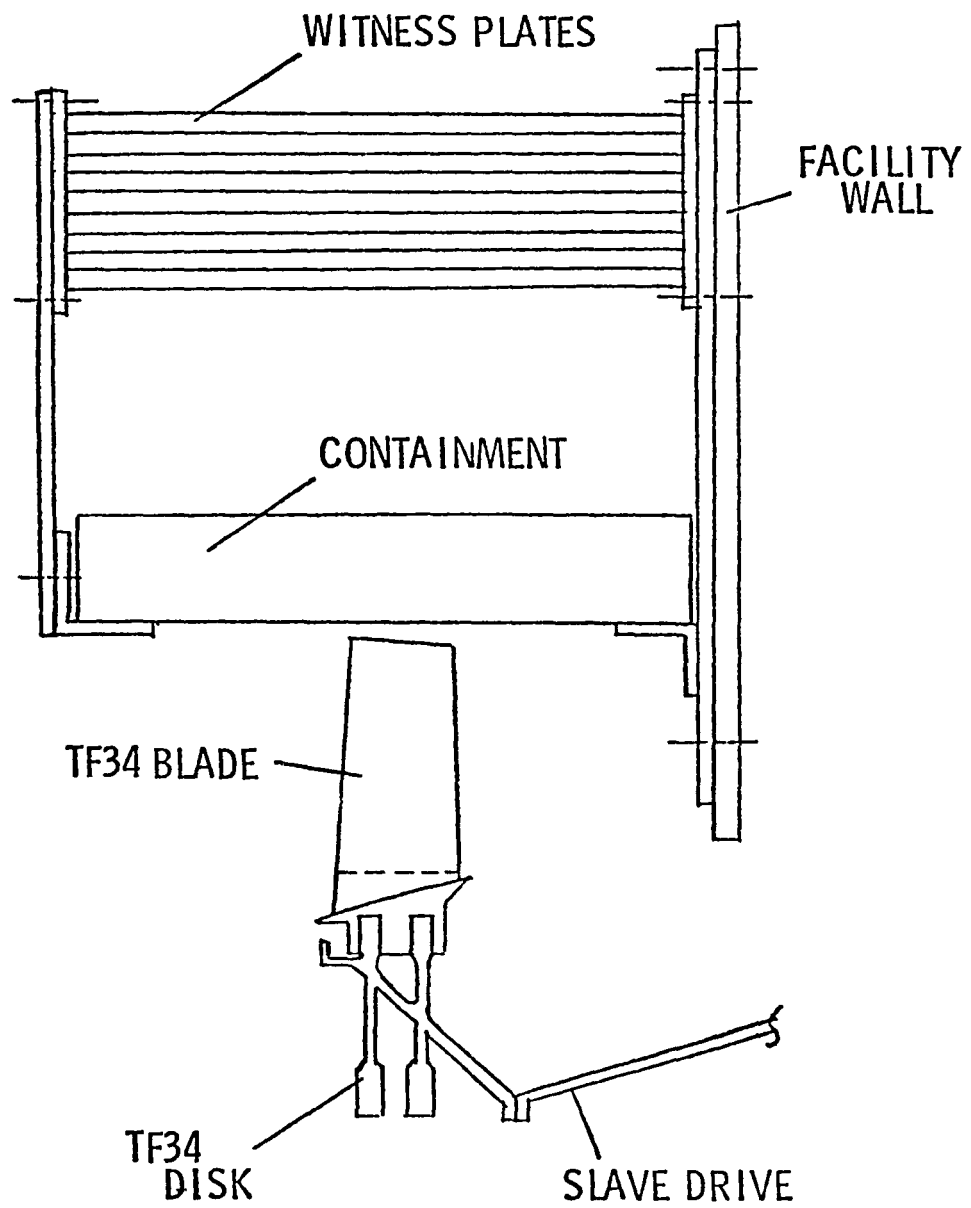


Figure 5. Containment Test Setup.

3.1.2 Test Plan

Two types of blades were used in the rotating tests. One was the standard titanium TF34 blade (Figure 6) which embodies typical current fan blade design practices. The other was a superhybrid blade (Figure 7) consisting of a titanium pinned root and leading edge spar, a graphite/epoxy shell, and a titanium foil outer covering. This configuration was intended to represent potential future blade construction.

In order to obtain the effects of change in impacting mass, some tests were conducted which released only the airfoil section of titanium blades while other tests involved the release of the blades below the base platform.

At the beginning of the program, the test matrix shown in Table I was generated. The tests defined by this matrix were intended to provide sufficient data to meet the objectives of the program.

3.1.3 Containment Design and Test Results

The basic design of the containment systems tested under this program was developed under NASA Contract NAS3-20118. It consists of a thin metal facing next to the fan rotor which is then backed up by aluminum honeycomb, Kevlar/epoxy, and dry Kevlar cloth. This type of system had demonstrated its ability to not only stop a released blade, but to capture it and any other resulting fragments while still remaining relatively round. It remained to be determined just how much Kevlar cloth, or how little, was required to just contain the released blade or part of blade.

The first series of tests was devoted to the determination of the material required for threshold containment for both an airfoil of a titanium TF34 fan blade and a complete blade. All previous tests had resulted in complete containment. The minimum number of Kevlar plies tested had been 16 plies which had withstood an impact of a complete TF34 titanium blade released at 5000 rpm. Fewer plies were therefore required to attain threshold containment. The first two containment designs to be tested under this program were intended to provide a sufficiently wide spread of Kevlar thicknesses so that,

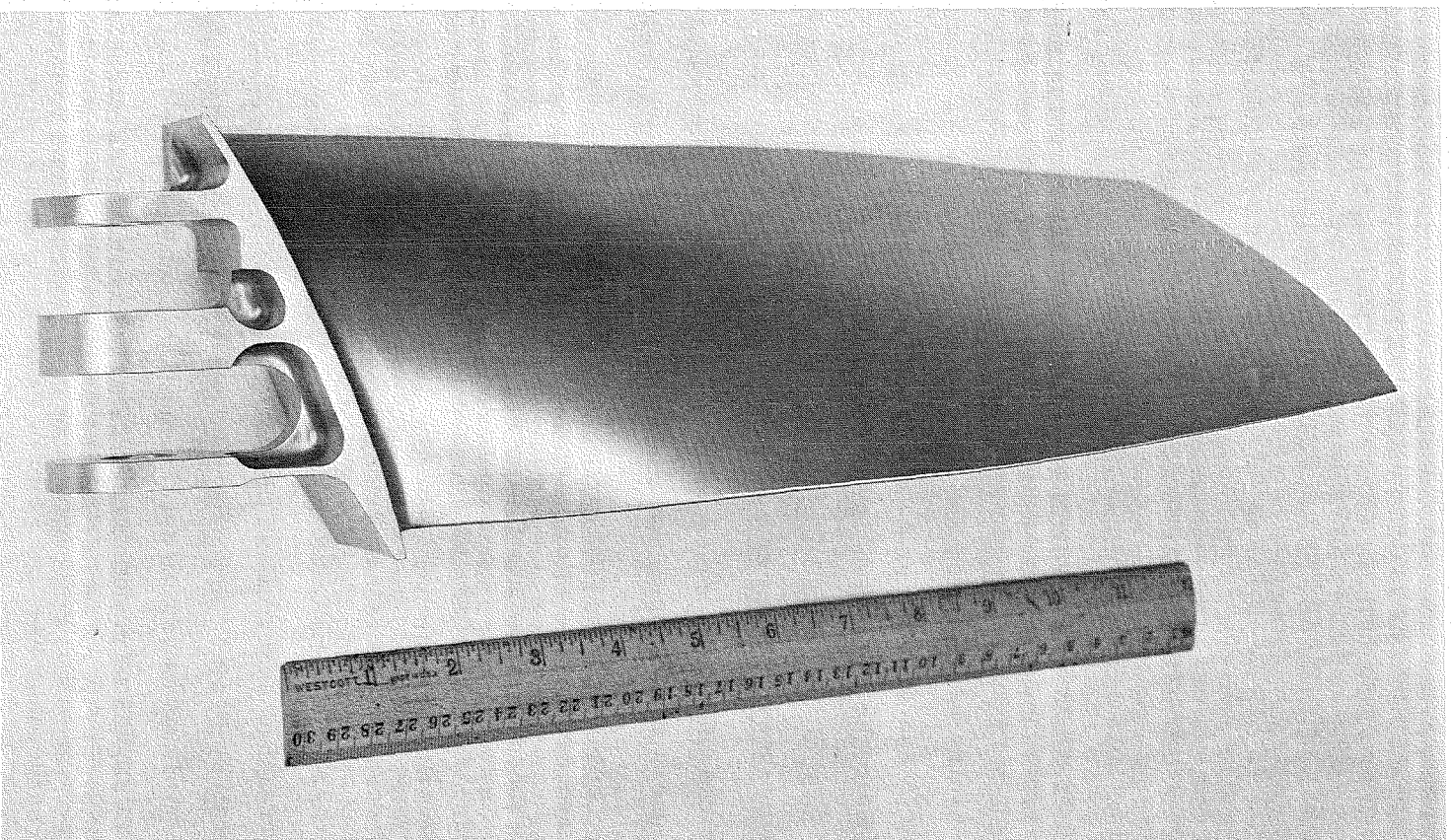


Figure 6. TF34 Titanium Blade.

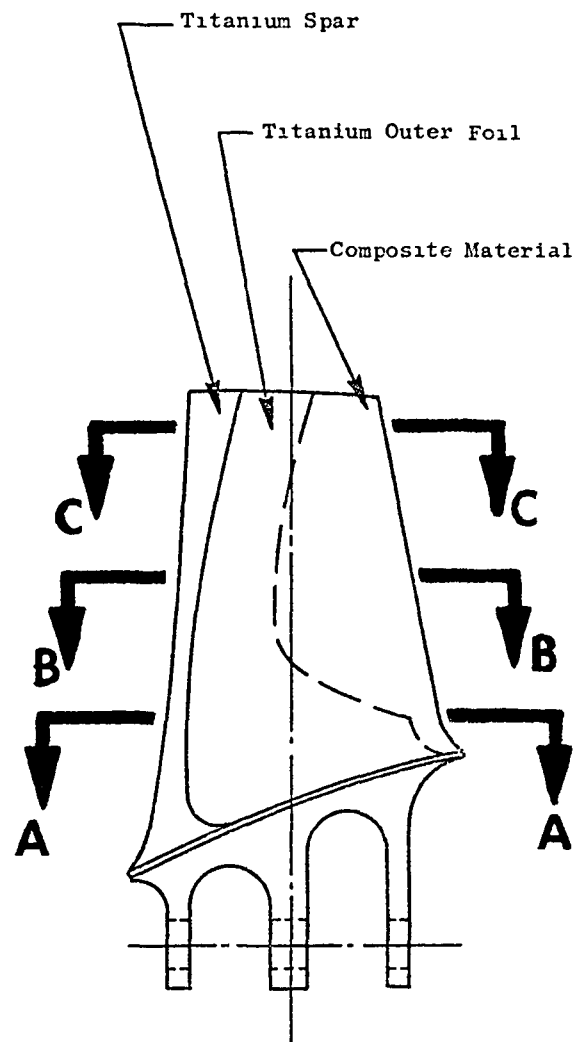
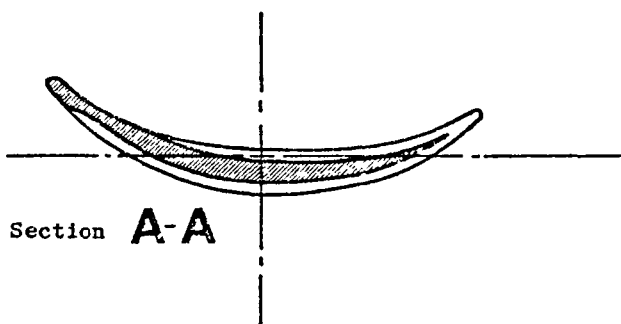
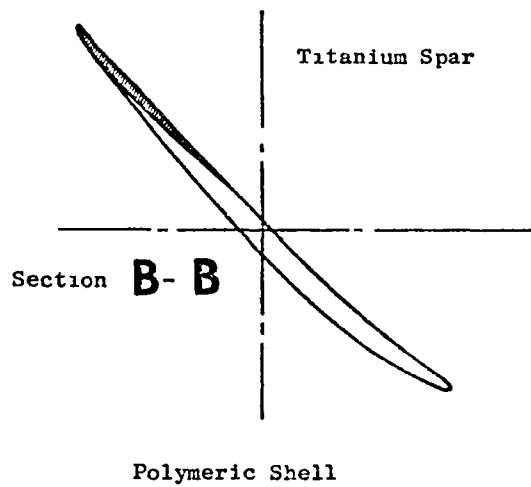
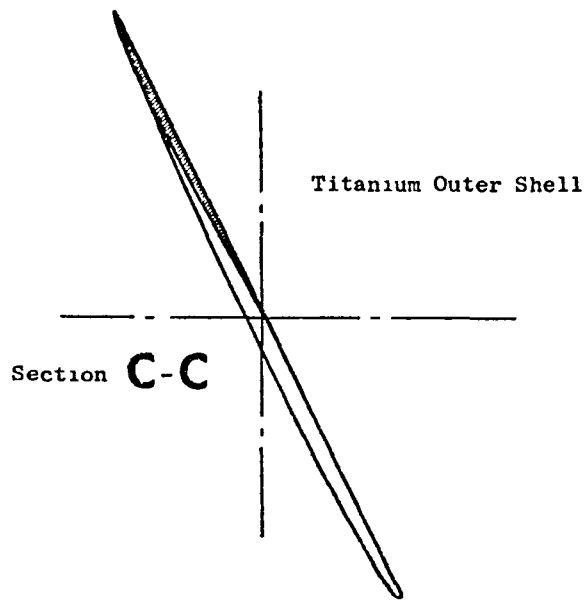


Figure 7. TF34 Superhybrid Titanium Composite TiCom Blade.

Table I. Spin Impact Test Program.

	Titanium Airfoil		Titanium Blade		Hybrid Blade
Tip Speed Object	V ₁	V ₂	V ₃	V ₄	V ₅
Containment					
Thickness of Kevlar 1	1	1	1	1	1
Thickness of Kevlar 2	1*1	1	1*1	1	
Thickness of Kevlar 3			1	1	
Thickness of Kevlar 4					1
End Retention Concept 1			1	1	
End Retention Concept 2			1	1	
To be Determined			1	1	
<p>*These tests will be single releases out of a full rotor into 360° targets.</p> <p>All other tests will be double release, with three following blades, into 180° targets.</p>					

by the use of only two different impact velocities, a situation would attain in which the Kevlar containment could be defeated. For these, and subsequent tests, three trailing blades were mounted behind each test blade to assure that the effects of the interaction between the released blade and the trailing blades were included in the test results. The test program shown in Table I was divided into two phases so that the results of the first phase could affect the design of the containment targets to be used in the second phase.

3.1.3.1 Phase I Testing

Ten 180° containment systems were constructed, by Accurate Plastic Inc. of Columbus, Ohio, for use in the Phase I testing. Four of these utilized 12 plies of Kevlar and six had eight plies. Two of the specimens which had eight plies also incorporated Kevlar felt as part of the containment system. These 10 systems were employed in the Phase I testing described below.

Test 1

Two TF34 titanium airfoils were released at 4500 rpm into a containment configuration which had 12 plies of dry Kevlar in one 180°-side and eight plies in the other. The containment systems were of typical lightweight construction with a thin steel facing, aluminum honeycomb, Kevlar, and thin aluminum back sheet. It was estimated prior to the test that the side with 12 plies would contain and the side with eight plies would be penetrated. The test setup is shown in Figure 8. In the actual test, the side with eight plies was not penetrated although the aluminum back sheet was ruptured. There was not indication of contact with the witness plate. The rotor and containment systems after test are shown in Figure 9. Typical damage to the flowpath side of the casings is shown in Figure 10. The backside (aluminum outer sheet) of the 12-ply containment system is shown in Figure 11 and that of the eight-ply system in Figure 12. The difference in damage to the Kevlar cloth was not as noticeable, but a progressive teardown of the structures showed that the Kevlar in the side with eight plies was pulled much more toward the center of the containment system (pulled away from the forward and aft ends) indicating that there was significantly greater radial deflection of the Kevlar due to the airfoil impact.

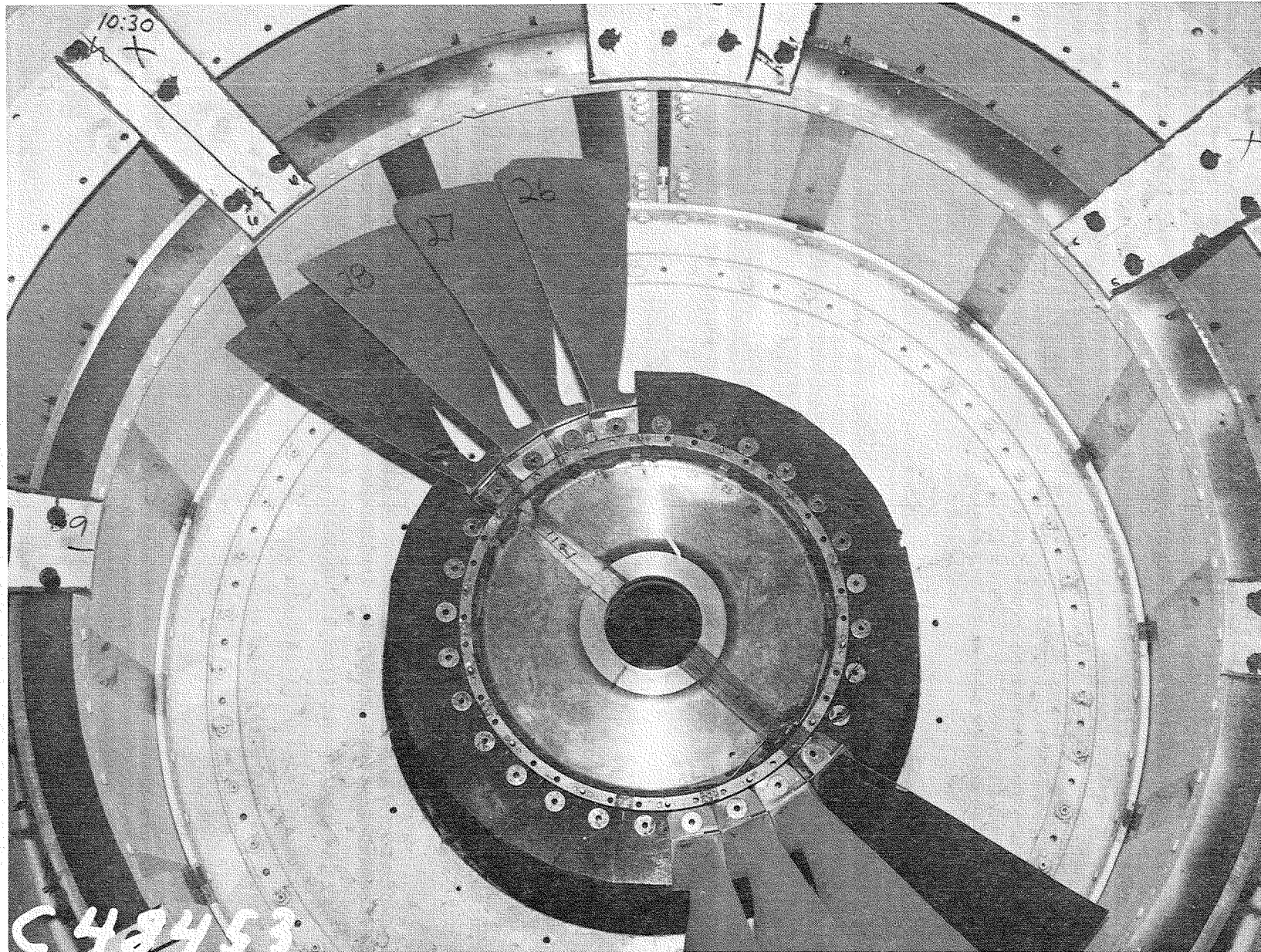


Figure 8. Test Setup - Test 1.

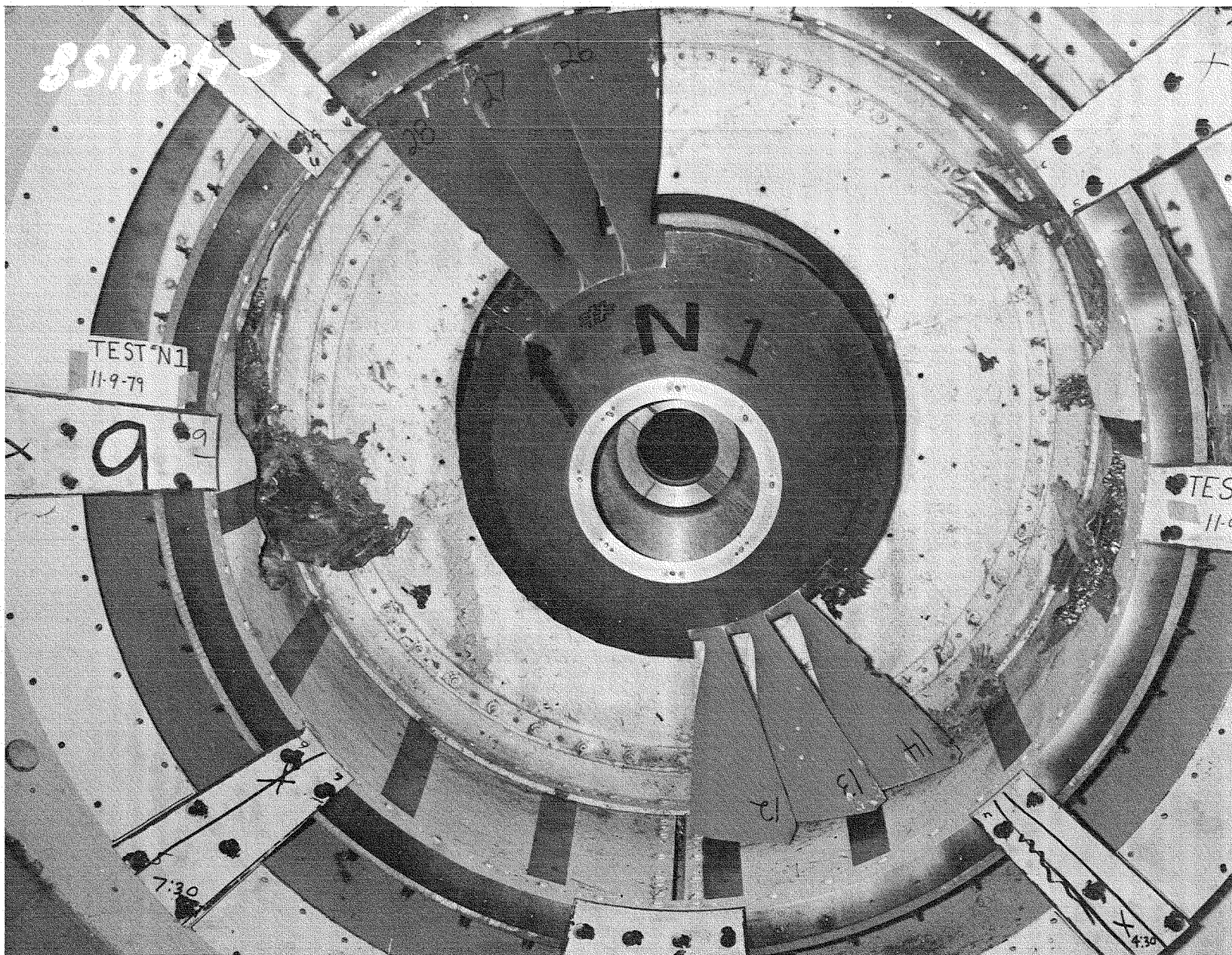


Figure 9. Test 1 - Overall View.

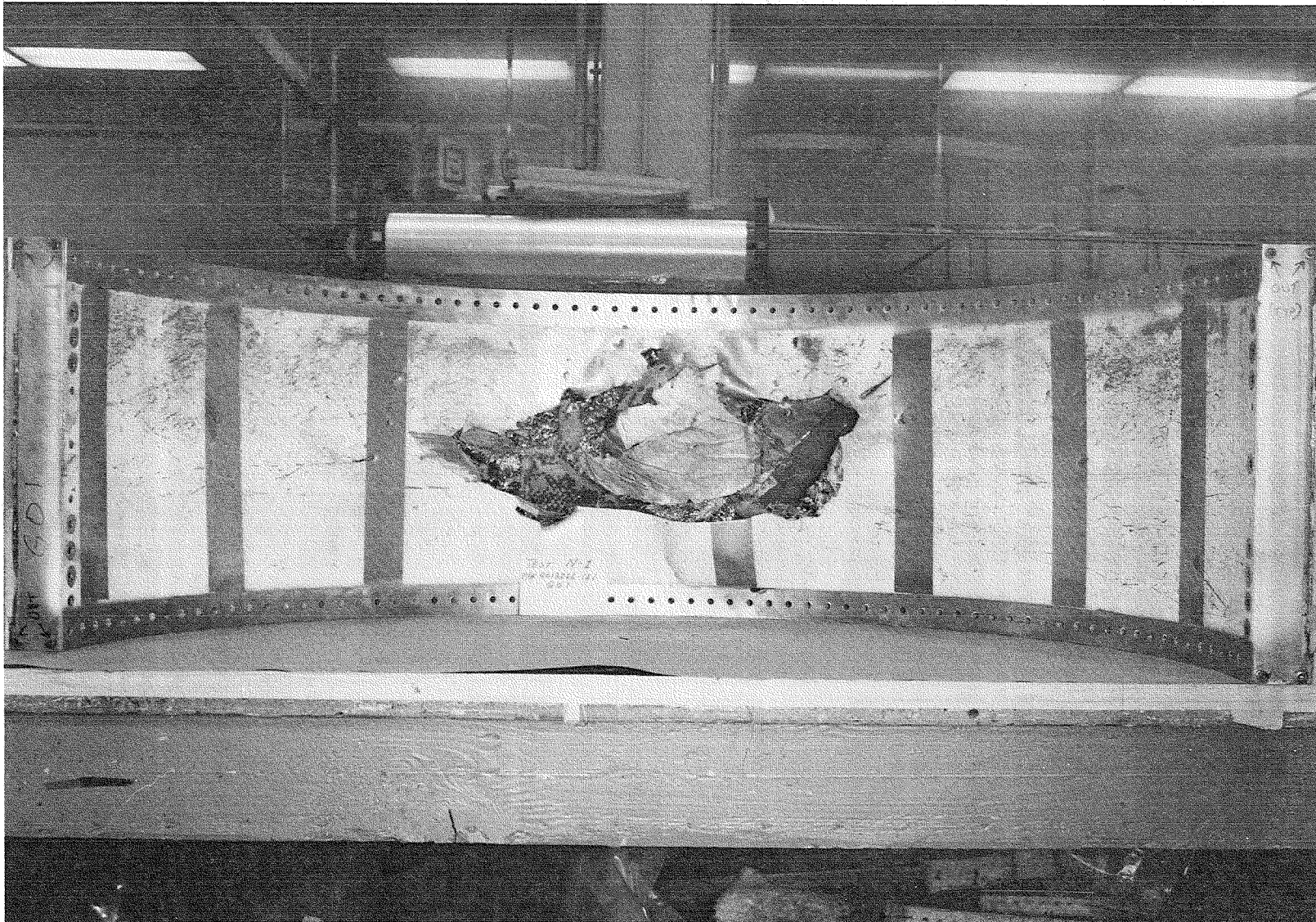


Figure 10. Typical Damage - Flowpath Side - Test 1.

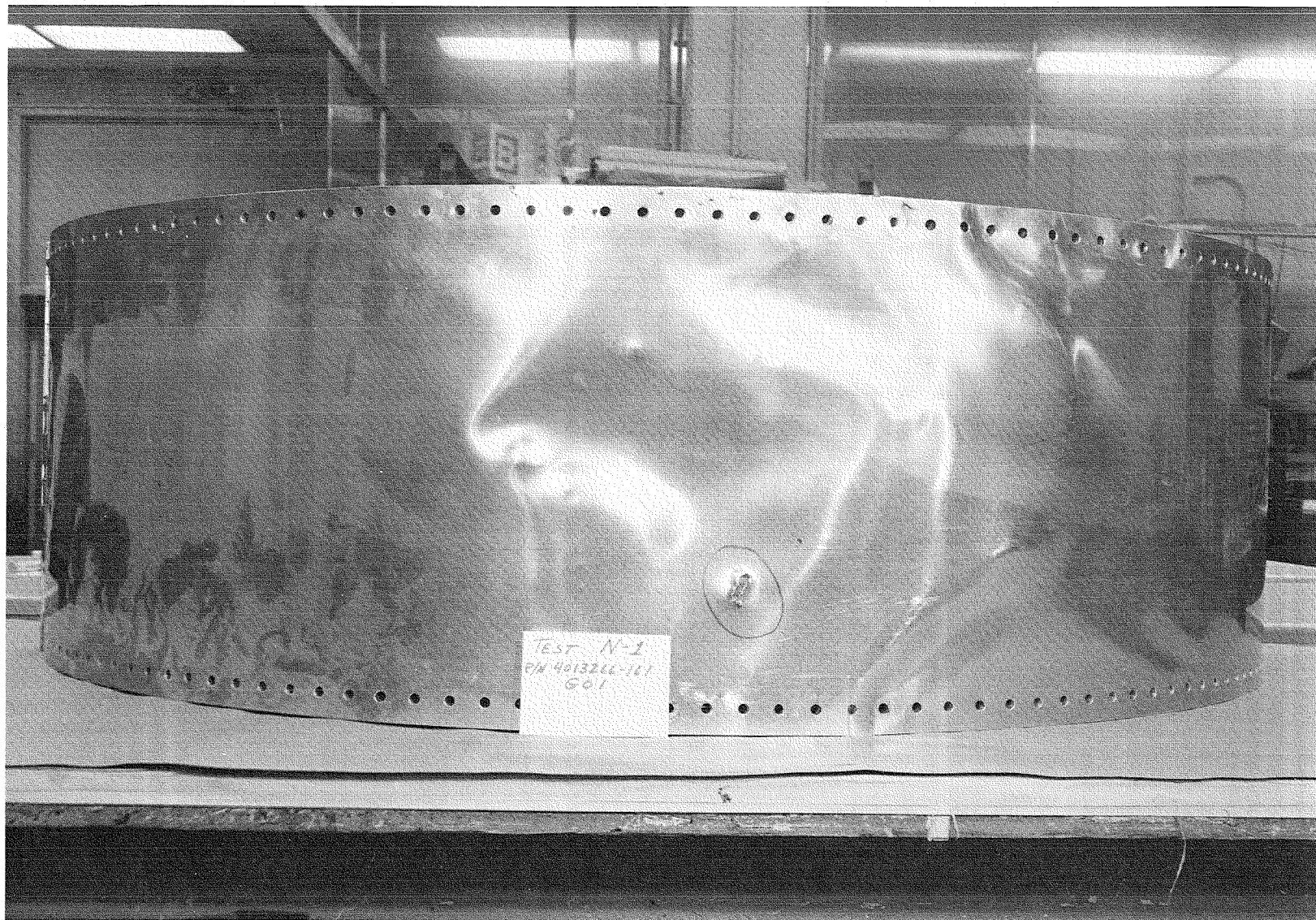


Figure 11. Exterior View - 12-Ply Side - Test 1.

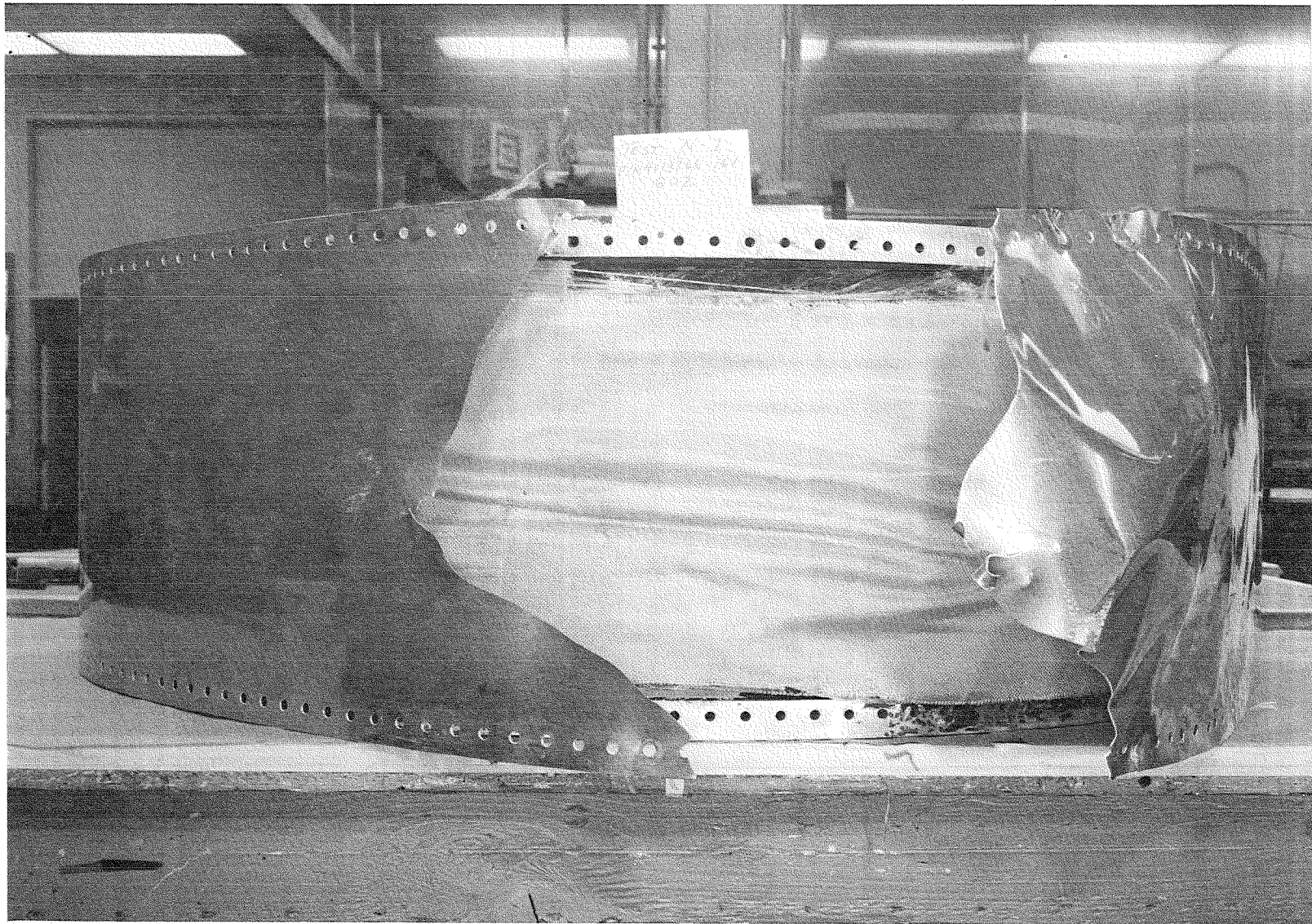


Figure 12. Exterior View - Eight-Ply Side - Test 1.

Test 2

Since Test 1 did not result in penetration of the Kevlar systems, it was decided to run Test 2 with the same containment configuration as Test 1 and increase the rotor speed from 4500 rpm to 5000 rpm. This resulted in a 25% increase in the energy of the released airfoils. The damage of the flow-path side of the 12-ply configuration is shown in Figure 13. Comparing Figure 13 to Figure 10, which shows the damage to an identical containment case when impacted by an airfoil at 4500 rpm (Test 1), it appears that the damage is somewhat greater at the higher release speed and the airfoil is more deeply embedded in the containment. Teardown from the backside, however, did not show any significant difference in the damage sustained by the Kevlar in Tests 1 and 2. It was obvious that threshold containment was not identified by these tests.

Test 3

This test was identical to Test 2 except that the blades were released below the platform resulting in a larger impacting mass and thus higher kinetic energies. The damage to the containment systems due to this test was much more severe than in Tests 1 and 2, but the blades were still retained by the Kevlar. The rotor/containment casing setup after the test is shown in Figure 14. Although the next following blade on each side interacted with the released blade and sustained a small dent in the leading edge near the root, no other damage was done to the remaining blades in the rotor. The back of the containment system containing 12 plies of Kevlar is shown in Figure 15 with the aluminum outer sheet removed exposing the Kevlar material. For the first time in the tests of this type, the impact had sufficient force to fail the axial joint of the Kevlar to the close-out beams. This joint was formed by locally rigidizing the Kevlar with epoxy adhesive and bolting it between the two steel bars which form the axial close-outs. The failure consisted of a combination of bolt failure and shear-out of the Kevlar/epoxy as shown in Figure 15. This phenomenon occurred only on the side which had 12 plies of Kevlar. On this side, the blade did not locally penetrate the Kevlar. The Kevlar plies moved outward as a unit thus applying a circumferential force which had to be resisted at the ends. This load was apparently

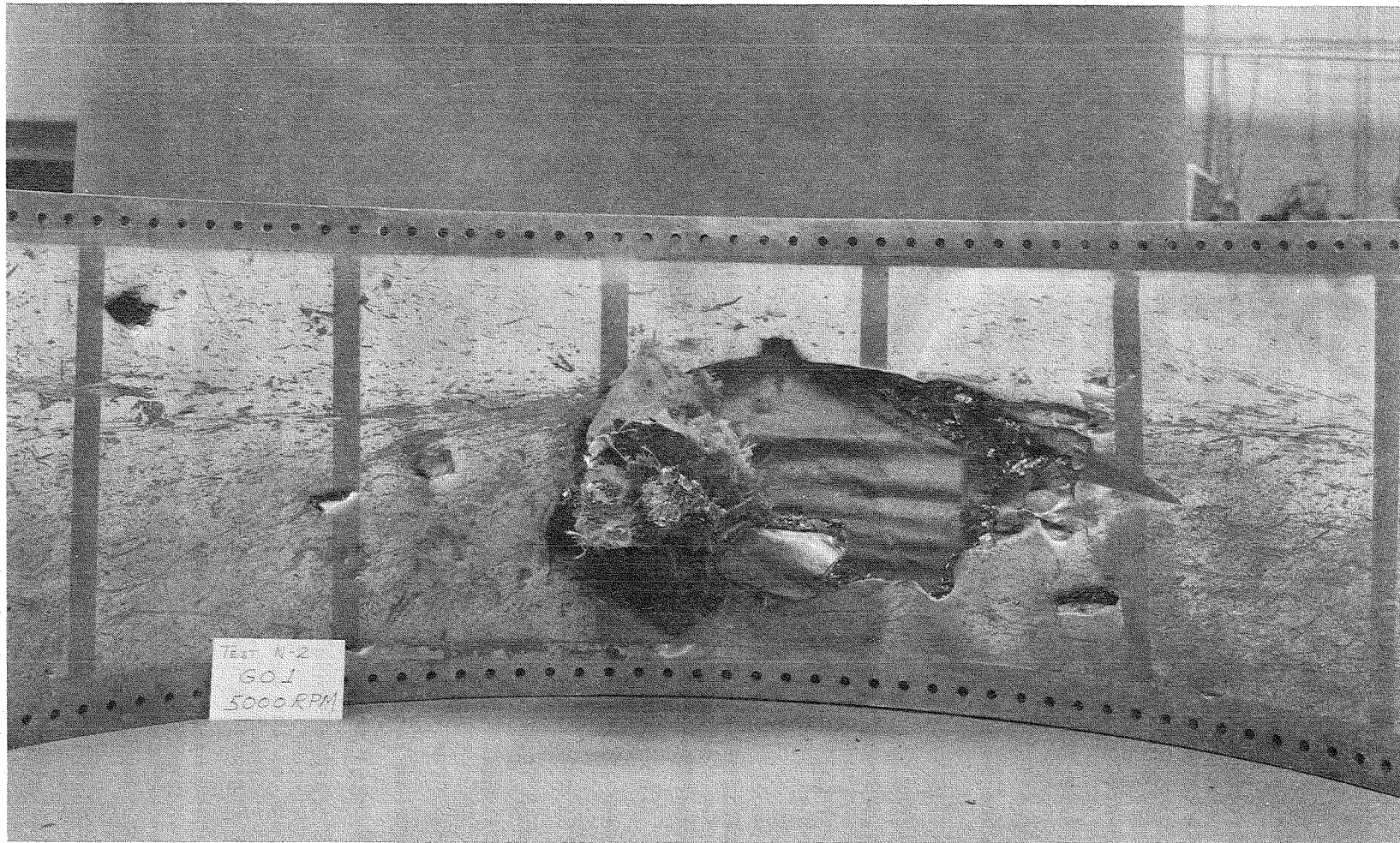


Figure 13. Interior View - 12-Ply Side - Test 2.

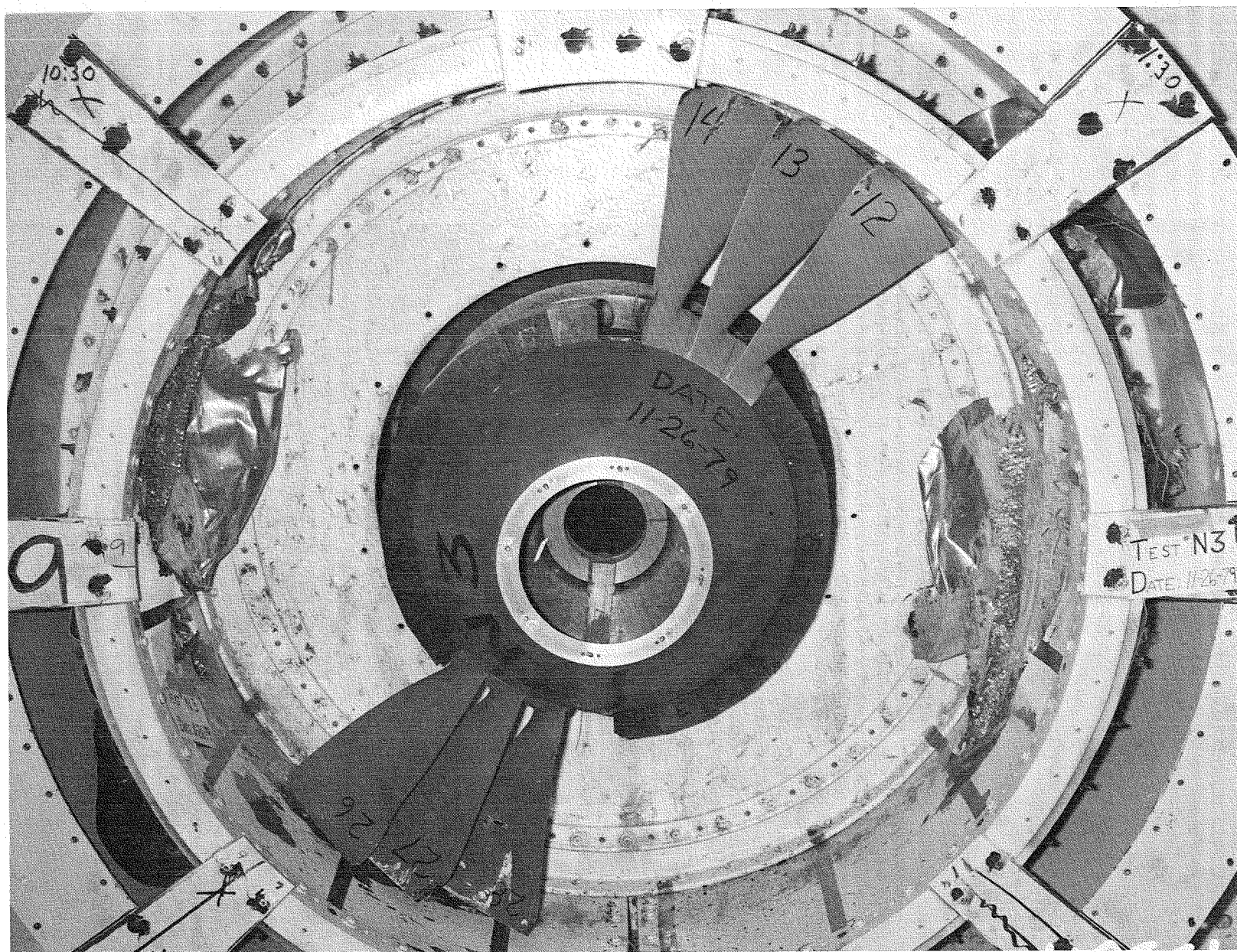


Figure 14. Test 3 - Overall View.

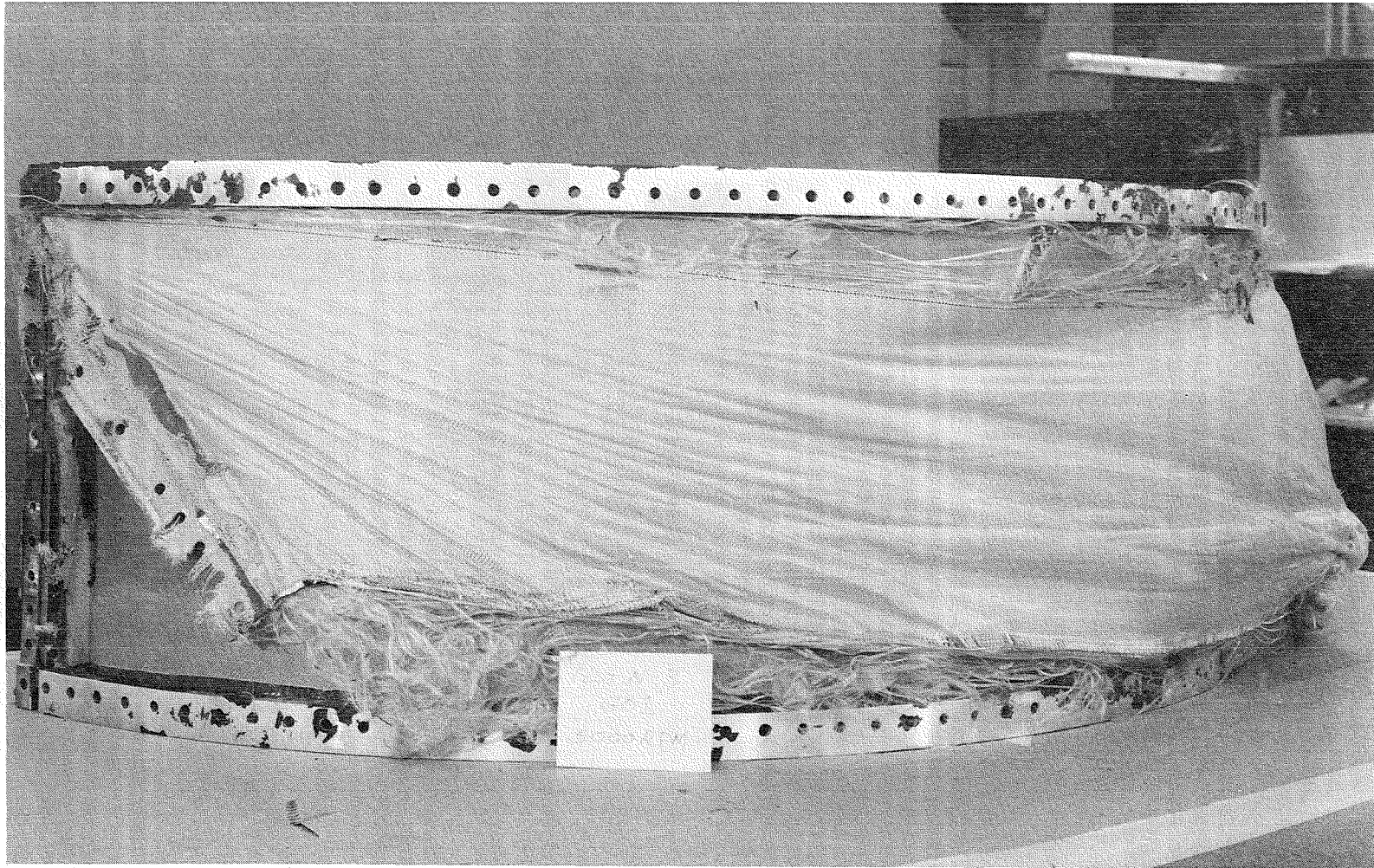


Figure 15. Exterior View - 12-Ply Side - Test 3.

sufficient to fail the end attachment. On the side with only eight plies of Kevlar, the blade root punched a hole entirely through the Kevlar although the blade as a whole was contained within the system. In this case, much of the energy was absorbed by fracturing the Kevlar and was thus not transferred circumferentially to the end attachments which did not fail. The eight-ply side, with the aluminum backing removed, is shown in Figure 16. As would be expected, the external damage, as can be seen by comparing Figures 15 and 16, was greater on the side that had less Kevlar. This difference in damage can also be seen in Figures 17 and 18 that show the interior of the containment specimen at the outer radius of the honeycomb sandwich of the 12-ply and eight-ply systems, respectively, where all the dry Kevlar has been removed.

Test 4

Since Test 3 did not completely defeat the system, even though the eight plies of Kevlar were just barely able to retain the blade, it was decided to increase the speed at which the blade was released to the maximum that could be obtained in the existing test setup. This speed turned out to be in the vicinity of 5300 rpm. The actual release speed was 5285 rpm and the containment targets were of the same configuration as Test 3. The damage to the containment systems was very similar to that noted in Test 3 with slightly greater penetration of the blades through the Kevlar. On the side with eight plies of Kevlar, the outward movement of the released blade was sufficient to impact the witness plate with considerable force. The dent left by this impact can be seen in Figure 19. Although the blade remained captured by the containment systems, it is questionable if it would have remained captured if its motion had not been stopped by the witness plate. The outside of the containment rings, with the aluminum back sheets removed, is shown in Figures 20 and 21. As can be seen in Figure 20, the blade root did not penetrate the outer plies of the 12-ply configuration while the root section came completely through the eight-ply Kevlar belt as shown in Figure 21. In both cases, the Kevlar material, at the point of impact and for a considerable distance circumferentially away from this point, was drawn toward the center (axially) of the containment ring. This movement left large areas unprotected in the event of subsequent impacts. Several methods of restricting this movement were experimentally evaluated later in this program.

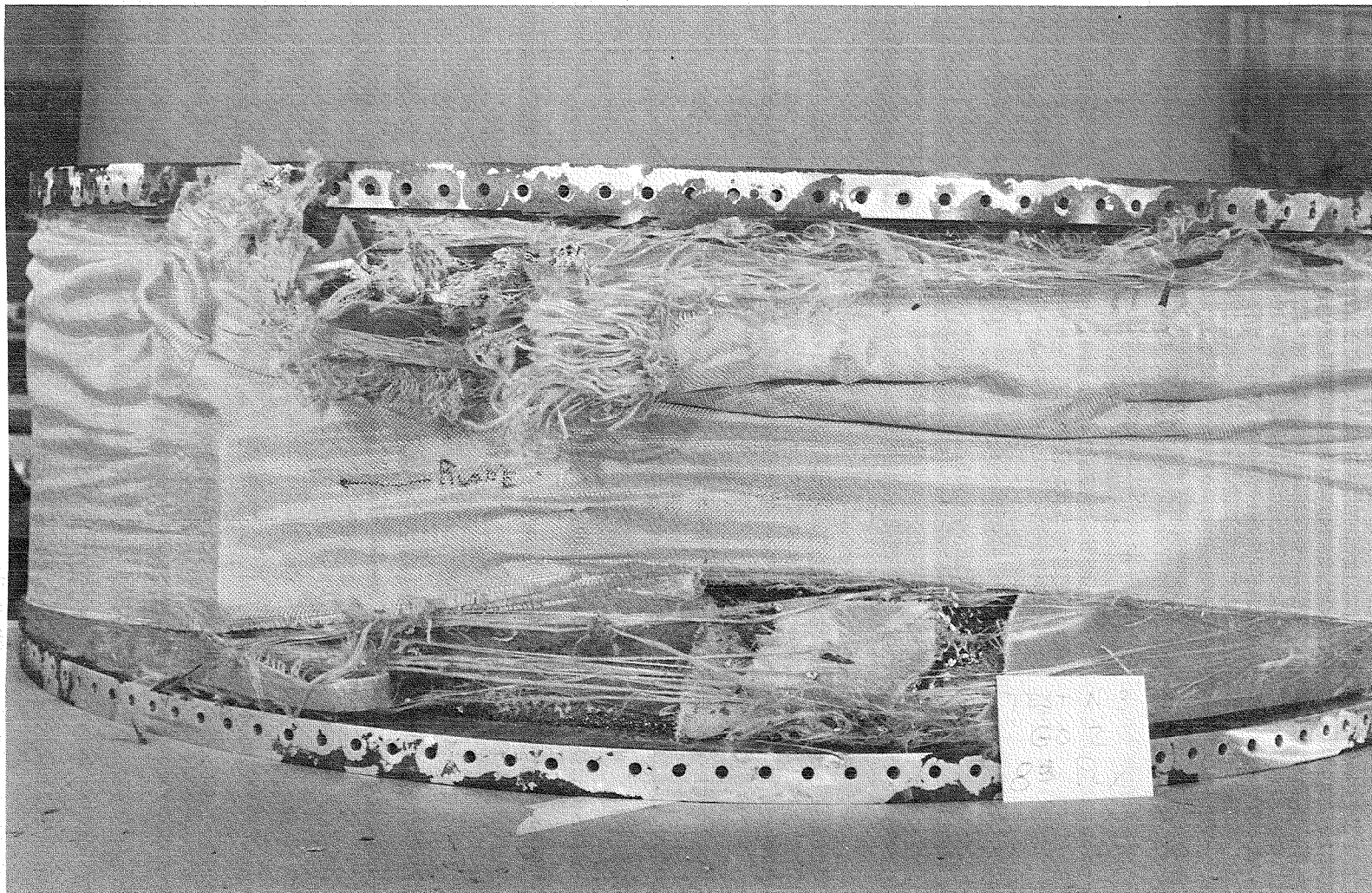


Figure 16. Exterior - Eight-Ply Side - Test 3.

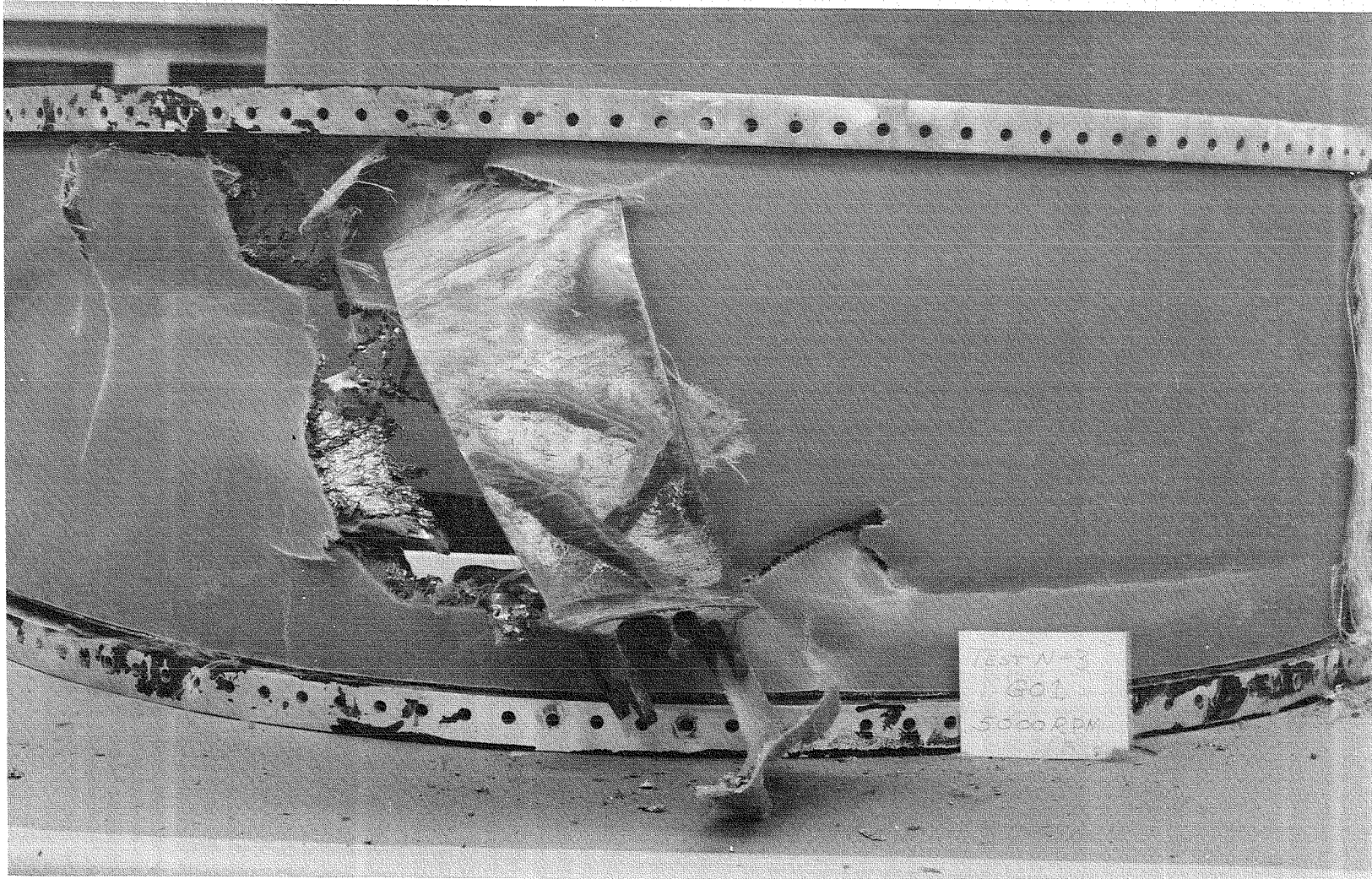


Figure 17. Exterior View - 12-Ply Side - Kevlar Removed -
Test 3.

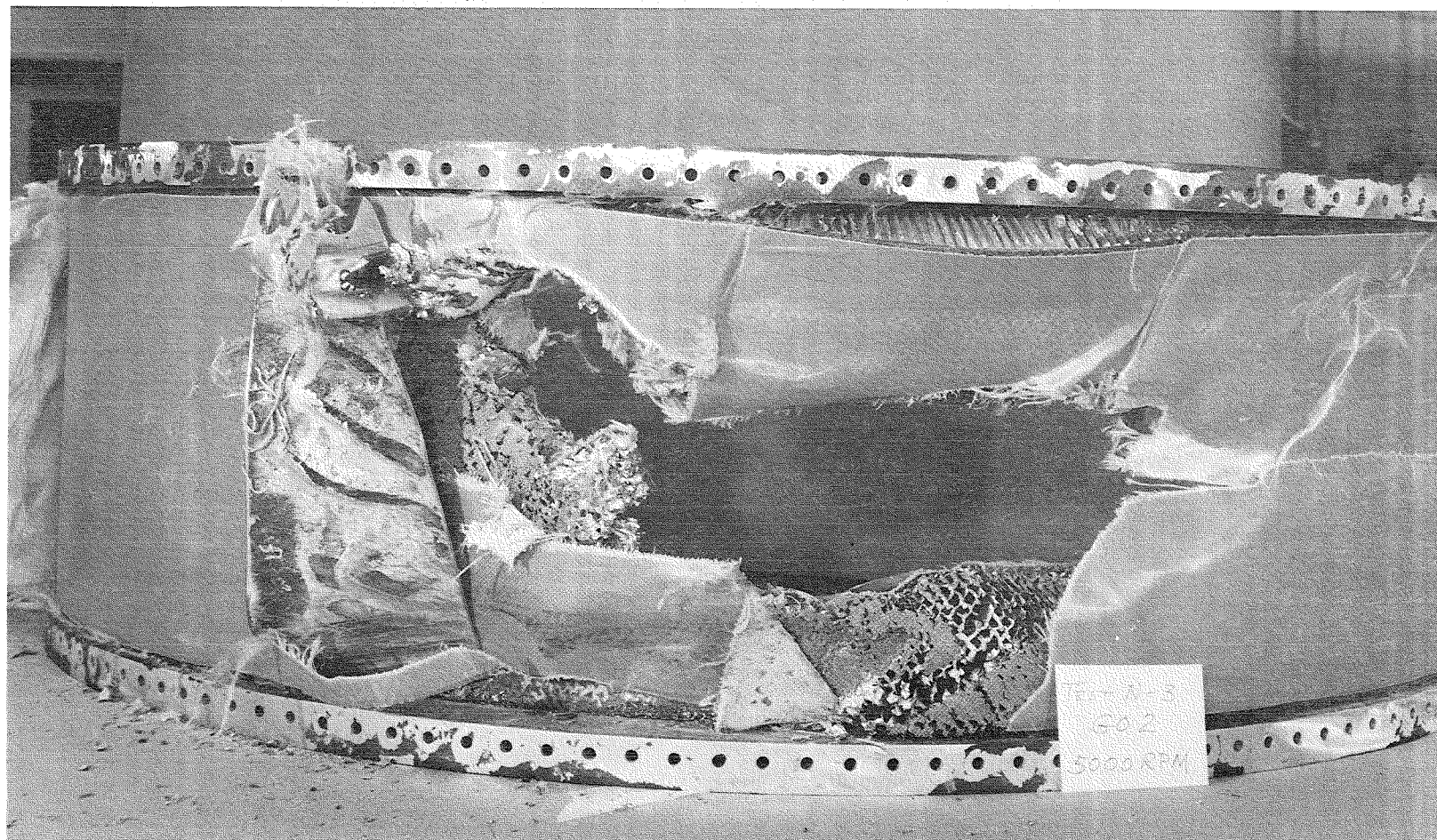


Figure 18. Exterior View - Eight-Ply Side - Kevlar Removed -
Test 3.

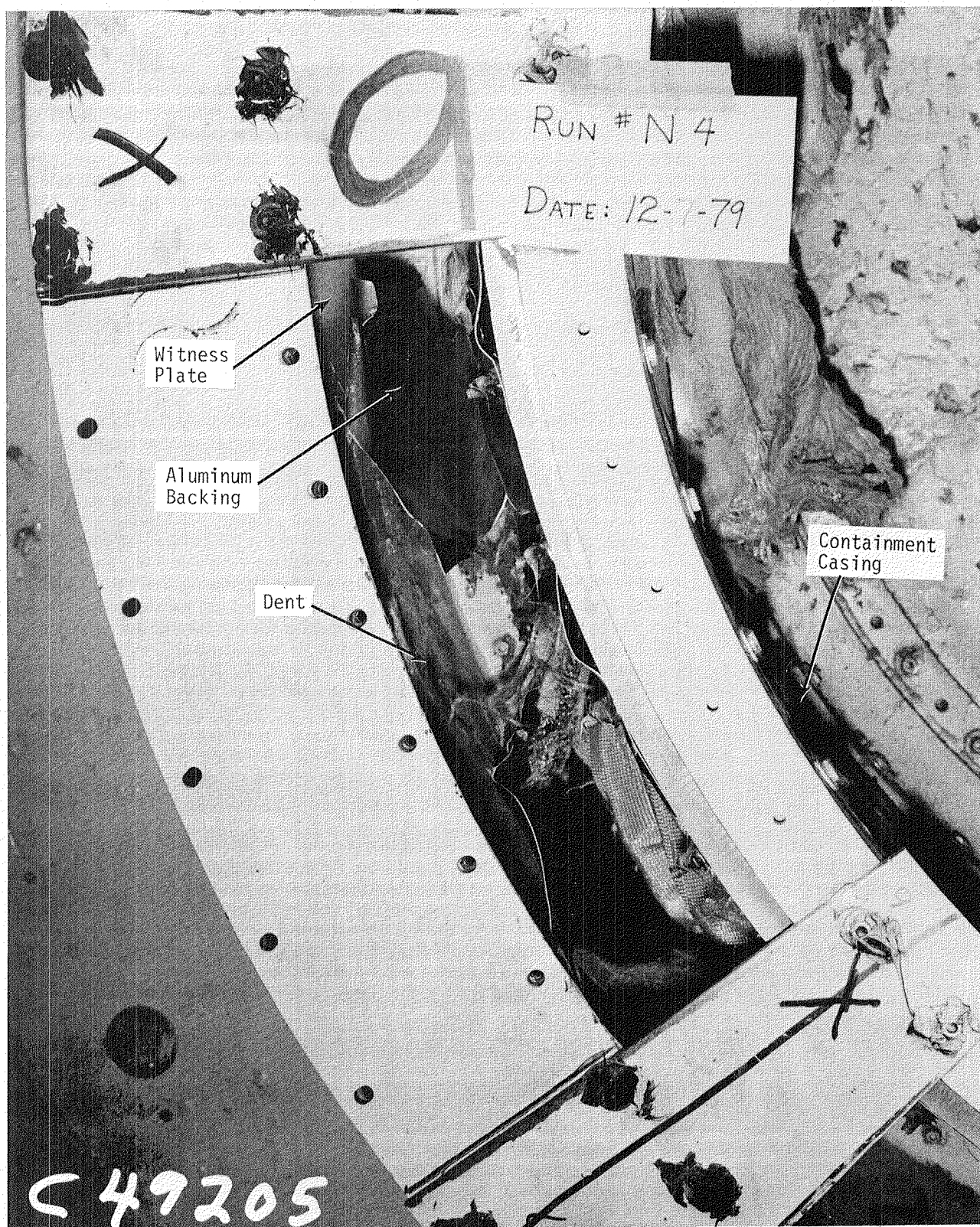


Figure 19. Witness Plate Dent - Test 4.

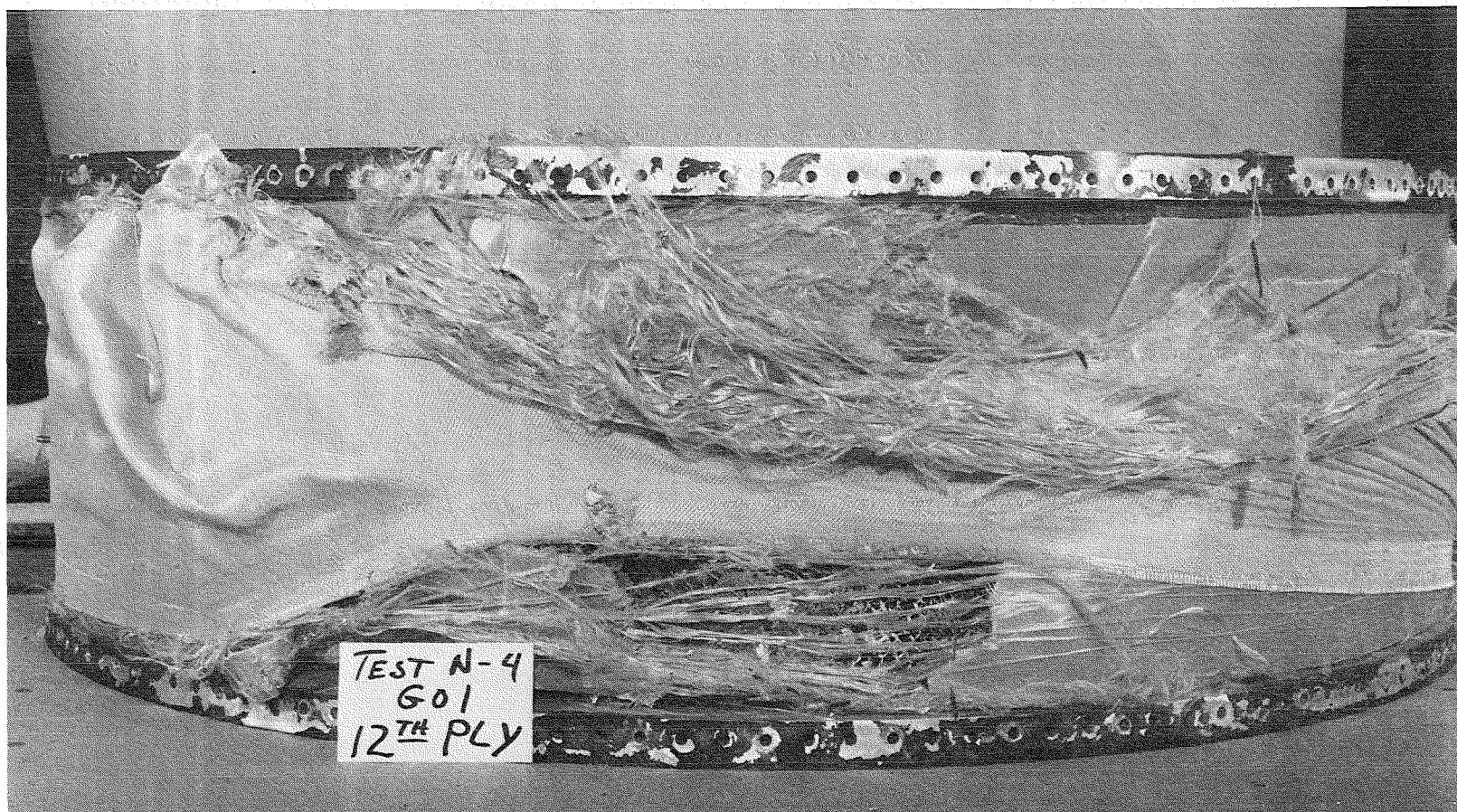


Figure 20. Exterior View - 12-Ply Side - Test 4.

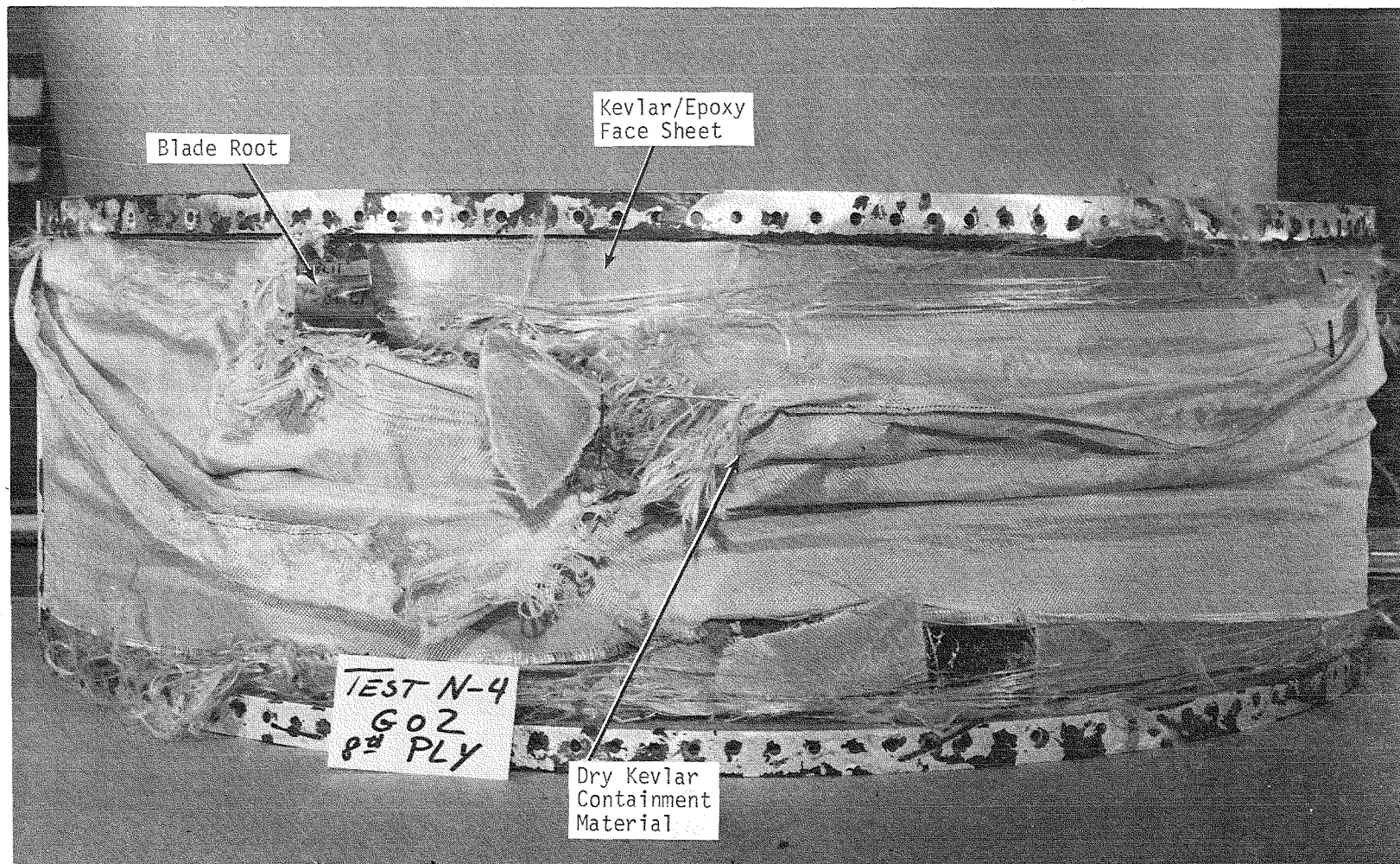


Figure 21. Exterior View - Eight-Ply Side - Test 4.

Test 5

The purpose of this test was to make an initial evaluation of the effects of adding Kevlar felt between the honeycomb sandwich and the dry Kevlar cloth. The purpose in using the felt was to attempt to enmesh the released blade in the very light, bulky, and tough felt, thus increasing the apparent area of the blade as it attempted to penetrate through the Kevlar cloth. Two methods of placing the felt were tested. These methods are shown schematically in Figure 22. The felt used in these tests was 56.06 kg/m^3 (3.5 lb/ft^3) density and the total thickness was 0.508 cm (0.20 in.). The remaining structure of the containment systems was similar to that used in Test 4 which had eight plies of dry Kevlar. Each containment system was impacted by a TF34 titanium blade released below the platform at a rotor speed of 5300 rpm. The overall damage to the containment systems was greater in this test than in the previous tests at similar release speeds and eight plies of Kevlar. This can be seen by comparing Figure 23 with Figure 21. The motion of the released blade was also different. In this test, the Kevlar felt wrapped around the sharp edges of the root section restricting its ability to penetrate the Kevlar cloth as it did in Test 4. However, this same feature apparently caused the blade to pull the Kevlar cloth further aft thus allowing much of the blade tip to be outside the containment system and resulting in a considerable portion of the containment ring being unprotected from any subsequent impact. There was more overall damage to the side in which the felt was installed per Concept B (Figure 24); however, the felt itself was more badly torn when installed per Concept A (Figure 25). Based on the results of this test, it is judged that the addition of Kevlar felt, in the density and thickness tested, did not provide any additional containment ability to the basic containment concept.

3.1.3.2 Phase II Testing

The second phase testing consisted of four tests which had balanced two blade releases into 180° containment systems and two tests involving single releases out of a virtually full rotor into 360° containment systems. Eight 180° containment systems were fabricated by Accurate Plastics Inc., and two 360° containment systems were fabricated by General Electric for this test

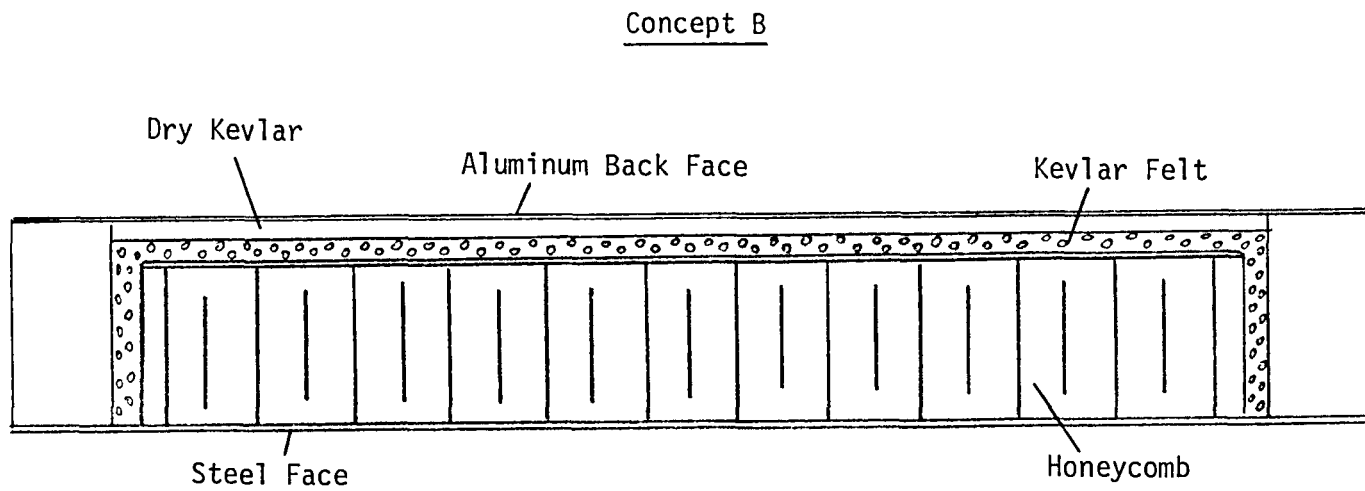
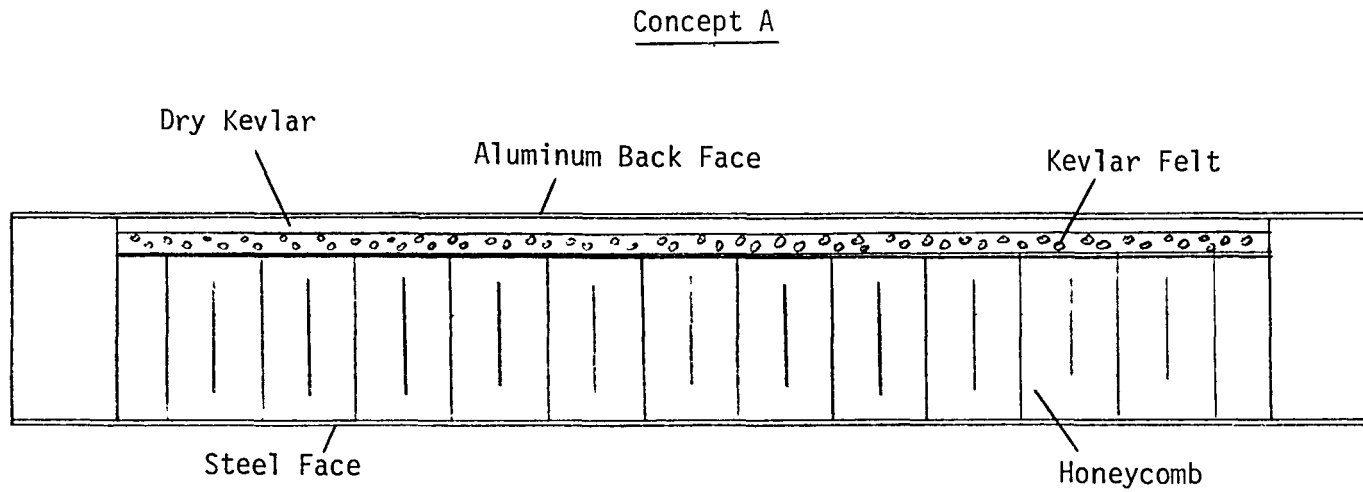


Figure 22. Kevlar Felt Concepts.

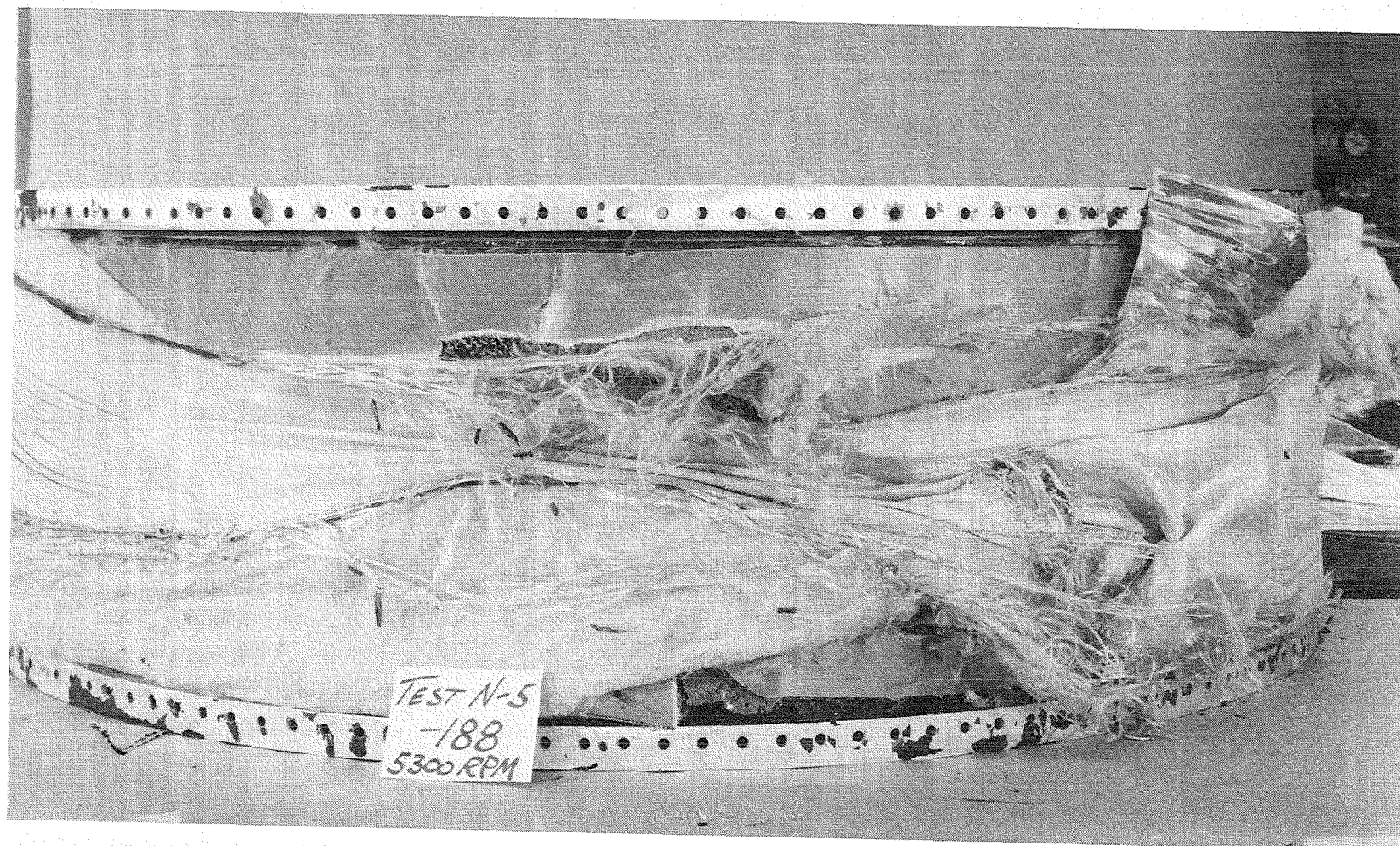


Figure 23. Exterior View - Test 5.

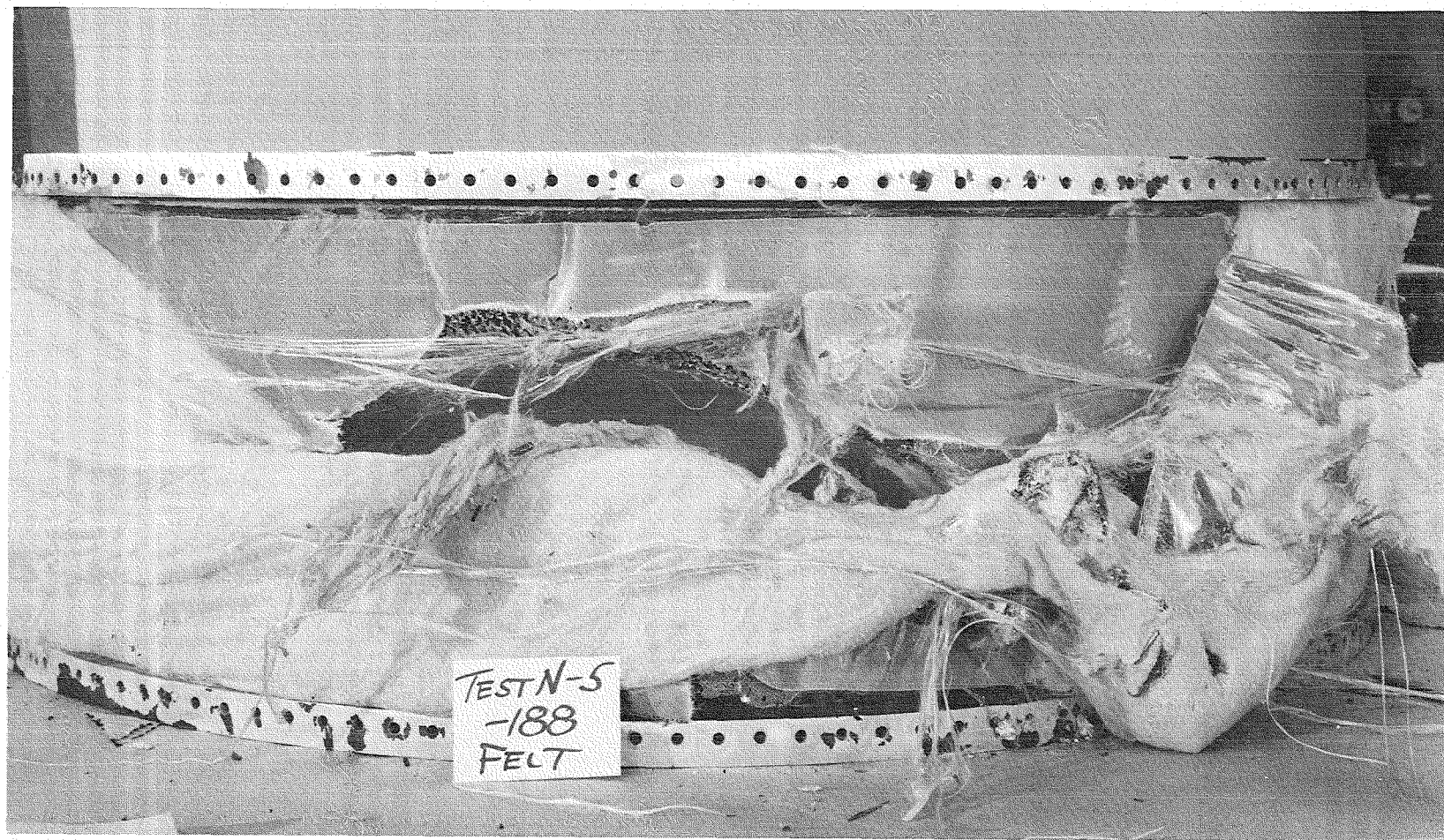


Figure 24. Exterior View - Test 5 - Cloth Removed - Concept B.



Figure 25. Exterior View - Test 5 - Cloth Removed - Concept A.

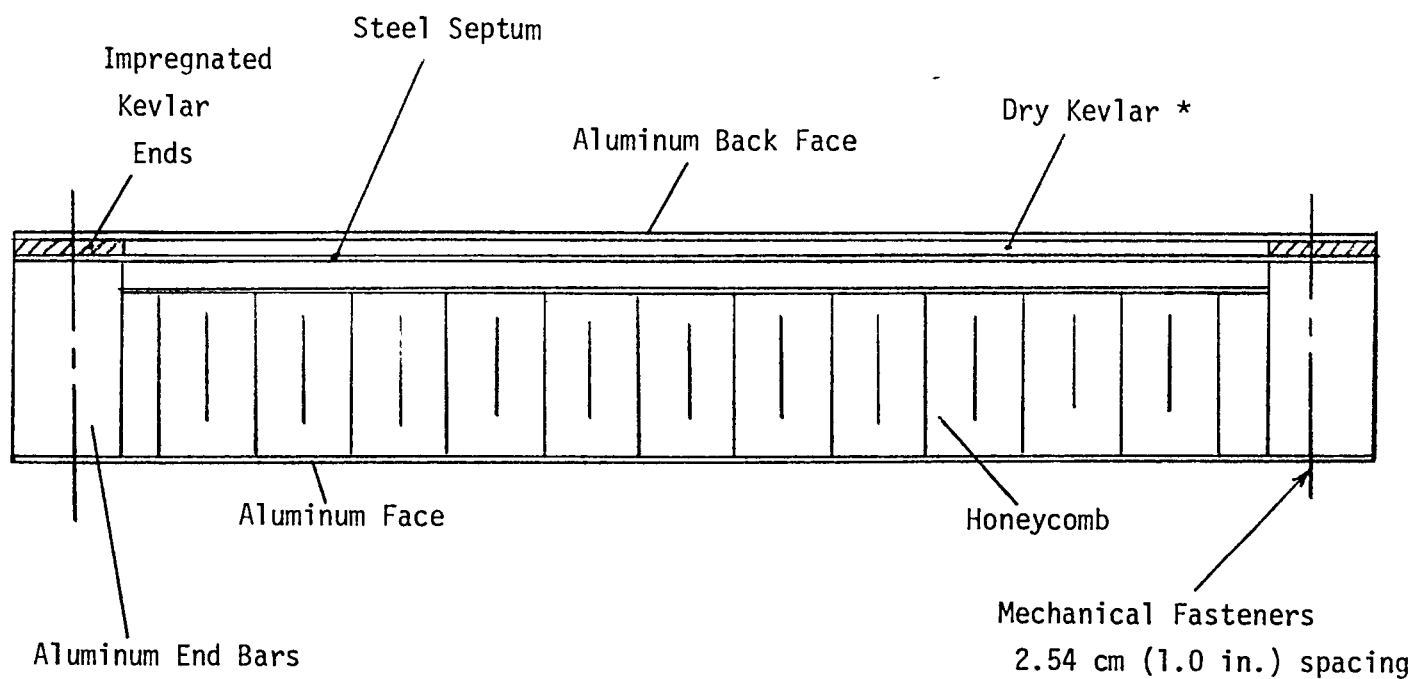
phase. Since the previous testing had shown significant axial movement, it was decided to try and restrict this movement on the Phase II tests. This was accomplished by impregnating the forward and aft ends of the dry Kevlar cloth with epoxy adhesive and curing it at room temperature. Holes were then drilled in these rigidized ends so that they could be mechanically attached to the end rings. Six of the eight 180° containment systems were fabricated in this manner as were both of the 360° systems. Other minor variations in the containment design are discussed below along with the test results.

Test 6

This was the first test to incorporate any form of restraint to the Kevlar in the fore and aft direction. It also investigated the difference in containment characteristics between the bidirectional-type weave (328) used in all previous tests and a more unidirectional weave (143). The effect of using aluminum next to the flowpath rather than steel was also investigated. A sketch of the systems tested is shown in Figure 26.

Two TF34 titanium blades were released below the platform at 5300 rpm. Both blades were contained by the containment systems and the end retention feature worked very well. There was no tendency for the Kevlar to be pulled out of position. This was a significant improvement over previous tests as can be seen by comparing Figure 27 which shows the damage to the side with 10 plies of 328-weave Kevlar with Figure 20 of Test 4 which was conducted under the same conditions with a containment system of 12 plies of Kevlar which were not restrained in the axial direction.

The side with the 328-weave Kevlar was somewhat thicker than the side with 143-weave Kevlar due to the slight per ply thickness difference of the two weaves. The containment characteristics of the 328 weave were much better than those of the 143 weave, even considering the thickness difference. The lack of tranverse fibers allowed the longitudinal fibers to split apart causing a much larger hole than was the case with the more bidirectional 328 weave. This difference can be seen by comparing Figure 28 with Figure 27.



- * Configuration 1 - 10 plies of 143-weave Kevlar
- Configuration 2 - 10 plies of 328-weave Kevlar

Figure 26. Test 6 Configurations.

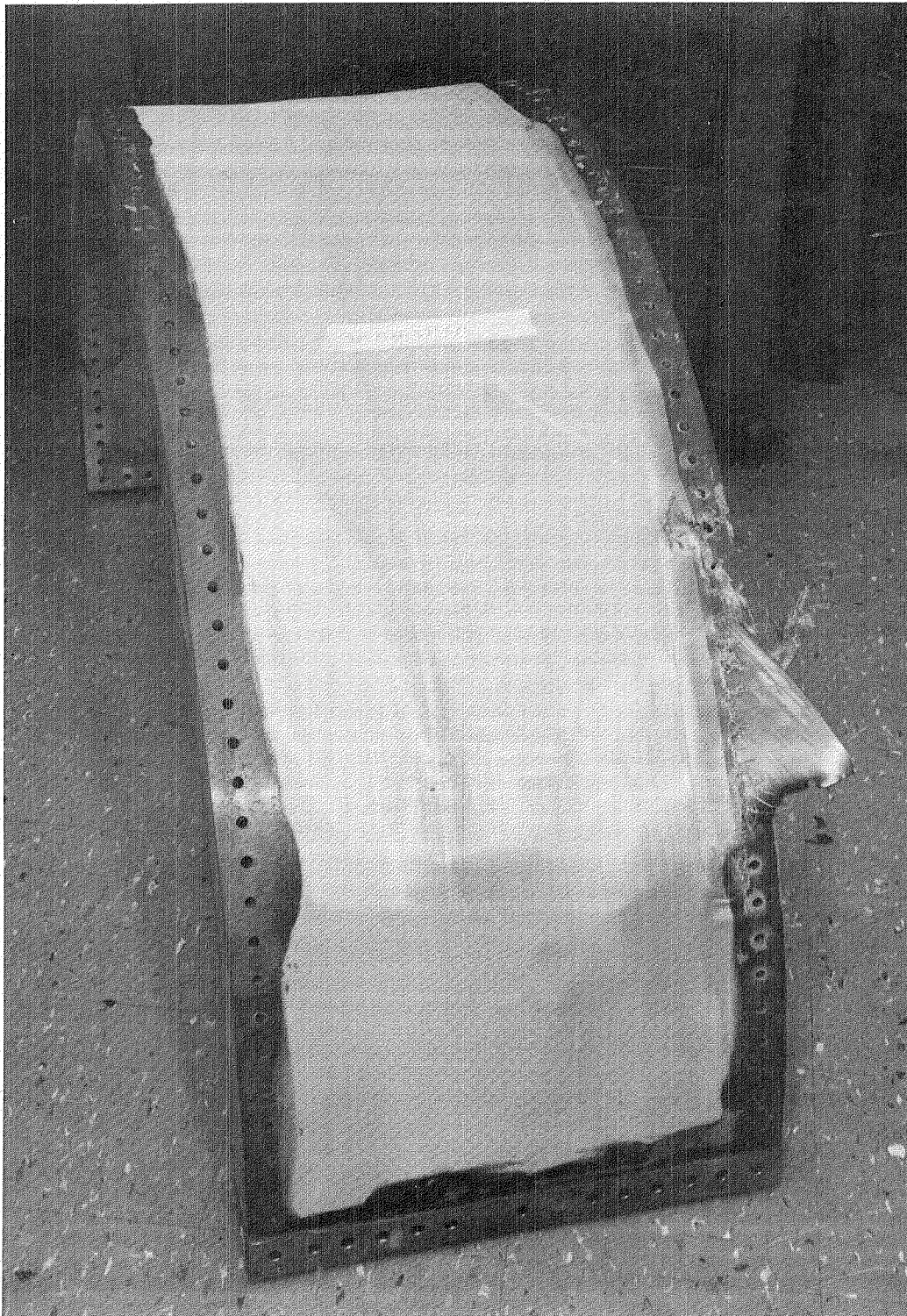


Figure 27. Exterior View - 10 Plies of 328-Weave Kevlar - Test 6.

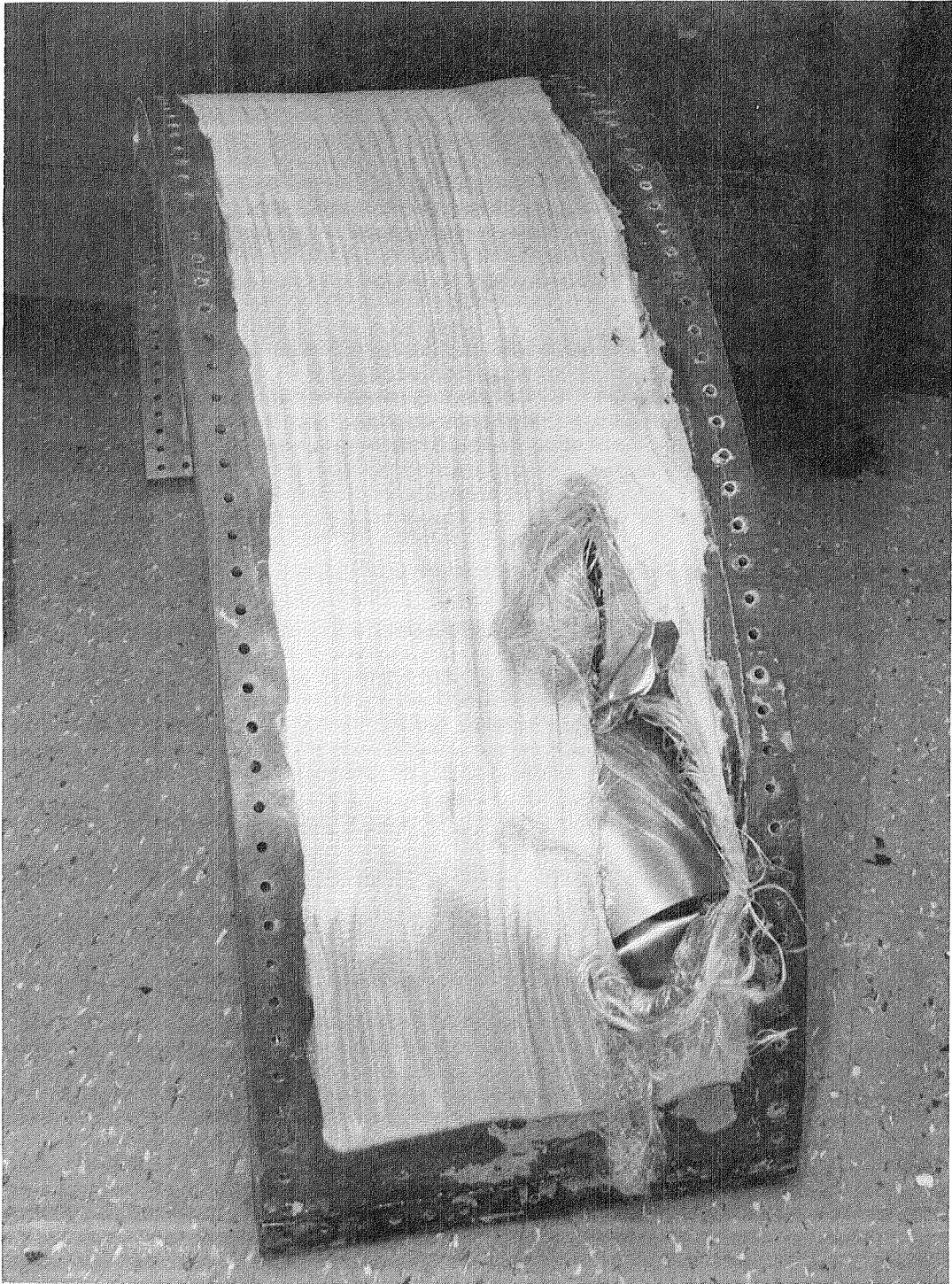


Figure 28. Exterior View - 10 Plies of 143-Weave Kevlar - Test 6.

The change from steel to aluminum on the flowpath face sheet did not appear to have any effect on the containment process and the face sheet was not torn up by the impact any more than the steel face sheets used in previous tests run under similar conditions. Since there was no net rotor unbalance, there was no information generated on the rub capability of the aluminum face. The condition of the aluminum face at the impact point is shown in Figure 29 and the condition away from the impact points is shown in Figure 30.

Test 7

Since the blades in the previous test were contained, the primary purpose of this test was to attempt to defeat the containment system by reducing the amount of dry Kevlar cloth. Both configurations tested had eight plies of cloth with the ends rigidized and bolted to the end rings. One side was identical to Concept A of Figure 22 except for the rigidized ends while the other side was the same as Configuration 2 of Figure 26 except that only eight plies of Kevlar were used. Two opposed titanium blades were released at a rotor speed of 5300 rpm to produce the same impact conditions as Test 6. Both containment halves were completely penetrated by the root sections of the blades. The root sections of both blades impacted the witness shield with sufficient force to dent the shield but not with enough to penetrate the shield which was 0.635 cm (0.25 in.) thick aluminum. The airfoil sections of the blades were still enmeshed in the containment system, but were not tightly held. It is possible that the blades could have come completely out of the containment if the root sections had not impacted the witness shield. The amount of blade penetration was about the same as can be seen in Figures 31 and 32. The Kevlar felt did not seem to affect the amount of root penetration or the damage to the flowpath side of the containment systems although the total size of the exit hole on the outside was smaller for the side which contained the felt.

It was judged that the containment configurations evaluated by this test represented, at very best, threshold containment and that the amount of Kevlar cloth employed in their construction would be insufficient for any production design.

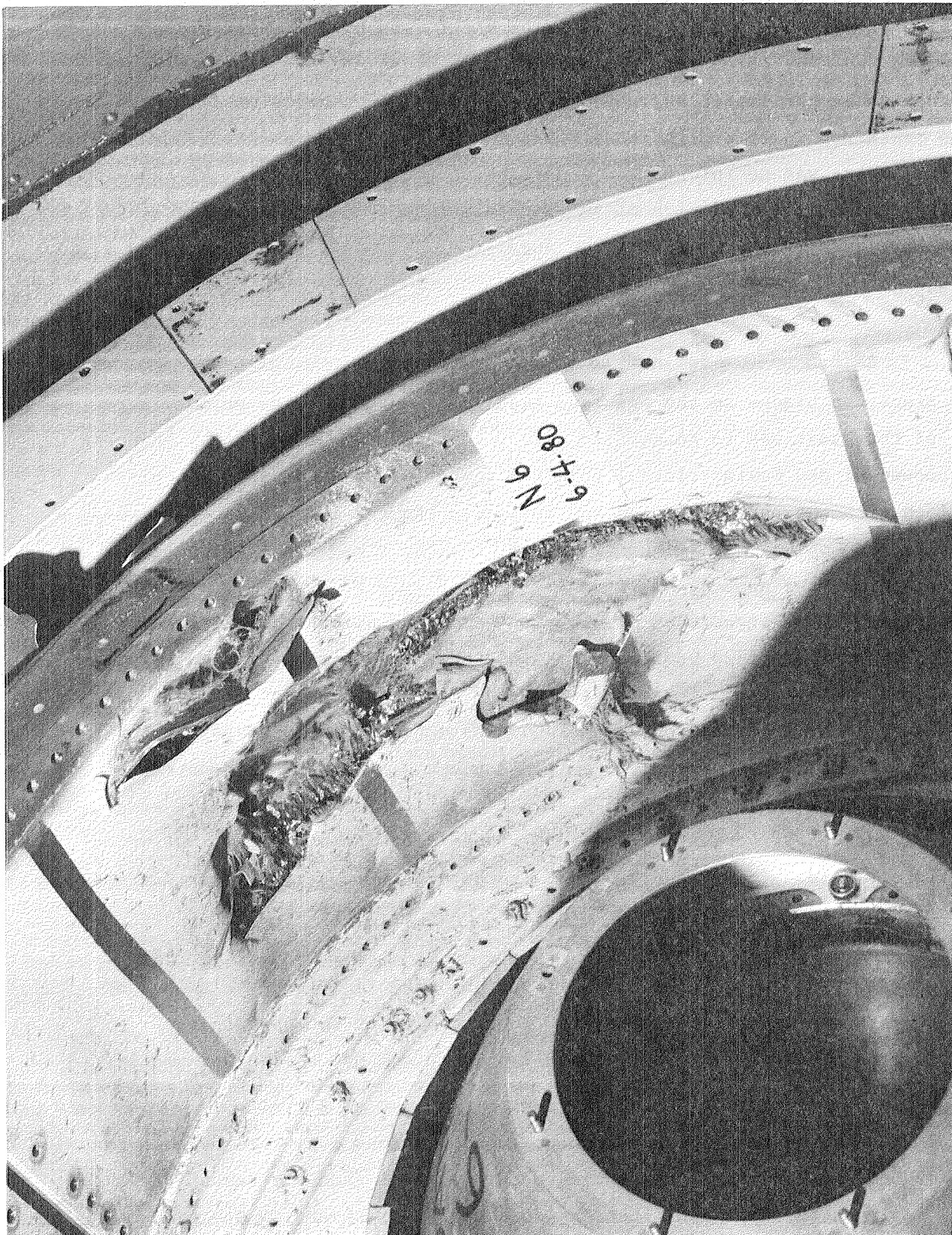


Figure 29. Aluminum Face Sheet - Test 6.

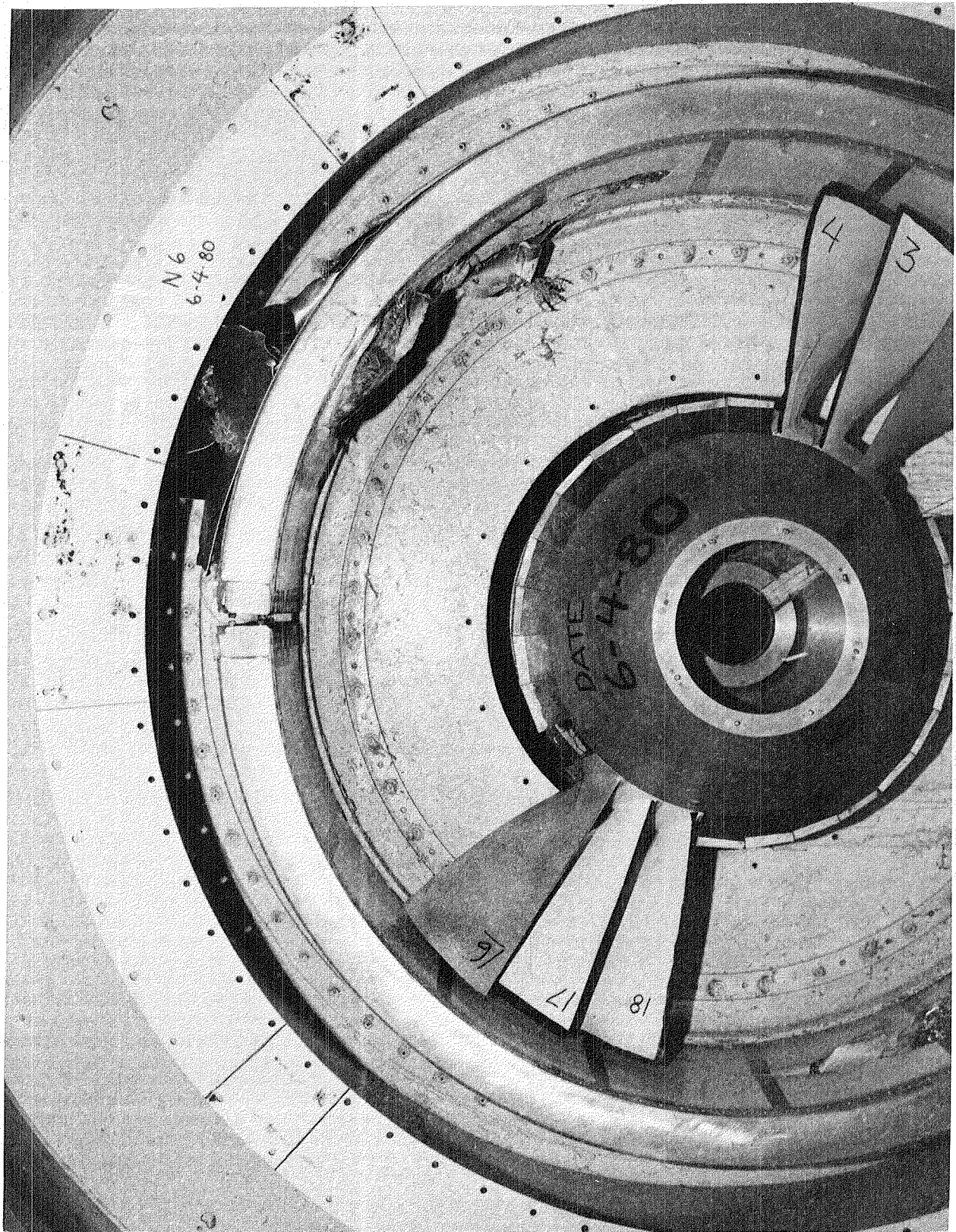


Figure 30. Test 6 - Overall View.

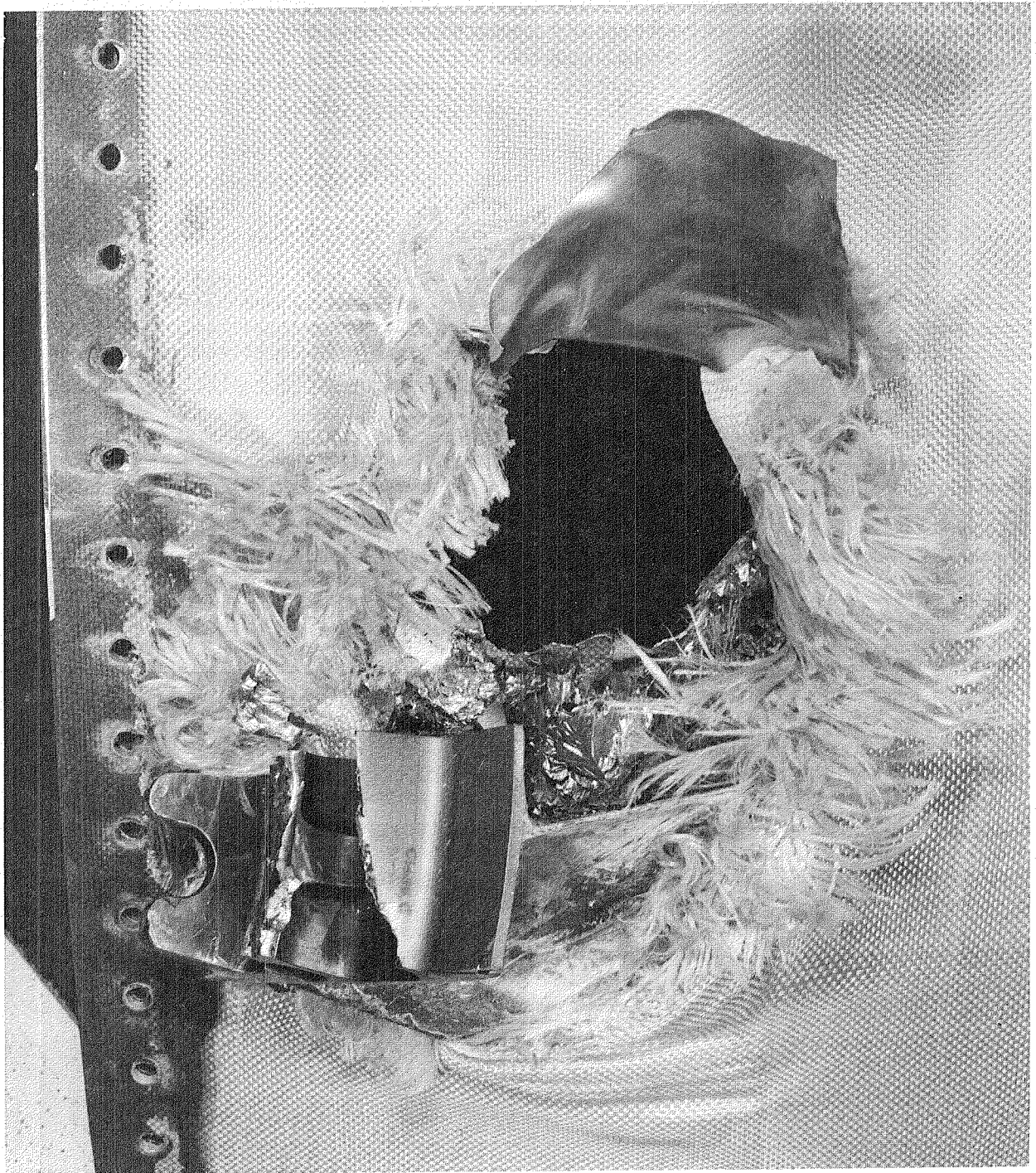


Figure 31. Exterior View - Test 7 - No Felt.

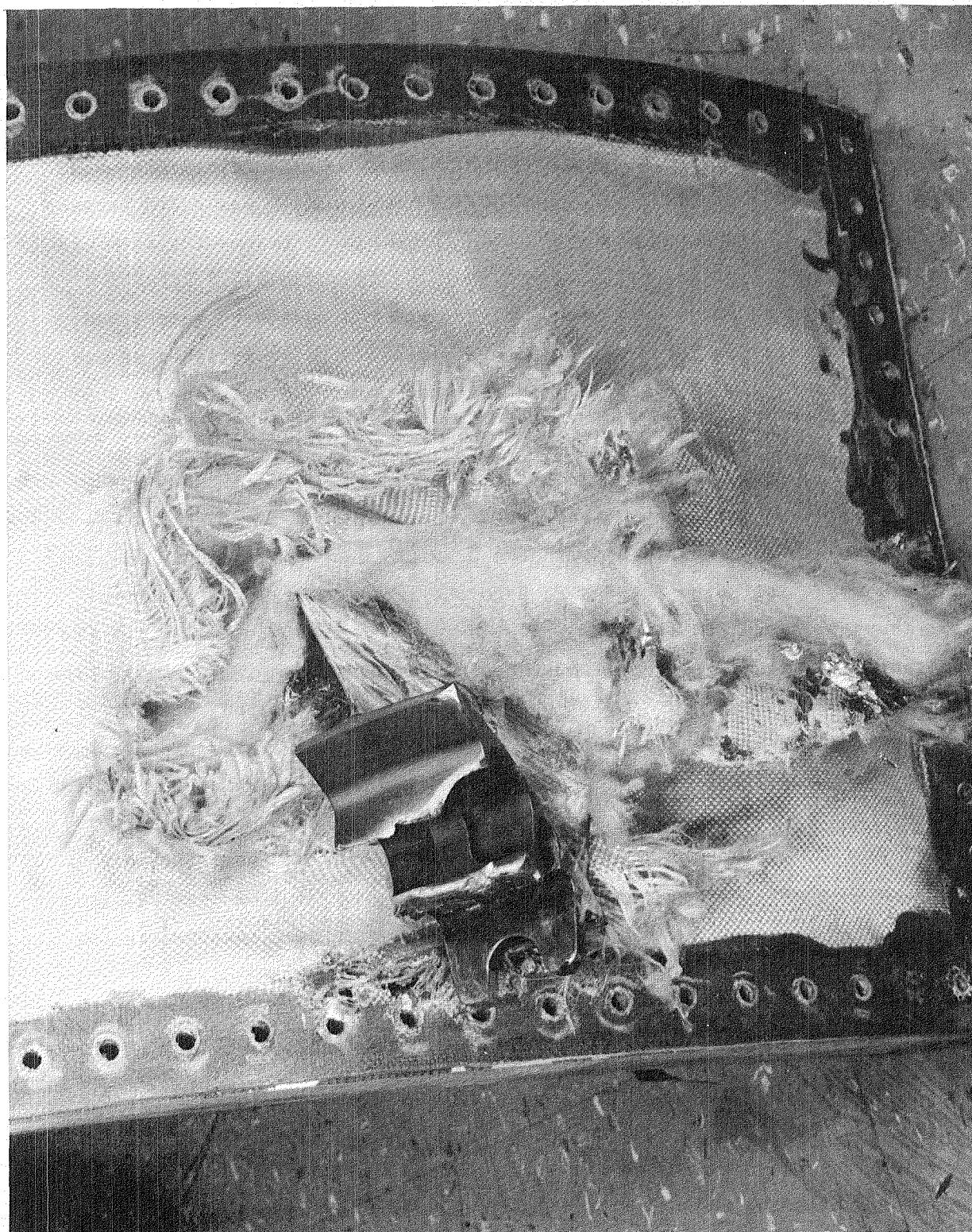


Figure 32. Exterior View - Test 7 - Kevlar Felt.

Test 8

This was the last test utilizing two opposite TF34 titanium blades as the released objects. One containment system was identical to Configuration 1 of Figure 26 except that only eight plies of the 143-weave Kevlar cloth was used and 1.016 cm (0.4 in.) of 192.2 kg/m³ (12 lb/ft³) Kevlar felt was added between the honeycomb sandwich and the steel septum. The other containment system was identical to Concept A of Figure 22 except that the felt was 192.2 kg/m³ (12 lb/ft³) instead of 56.06 kg/m³ (3.5 lb/ft³) and the ends were restrained. The ends of the Kevlar in both systems were rigidized with epoxy adhesive and bolted to the end rings. The blades were released below the platform at 5000 rpm.

Although the heavier felt did not tear nearly as readily as the lighter felt used on previous tests, the blade roots punctured both the felt and the woven cloth on both specimens. As with the previous test using the 143-weave cloth, there was a splitting tendency due to the small number of transverse (axial) fibers allowing the released blade, encased in the felt except for the root section, to virtually escape from the containment system (Figure 33). The blade would probably have come out except that the root struck the witness plate preventing further radial motion. The damage to the witness plate can be seen in Figure 34. The system with 328 weave was not as severely penetrated but the root section did come completely through the containment in a manner similar to Test 7. Although the heavier felt may have helped some (compare Figure 35 which shows the damage from Test 8 with Figure 32 from Test 7), it was a marginal improvement. This blade too may not have been retained in the containment system if it had not struck the witness shield.

Test 9

This was the only test run during this program using simulated super-hybrid blades, shown in Figure 7, as the released projectiles. It was anticipated that, since these blades were lighter than the all-titanium blades previously used and the composite portion should break up more readily, the amount of containment required to contain these blades would be less than that required to contain the titanium blades. With the blades being released

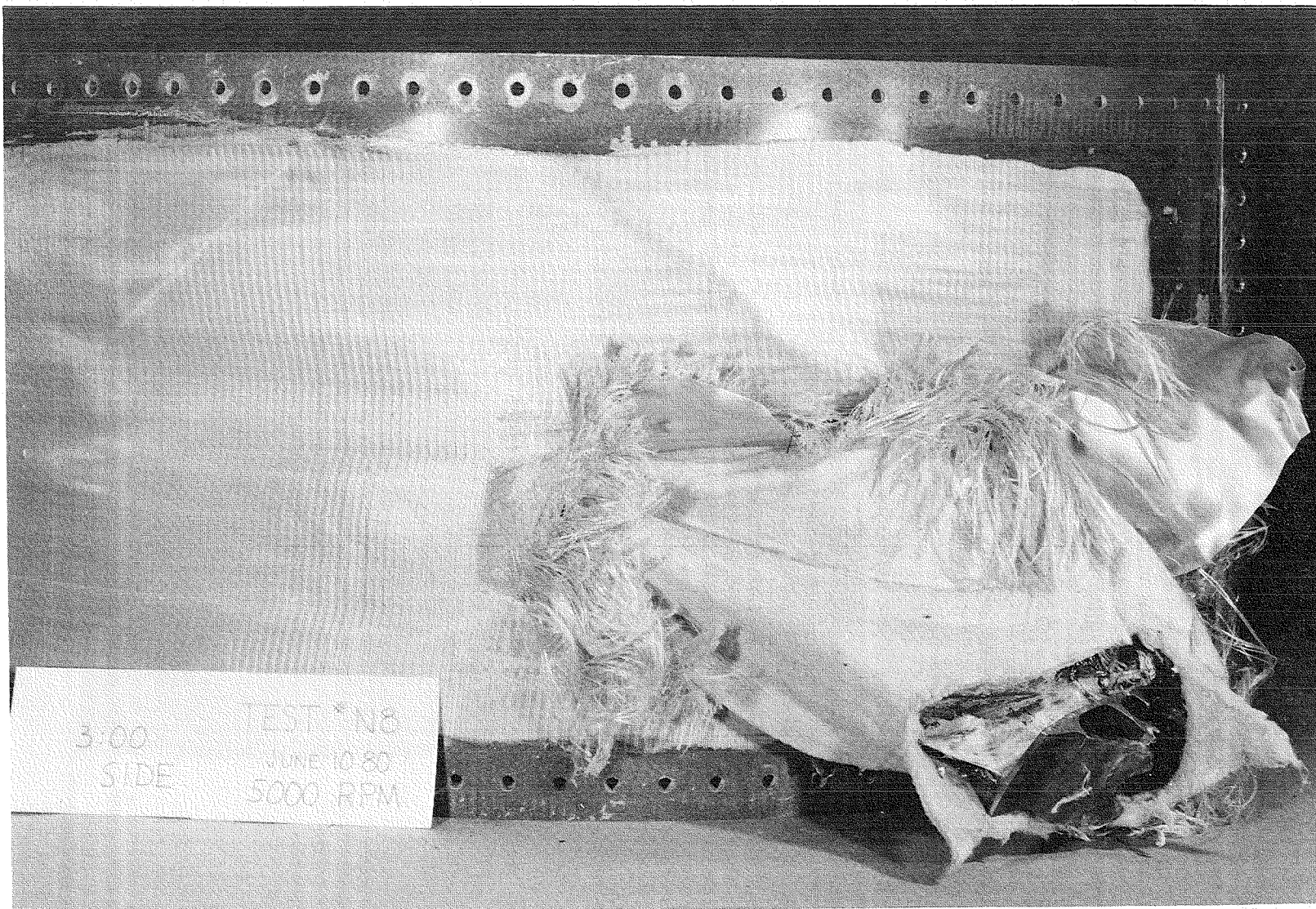


Figure 33. Exterior View - Test 8 - 143-Weave Cloth Plus Felt.

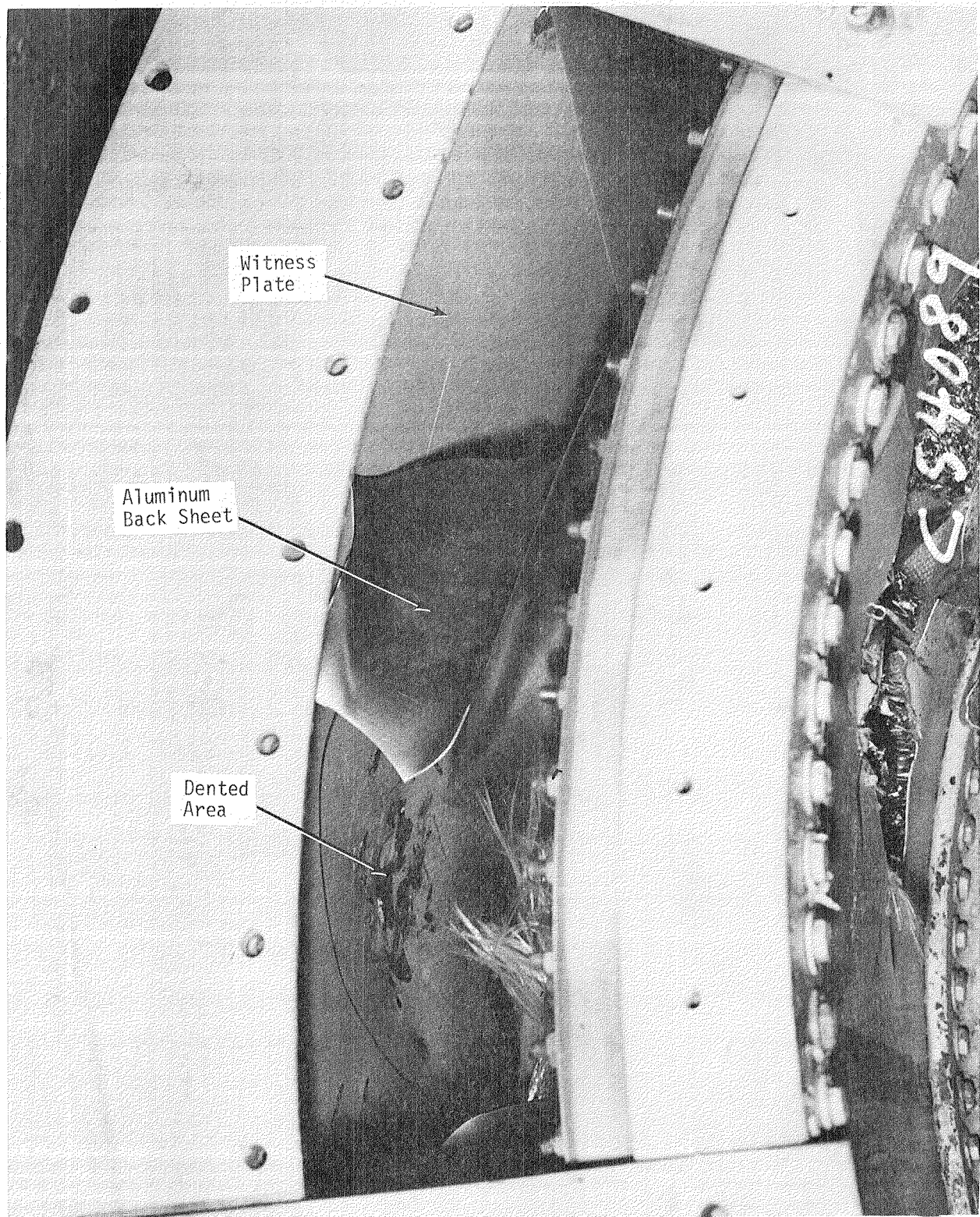


Figure 34. Witness Plate Damage - Test 8.

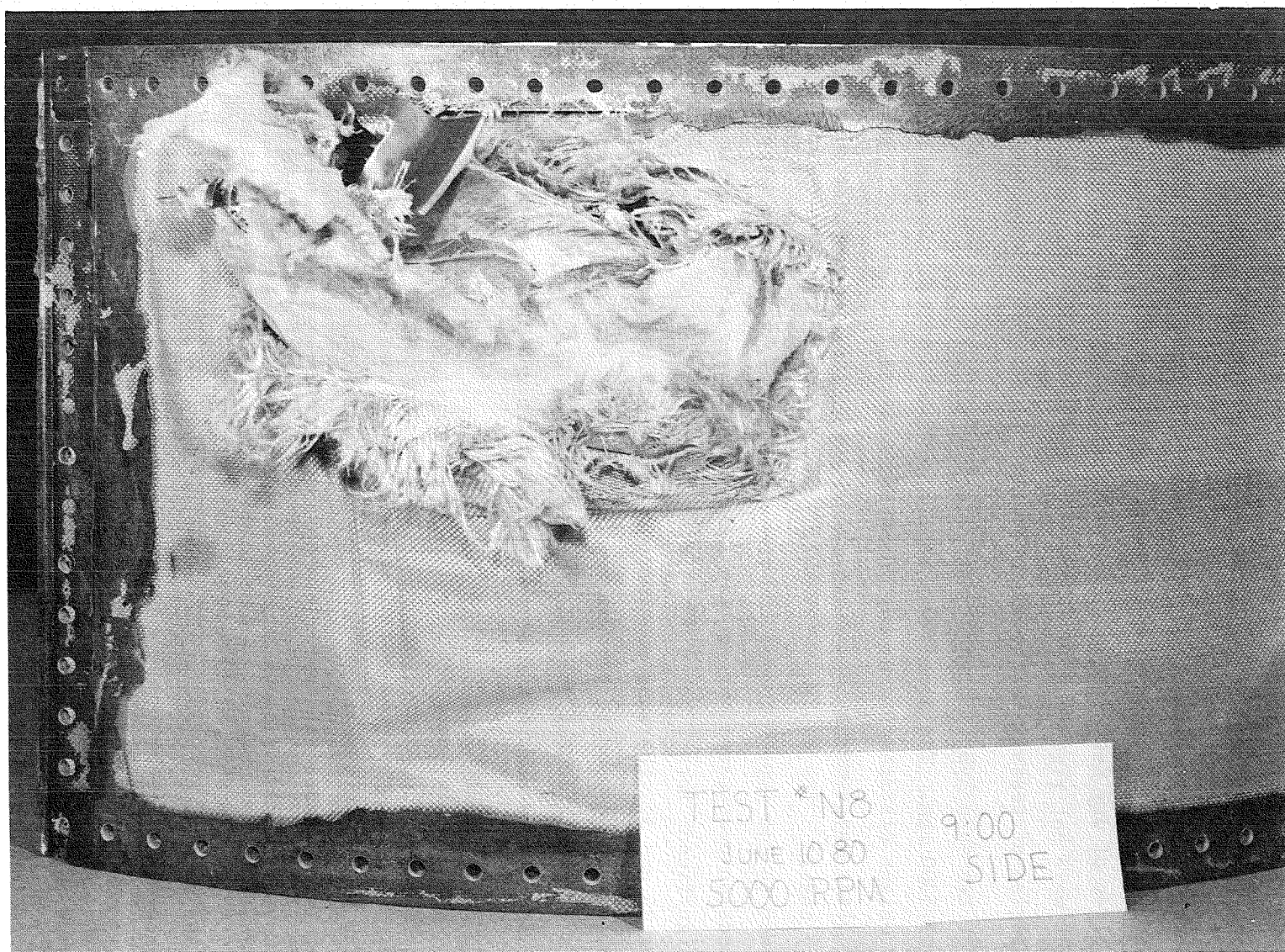


Figure 35. Exterior View - Test 8 - 328-Weave Cloth Plus Felt.

below the platform, the released weight of the superhybrid blade was 0.899 kg (1.982 lb) compared to the released weight of a titanium blade of 1.013 kg (2.234 lb).

Both of the containment systems used in this test were of the same design and constructions as those used in Tests 1 through 4. One of the systems had eight plies of dry Kevlar 328-weave cloth and the other one had six plies. The ends were not rigidized and restrained but were free to move as in the first series of tests.

The two superhybrid blades were released below the platform at a rotor speed of 5300 rpm. The damage was severe to both systems. Due to the different weight distribution of the superhybrid blade, the motion of the released blade was somewhat different than that of the titanium blades previously tested. The superhybrid blade seemed to have a higher axial (aft) component to the impact force. On the side with six plies of Kevlar, the root section penetrated through the Kevlar and impacted the witness plate with significant force, but did not penetrate it. As can be seen in Figures 36 and 37, the root section was completely outside the containment system, and the composite portion of the blade was badly fragmented. Some of this composite debris trapped in the containment system can be seen in Figure 38. It is possible that the root section and attached titanium spar would have escaped the containment system if it had struck the witness plate. The six-ply containment system was therefore considered inadequate to contain a superhybrid blade under the conditions tested.

The superhybrid that impacted the side that had eight plies did not completely penetrate the Kevlar cloth; however, the more aft direction of the blade moved the Kevlar cloth considerably aft as shown in Figure 39. This damage can be compared to that caused by an all-titanium blade released under the same conditions into an identical containment system during Test 4 as shown in Figure 21.

Test 8 was the second test in which the circumferential restraint was broken as shown in Figure 40. This is probably why the root section did not penetrate through the Kevlar cloth; since, with the circumferential restraint

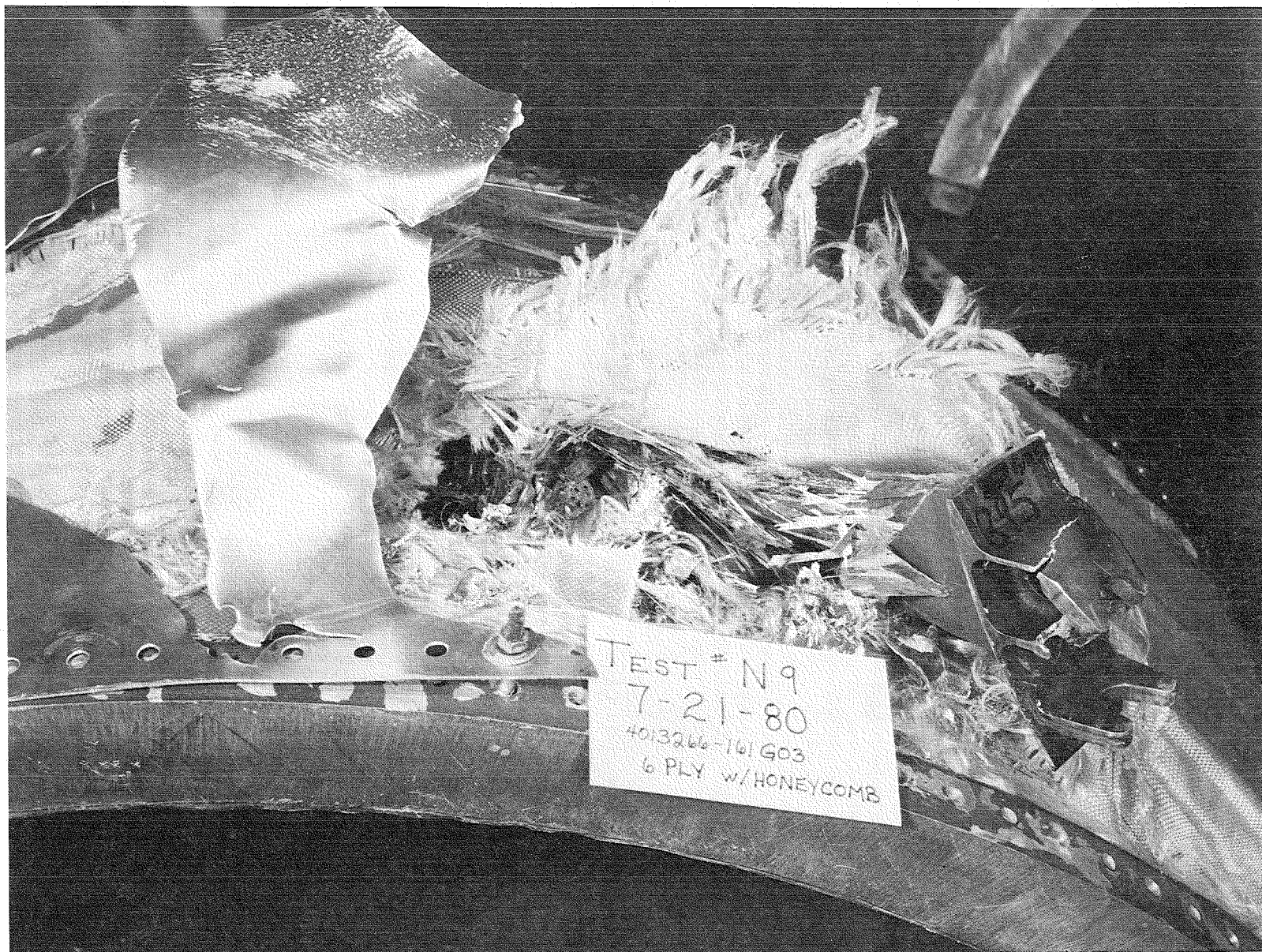


Figure 36. Exterior View - Test 9 - Six-Ply Side.

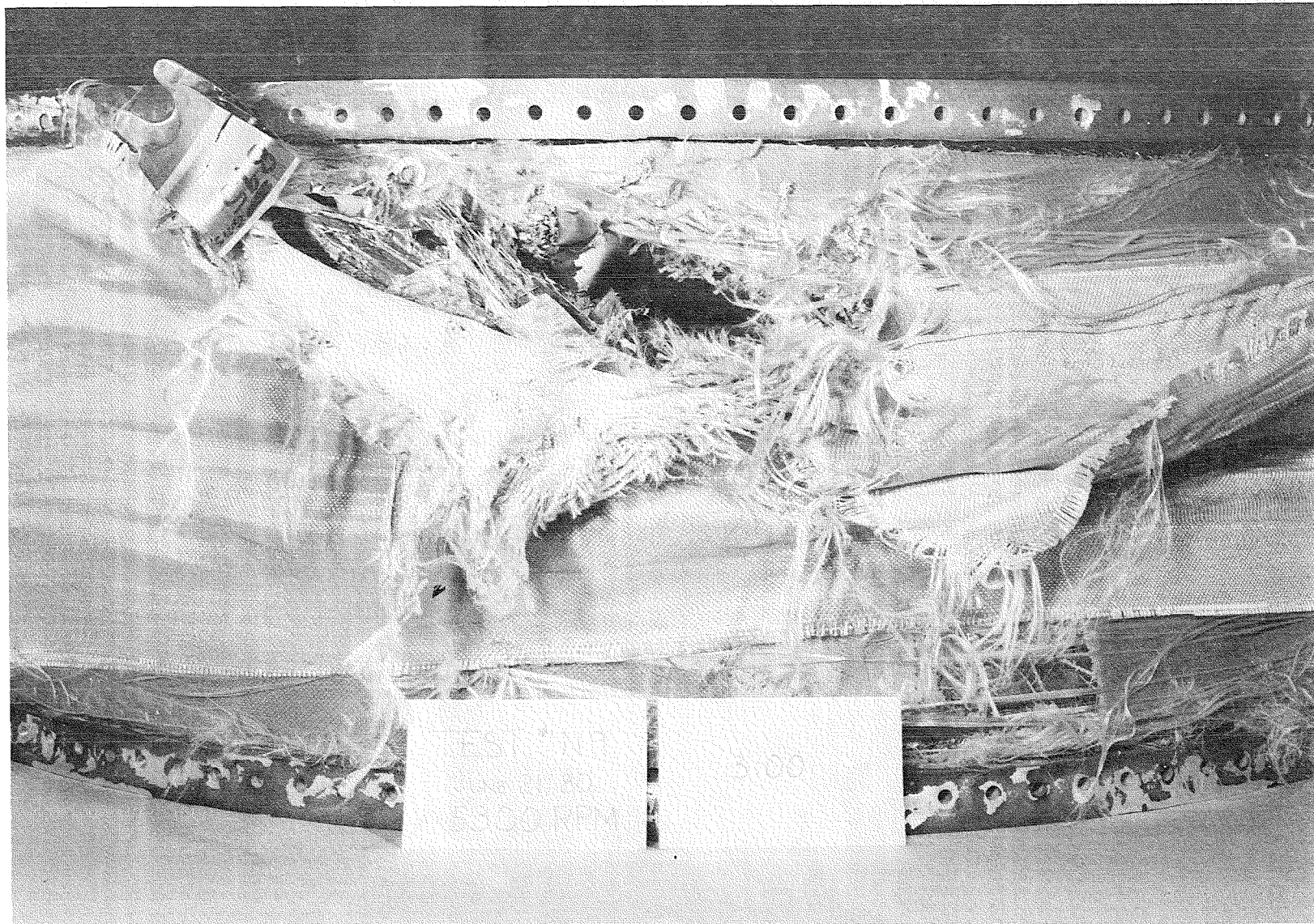


Figure 37. Exterior View - Test 9 - Six-Ply Side - Aluminum Cover Removed.

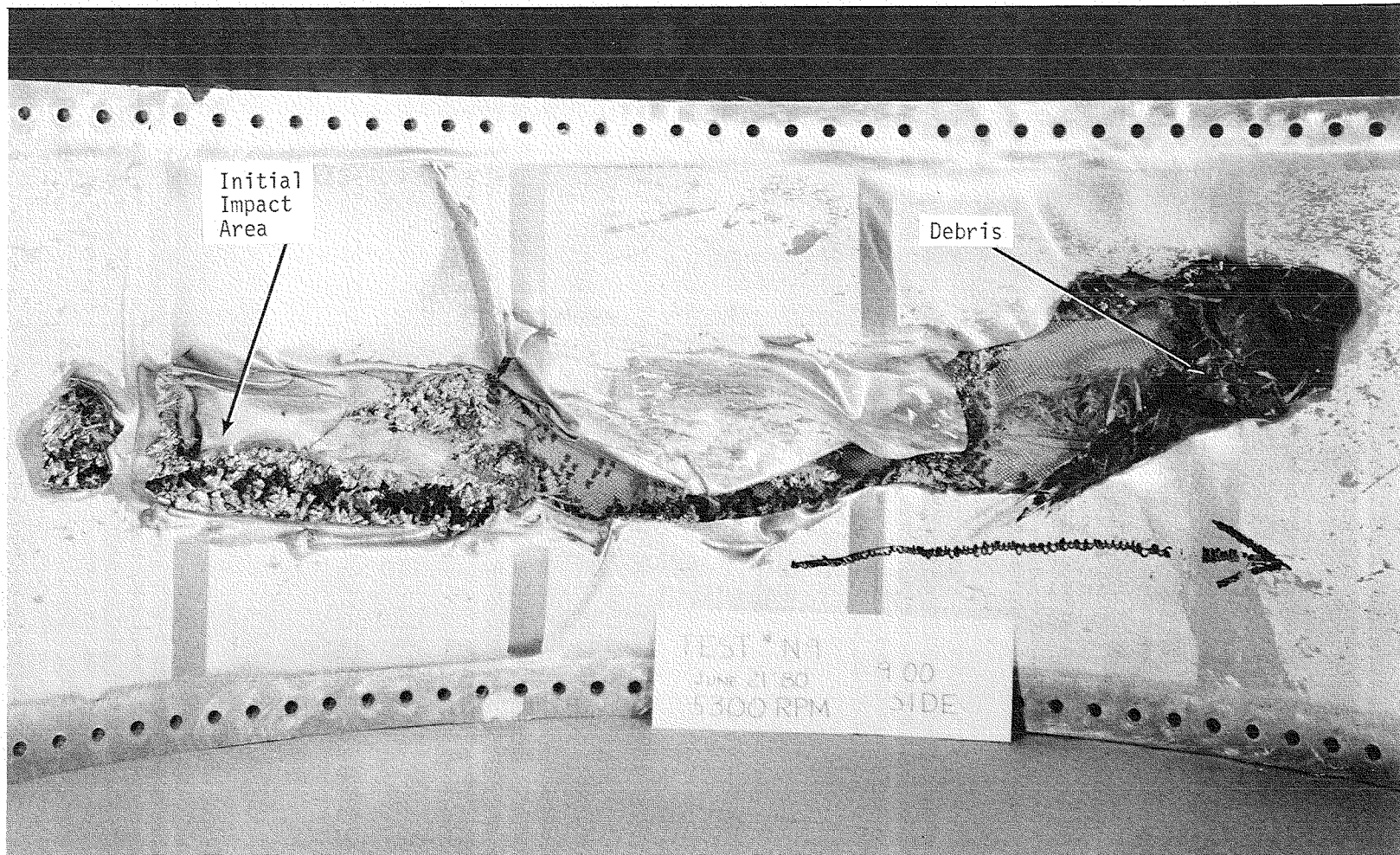


Figure 38. Interior View - Test 9 - Composite Debris.

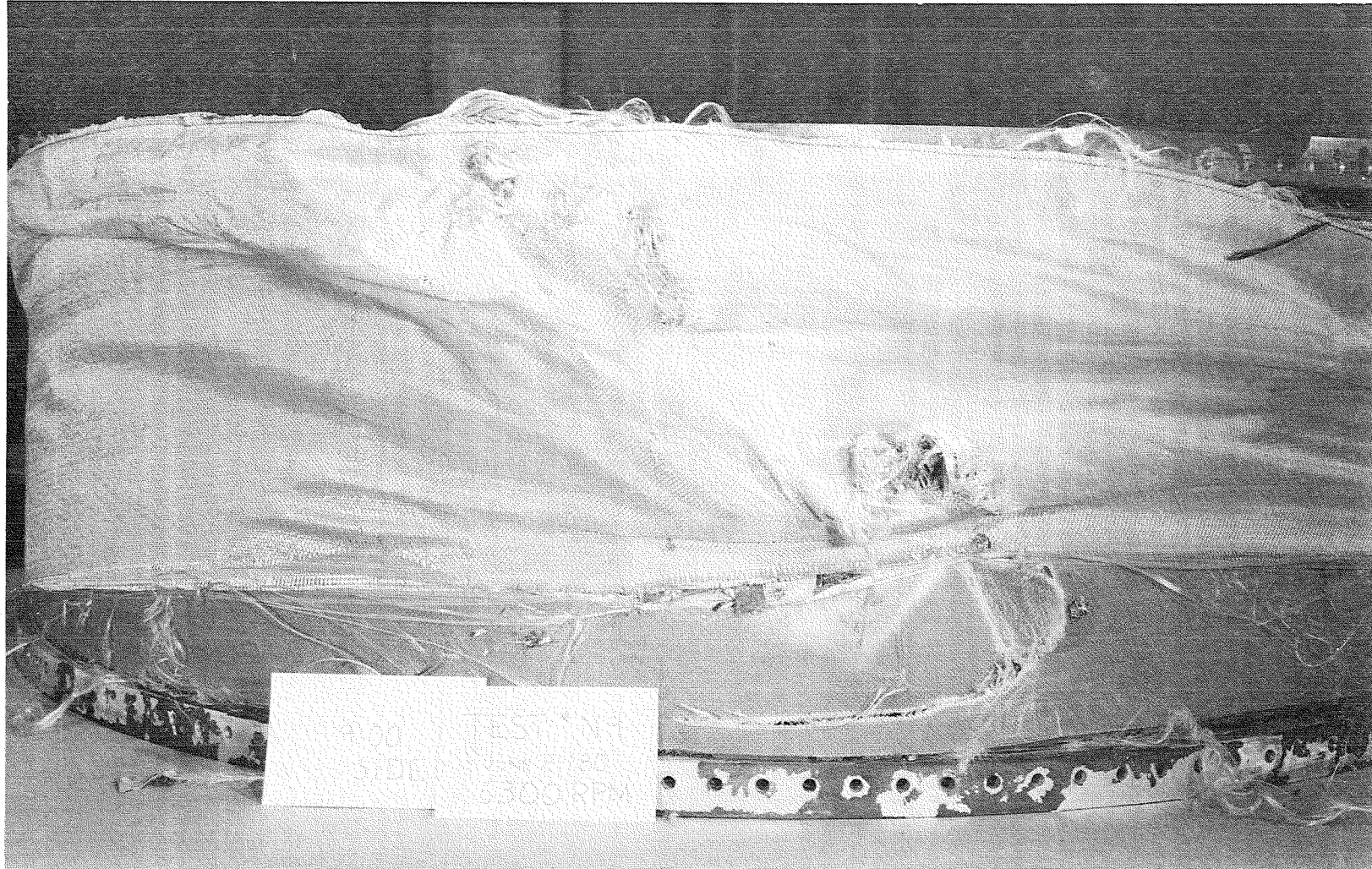


Figure 39. Exterior View - Test 9 - Eight-Ply Side.

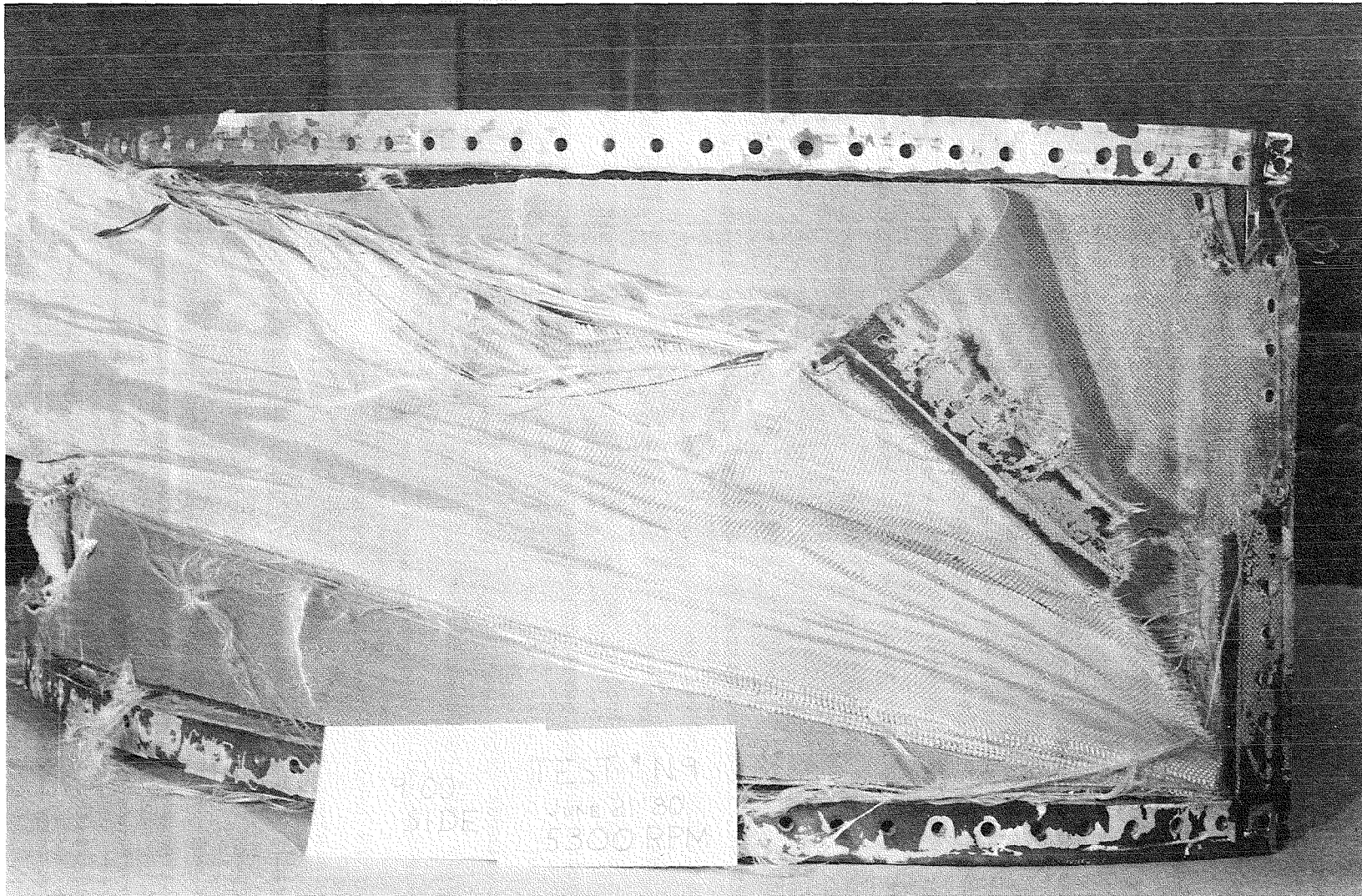


Figure 40. Broken Circumferential Restraint - Test 9.

released, the cloth was free to move radially outward without adding additional strain to the fibers. If this restraint had remained intact, it is expected that the root section would have penetrated the eight plies of Kevlar in a manner similar to that shown in Figure 21.

Based on the results of this test, it appears that, since the root section does most of the damage, there is no significant difference in the amount of containment required for a superhybrid blade versus an all-titanium blade when the blade is released below the platform.

Test 10

The data from the previous nine tests were analyzed to determine what would be an acceptable amount of containment if one was considering the design concept for commercial application. Under these conditions, it was considered unacceptable to have major penetrations of the containment system, even though the blade would not escape. The last two tests of this program were intended to demonstrate the adequacy of the resultant design criteria in as realistic a manner as possible without having actual engine hardware. The two tests involved first, the release of a single TF34 titanium airfoil out of a nearly full rotor, and second, the release of a single TF34 titanium blade, below the platform, out of a nearly full rotor. The containment systems in both tests were made as continuous 360° structures rather than the 180° structures used in previous tests. This feature combined with the use of a nearly full rotor permitted the effect of the impact on casing deformation and potential rotor/casing interaction to be evaluated.

Test 10 involved the release of a single TF34 titanium airfoil into a 360° containment case which had eight plies of Kevlar cloth. These plies were rigidized on the forward and aft ends by applying a room temperature curing epoxy adhesive. The rigidized ends were then bolted to the end rings as was done in Tests 6, 7, and 8 except that the bolt spacing was increased from 2.54 cm (1.0 in.) to 7.62 cm (3.0 in.). The test setup is shown in Figure 41. The airfoil to be released is identified as Blade 1. The holes in the blade base are used to attach the explosive carriers to the blade. As can be seen, two blades were not installed. This was due to the

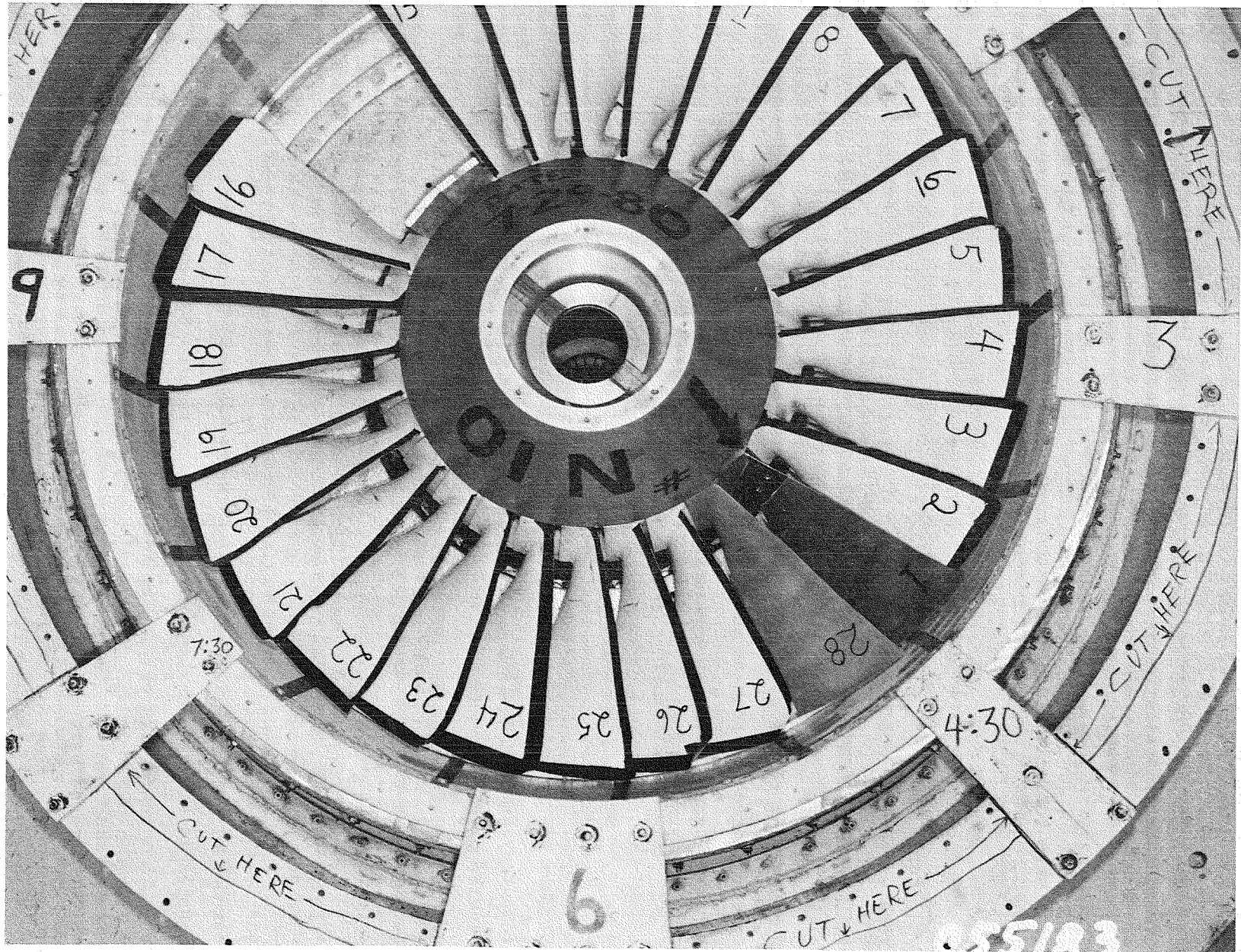


Figure 41. Test Setup - Test 10.

fact that there was no blade removal slot built into the containment case, preventing the installation of the last two blades when the containment case is in position. Due to the method of attaching the containment case to the facility wall, the rotor could not be installed before the casing. Weighted blocks were installed in place of the missing blades to provide a proper balance for the rotor.

The airfoil was released at a rotor speed of 5000 rpm and was contained in a typical manner. It nested into the sandwich structure as shown in Figure 42 and did not penetrate the outer plies of Kevlar cloth (Figure 43). The containment case away from the impact point was not significantly affected and the rotor unbalance due to the airfoil loss was not sufficient to cause the blade tips to rub on the casing. It was considered that this test was a successful demonstration of the lightweight containment concept as it would be applied to a commercial application having the energy absorbing requirement exemplified by the test.

Test 11

This was the last test to be performed under this program. The containment system was similar to that used in Test 10 except that 10 plies of Kevlar were used and the bolt spacing attaching the rigidized ends to the fore and aft rings was increased to 10.16 cm (4.0 in.). The rotor configuration was the same as was used for Test 10 except that the test blade was released below the platform. The release speed was again 5000 rpm. A corner of the blade platform penetrated through the Kevlar cloth as shown in Figure 44. The mechanical attachment of the rigidized edges to the aluminum rings failed locally in the area of the impact. The mode of failure was shear-out of the holes in the rigidized Kevlar as seen in Figure 45. There are holes in both the Kevlar and the aluminum ring on 2.54 cm (1.0 in.) center, but there were only bolts in every fourth hole. This is the first time this type of edge attachment failed during the test program, but it is also the largest bolt spacing that was used. Almost identical test conditions were achieved during Test 6 where the attachment, using bolts in every hole, did not fail. Otherwise, the local damage was similar to that noted during

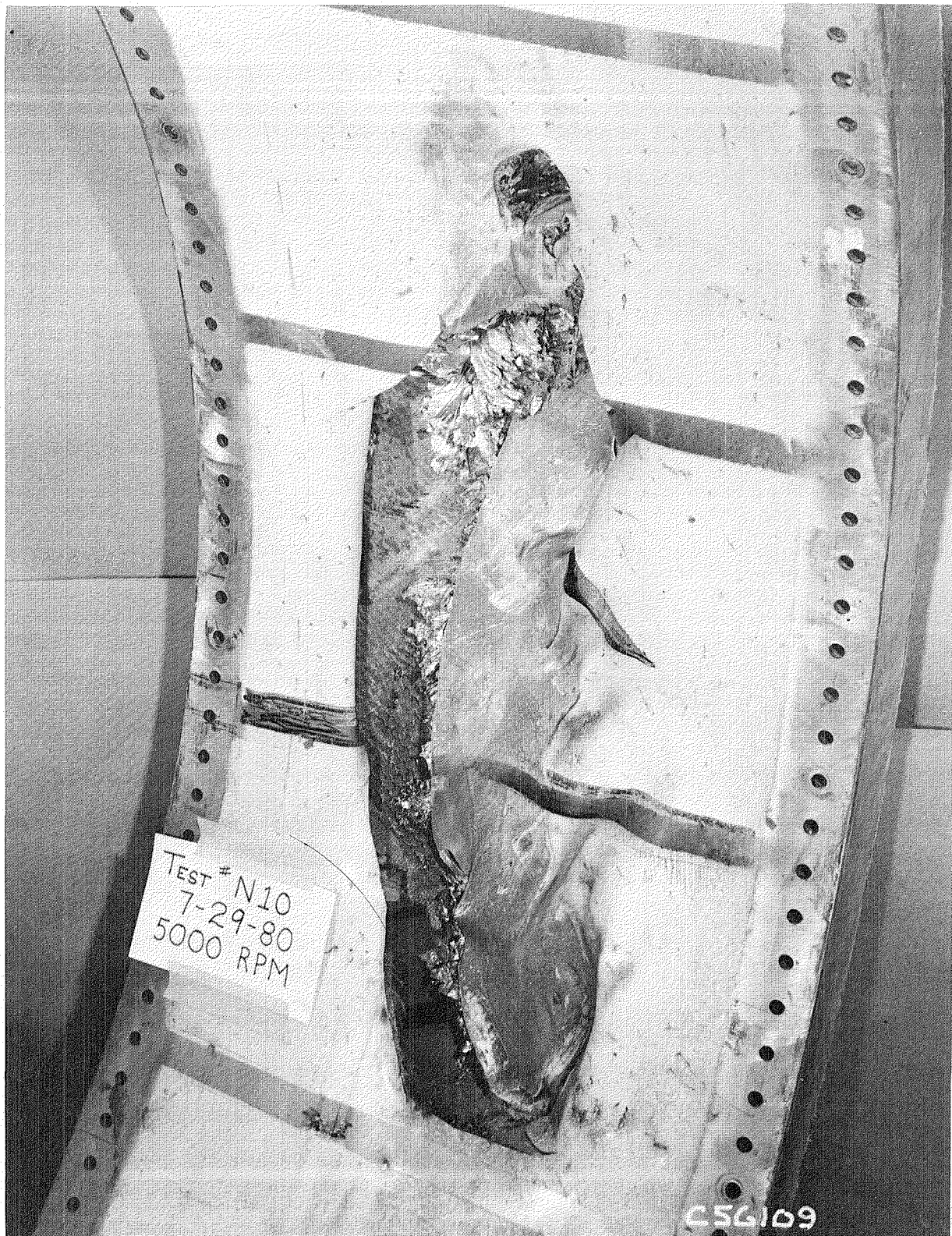


Figure 42. Interior View - Impact Area - Test 10.

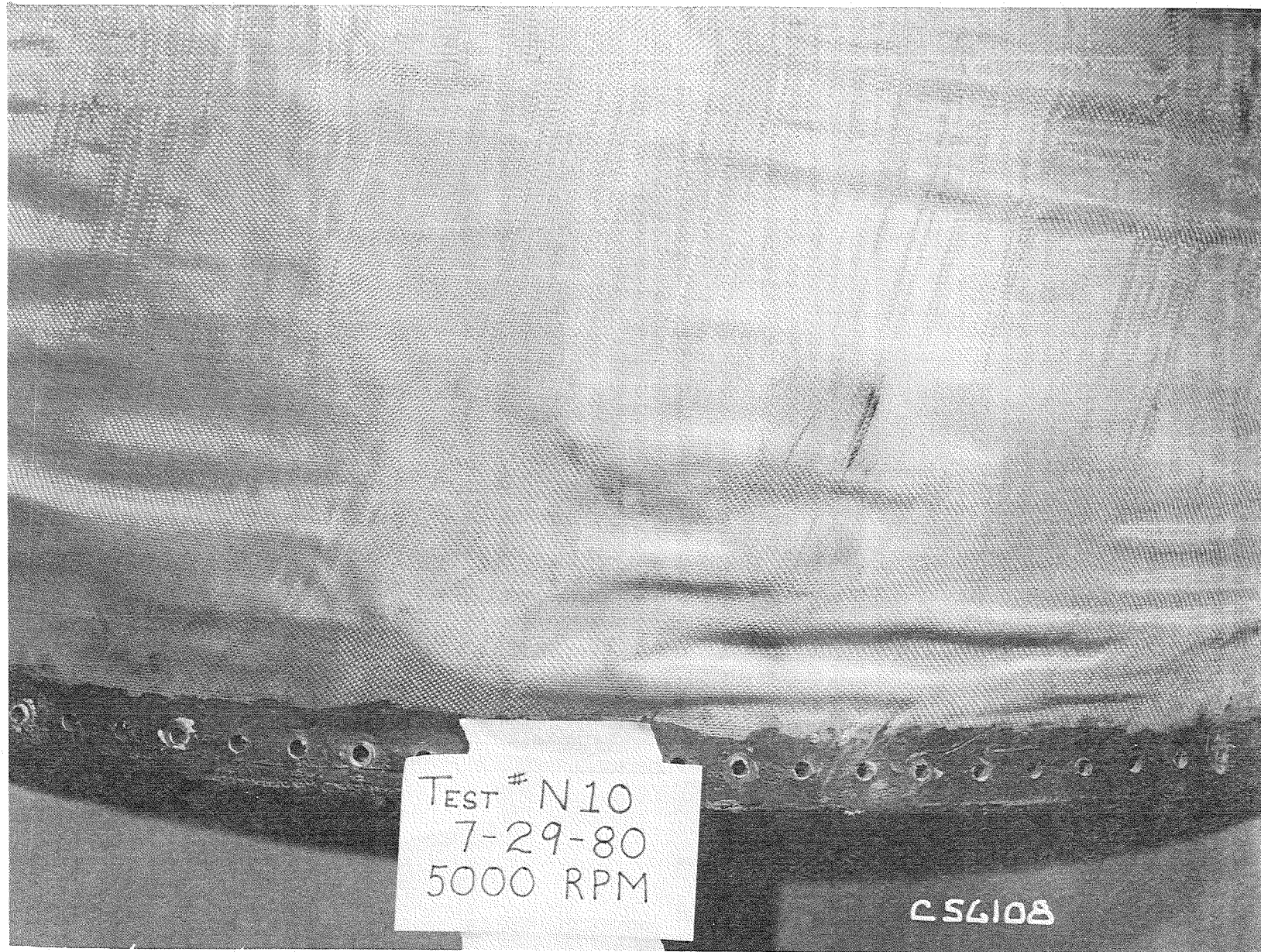


Figure 43. Exterior View - Impact Area - Test 10.

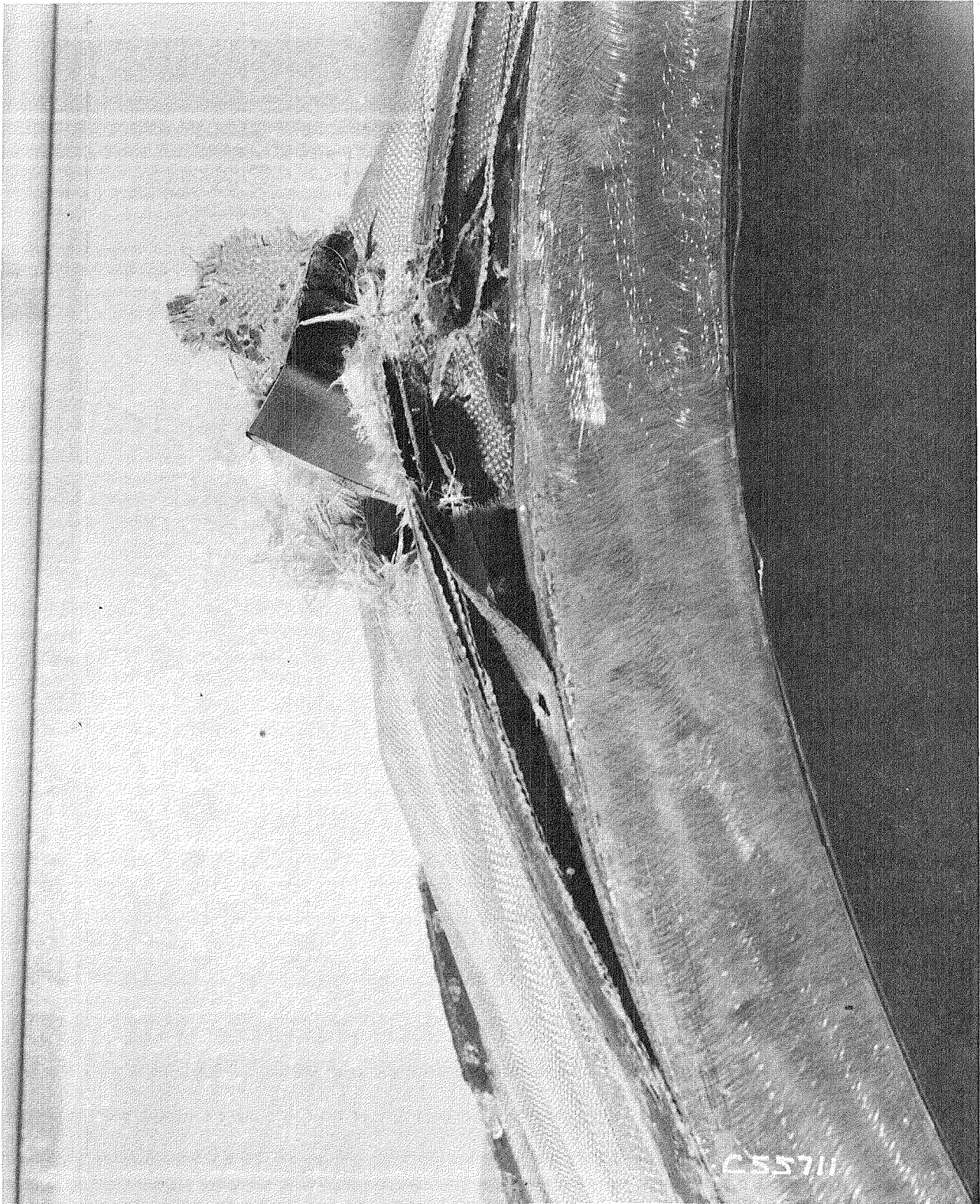


Figure 44. Blade Platform Penetration - Test 11.

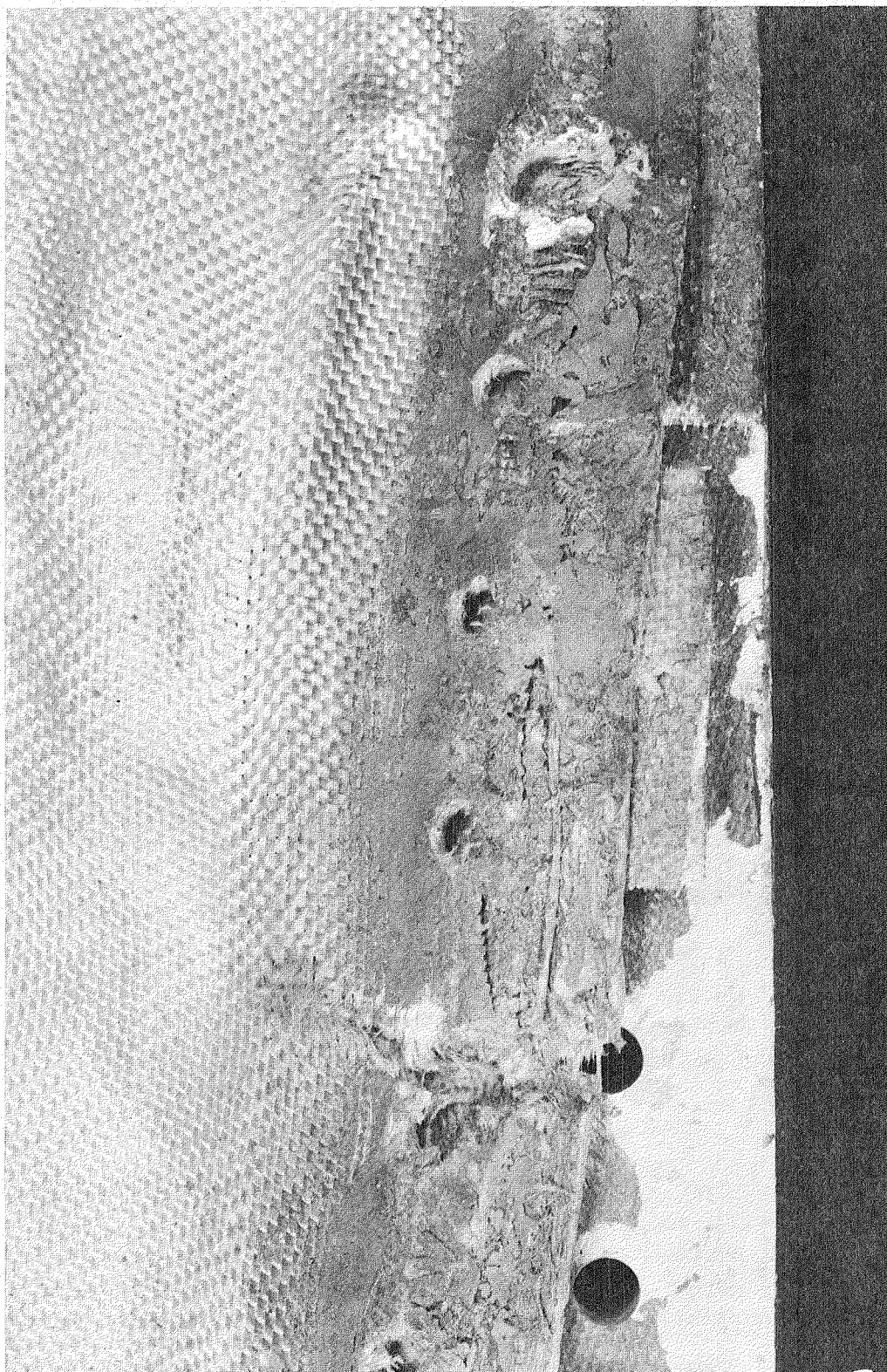


Figure 45. Edge Attachment Failure - Test 11.

Test 6. The damage in the impact area was typical and is shown in Figure 46. The rotor unbalance due to the blade loss was sufficient for the rotor blade tips to rub on the inner surface of the containment case. A typical rub area can be seen between 6 o'clock and 9 o'clock in Figure 47. A closeup of this area is shown in Figure 48. The face sheet was locally grooved, and there were several small circumferential cracks (Figure 48) but nothing which would significantly degrade the structural integrity of the case. In spite of the impact and the tip rubs, the casing remained round.

Although the blade was well contained, a corner of the platform was protruding through the outer Kevlar plies. If the criteria of no penetration in a commercial application is adhered to, two more plies of Kevlar would be required for this design. Otherwise, the test was very successful and the casing stood up well to the conditions imposed by the high rotor unbalance.

3.2 DATA ANALYSIS

In order to make the data generated during this program useful for the design of large turbofan engines, some means must be found to relate the containment parameters to the energy of the impacting object. For the thickness and materials used for the inner (flowpath) facing during their program, their energy absorbing capability was very small compared to the total energies involved. It was decided, therefore, to just relate the thickness of the Kevlar cloth to the kinetic energy of the released object. The velocity at the center of gravity of the object was used to compute this energy. Previous experience with metal containment systems has indicated that the relationship $t = k \sqrt{E}$ where:

t = thickness of containment material

k = an empirical constant

E = kinetic energy

provides a reasonable estimation of the amount of containment material required. This method was therefore used to evaluate the data generated during this program.

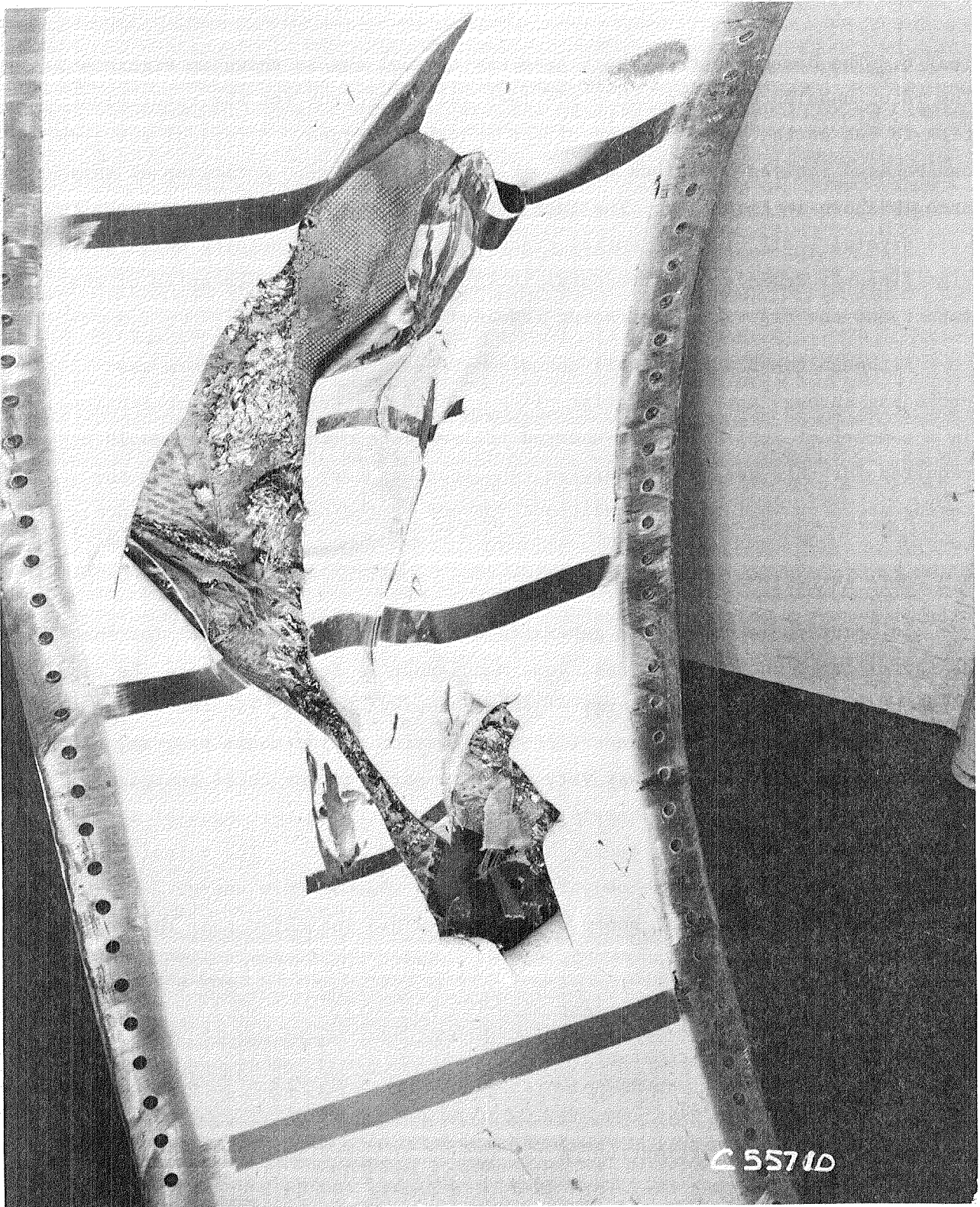


Figure 46. Impact Area - Test 11.

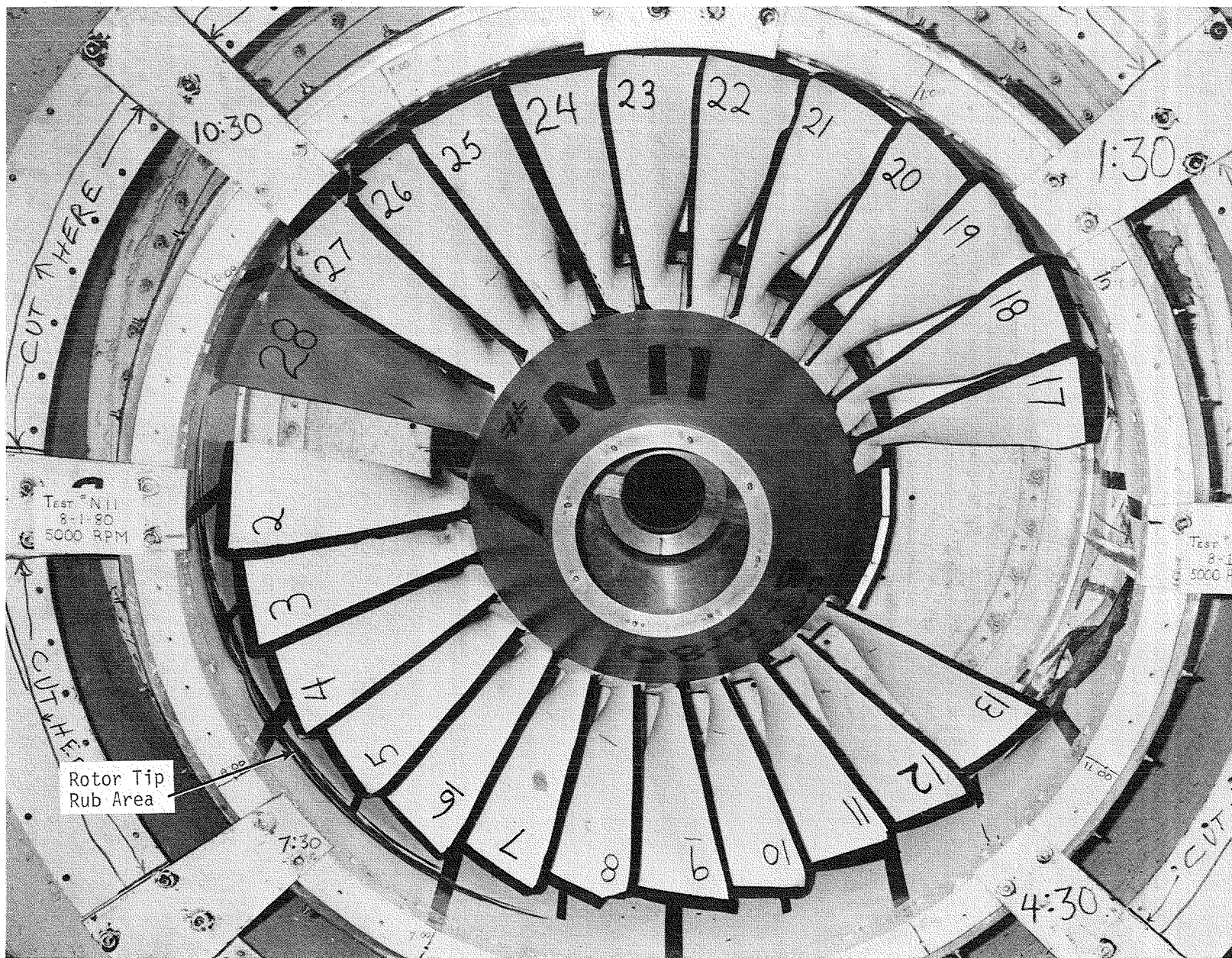


Figure 47. Test 11 - Overall View.

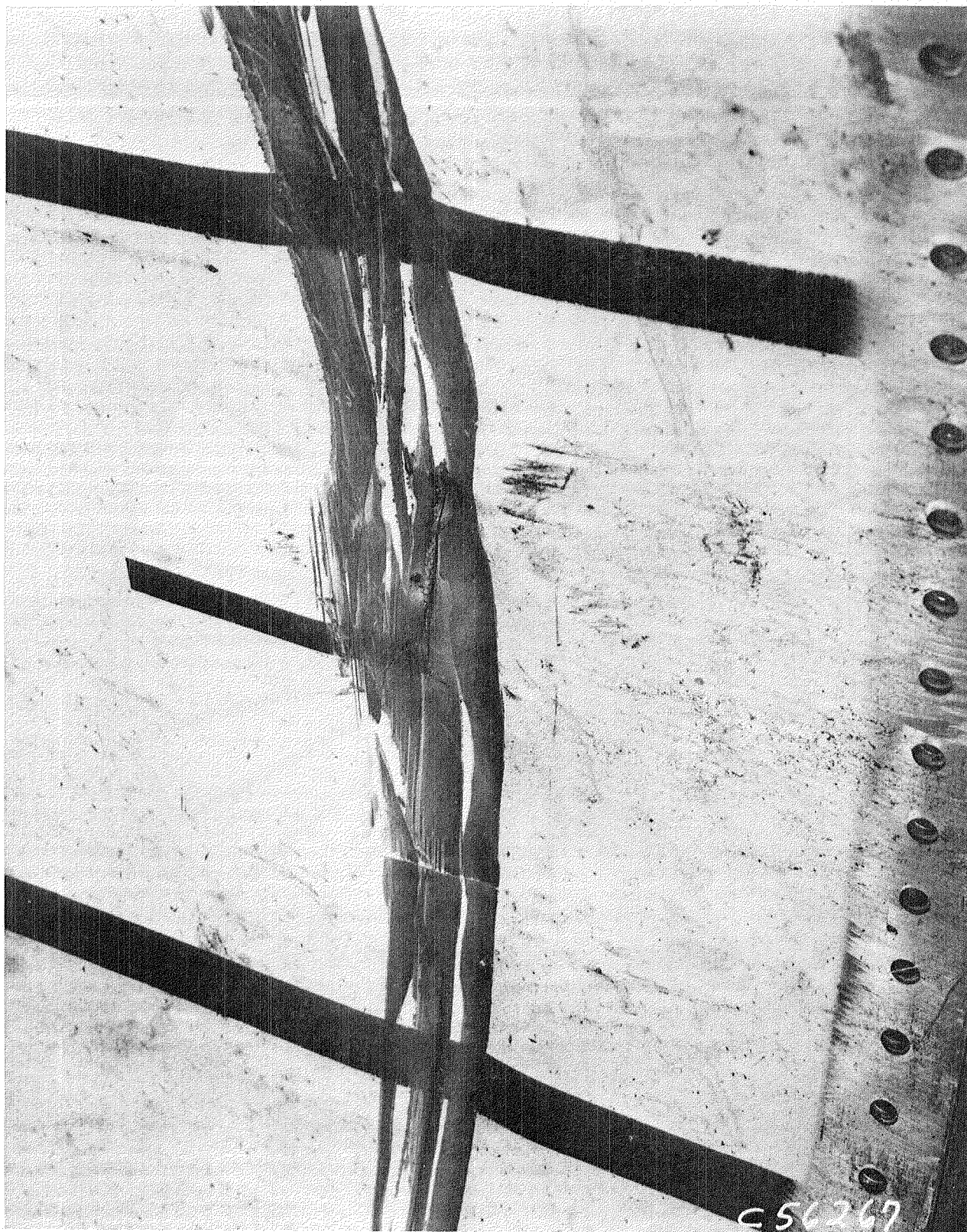


Figure 48. Closeup of Rub Area - Test 11.

A number of minor variations of the basic lightweight containment concept were evaluated during this program. The only one which seemed to have any major effect on the containment process was the one which provided fore and aft edge restraint to the Kevlar cloth. For this reason, the data generated on specimens which incorporated the restraint were plotted separately. The data showing the test results for those containment systems having the forward and aft edges of the Kevlar unsupported are shown in Figure 49 while that for the systems with supported edges are shown in Figure 50.

Since safe commercial design will require that the containment systems provide more than just threshold containment capability, the design curves based on the relationship $t = k \sqrt{E}$ and shown in Figures 49 and 50 were drawn to the left of the data points representing noncontainment and threshold containment. The point represented by the half-filled-in square in Figure 50 thus introduces some conservatism in the design. The number of bolts used to help restrain the edges of the Kevlar in this test was only one-fourth the number used in the fully contained test represented by the open circle. Based on a comparison of the two tests, it was felt that if a greater number of bolts has been used for this test full containment would also have been obtained and the design curve could have been drawn to the right of the open circle. Since this conclusion was not actually demonstrated by test, the design curve was assumed somewhat to the left of this point. The K-factors shown for the design curves are applicable only when using the International System of Units (centimeters and joules). If English Units (inches and foot-pounds) are used, the K-factors are 0.00141 for the edges free and 0.00125 for the edges fixed.

For any reasonable length containment system, the weight added by rigidizing the ends and bolting them down results in a heavier containment system than if the edges are left free. The weight added by the epoxy used to rigidize the ends, along with the weight of the bolts, is greater than the weight that can be saved by the reduction in the amount of Kevlar required. The concept with the rigid ends, however, does provide much better protection against subsequent impacts, and the designer should carefully consider this aspect, with respect to his particular application, when choosing which approach to employ.

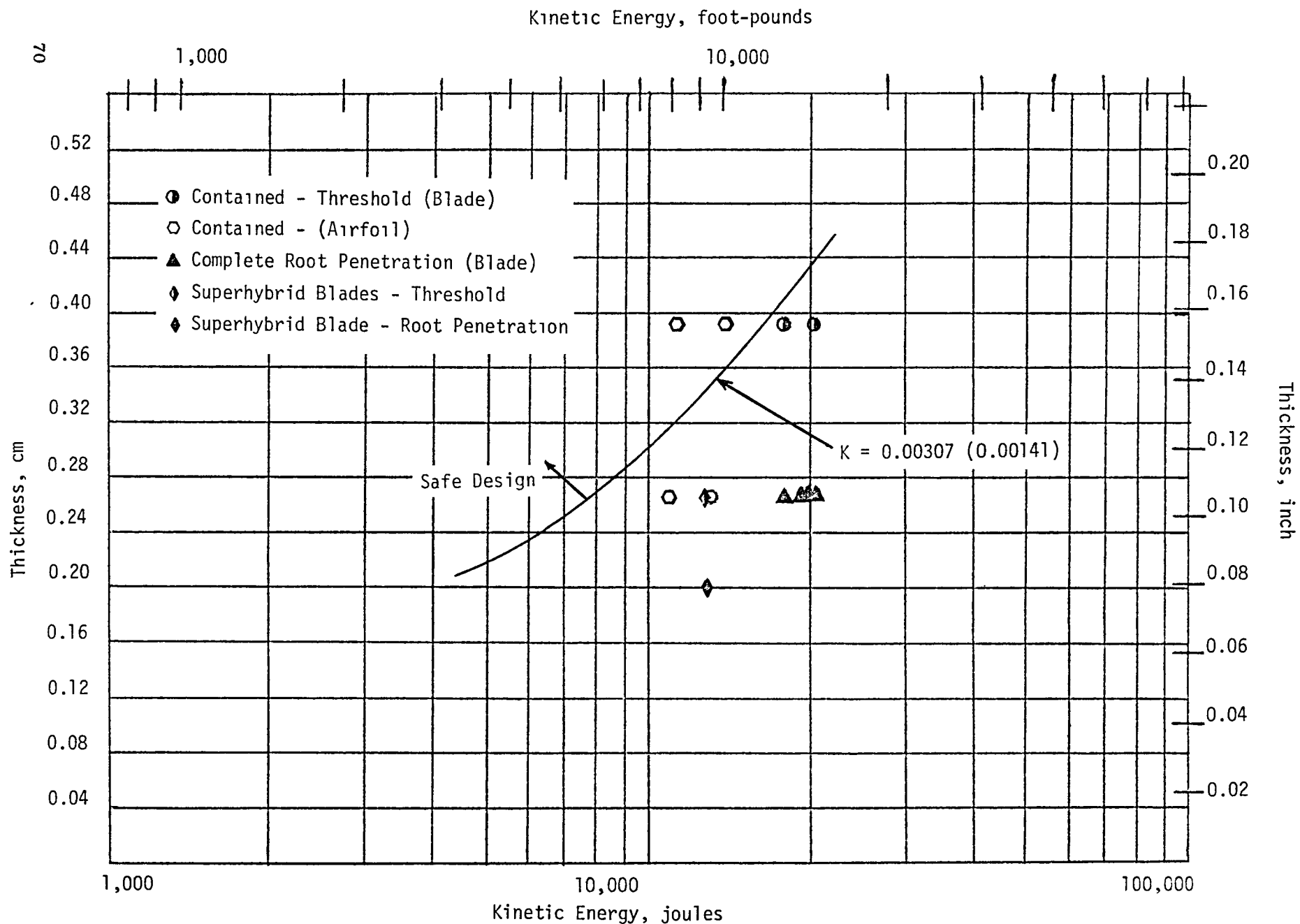


Figure 49. Test Data - Free Edges.

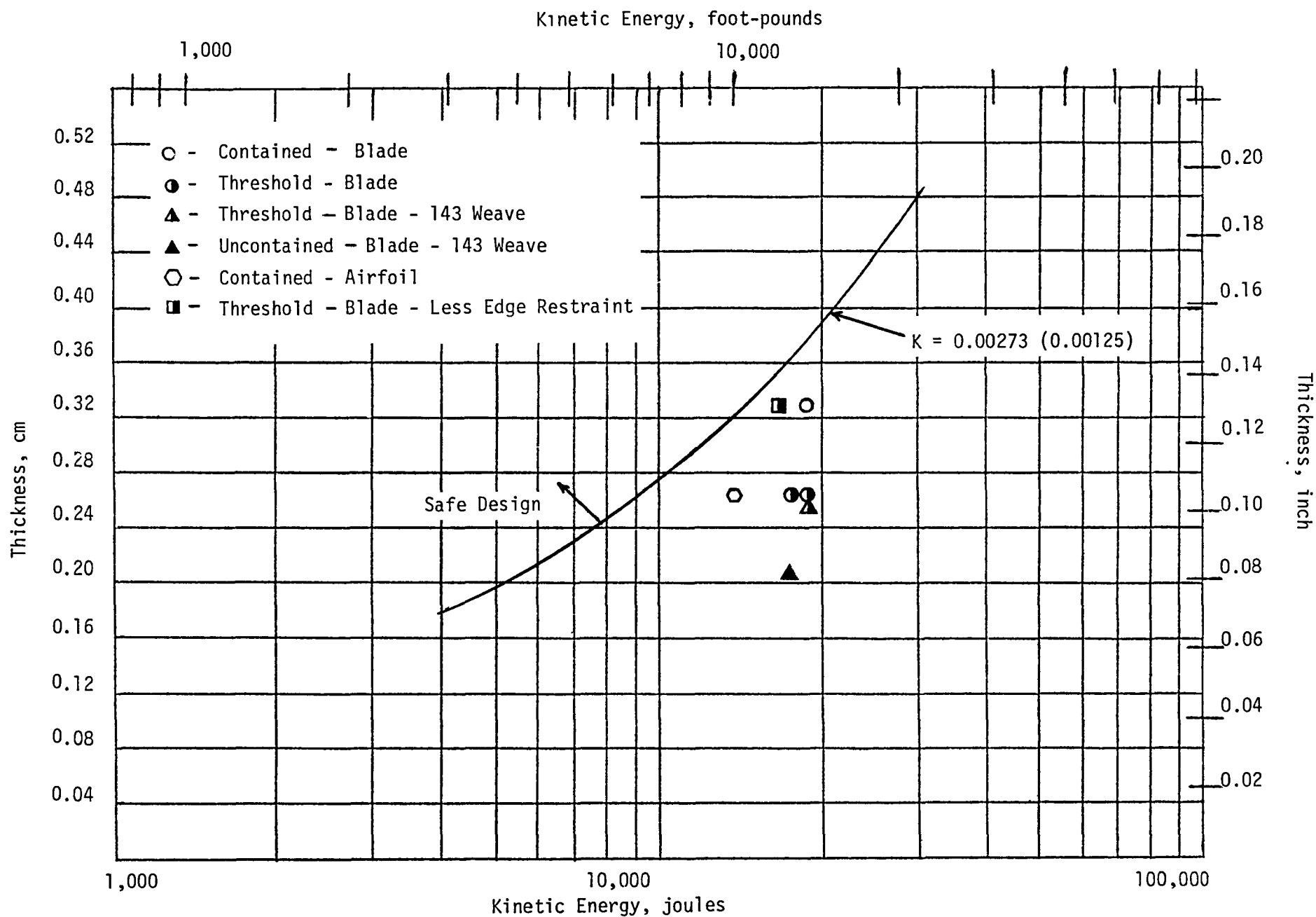


Figure 50. Test Data - Restrained Edges.

3.3 FULL SCALE CONTAINMENT SYSTEM DESIGN

The containment concept developed during this program was demonstrated using TF34 size hardware and involved maximum energy levels in the 20,000 J (14,750 ft-lb) range. The information thus generated was then extrapolated to develop lightweight containment designs for larger turbofan engines which have much bigger and heavier blades and thus involve much higher energy levels. The CF6 engine size and general operating parameters were used as the basis for designing these large scale, lightweight containment systems.

Since it is unlikely that new containment concepts would be used to retrofit existing engines, it is new engine design that must be considered. It is possible that these new designs may incorporate materials other than titanium in their fan blade design; therefore, several lightweight containment designs were generated to account for this possibility. Three potential blade constructions were considered. These were a typical titanium fan blade, a superhybrid concept similar to that tested under this program, and a boron/aluminum blade.

For all of these blades, it was decided, in the interest of safety, to employ the concept of rigidizing the ends of the dry Kevlar cloth with epoxy adhesive. Since the thicknesses of Kevlar required for these designs is much greater than that tested during this program, it is possible that, due to the greatly increased section properties of the rigidized ends, it will not be necessary to bolt these ends of the end rings. Therefore, in the weight calculations for the lightweight design, the epoxy rigidizing agent was included but not any bolting hardware.

The baseline state-of-the-art containment design, against which the lightweight designs are evaluated, is shown in Figure 51. This design is a ribbed steel ring weighing 200 kg (486 lb) and was designed to contain a titanium blade which had a kinetic energy at blade release of 211,500 J (156,000 ft-lb) at the blade center of gravity.

A lightweight containment system designed to provide adequate protection from an all-titanium blade released under the same conditions and producing

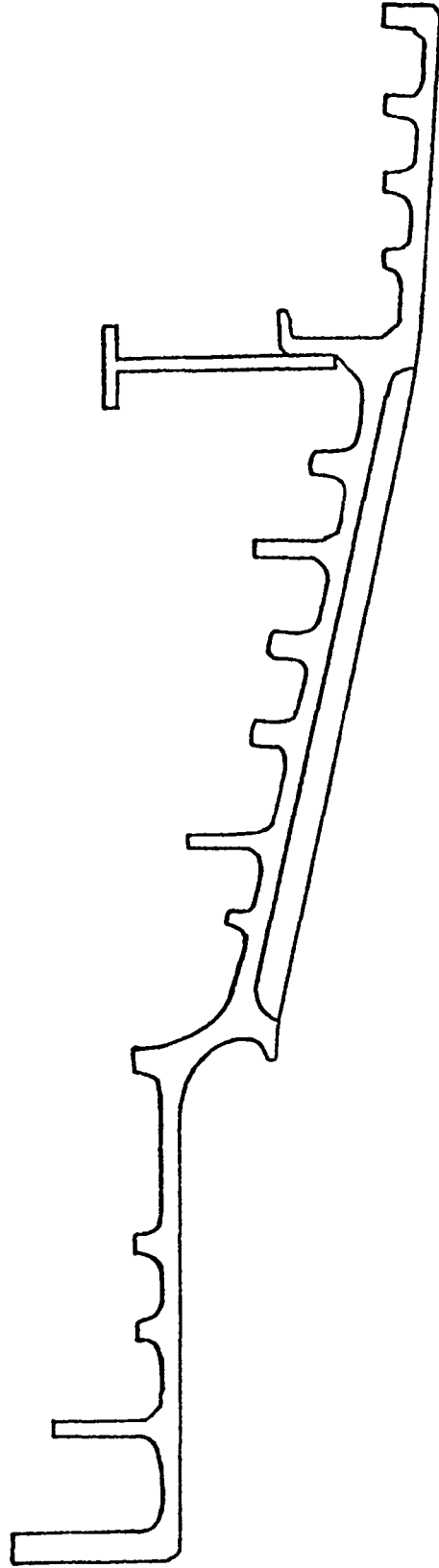


Figure 51. Baseline Containment Design.

the same energy as stated above is shown in Figure 52. This design is based on the curve shown in Figure 50 which gives the relationship between Kevlar thickness and kinetic energy of $t = 0.00273 \sqrt{E}$ where t is in centimeters and E is in joules. This results in a Kevlar thickness of 1.256 cm (0.50 in.). The thicknesses of the steel and the graphite/epoxy used to form the basic structural sandwich were chosen, along with the honeycomb depth, to provide the same casing stiffness as the all-steel baseline case. The resulting design, shown in Figure 52, weighs 171.5 kg (378 lb). This total weight is made up of the following items:

	<u>kg (lb)</u>
• Steel Inner Shell and Flanges	87.3 (192.5)
• Graphite/Epoxy Shell	9.8 (21.5)
• Honeycomb Core	8.2 (18.0)
• Glass Epoxy Liner	0.9 (2.0)
• Kevlar/Epoxy Cover	3.5 (7.8)
• Adhesive	5.4 (12.0)
• Tip Rub Material	7.2 (15.9)
• Kevlar Containment	35.7 (78.6)
• Miscellaneous	2.3 (5.0)
• 7% Weight Margin	11.2 (24.7)

From this breakdown, it can be seen that the actual containment material, Kevlar, is only a small part (20%) of the overall containment system weight. The remainder of the weight is primarily devoted to providing the structural strength and stiffness required to support an inlet and prevent rotor/case interaction. In spite of this, the lightweight containment concept shown in Figure 52 provides a 50 kg (108 lb) weight savings over the baseline containment system (Figure 51) for the same type of fan blade released under the same conditions.

Since the lightweight containment system would be primarily used in new engines design, the type of fan blade that might be used in these engines, other than the typical titanium blade, must be considered. Two of the leading candidates to replace the titanium blades are boron/aluminum blades and super-hybrid blades. It is not anticipated that the basic lightweight containment

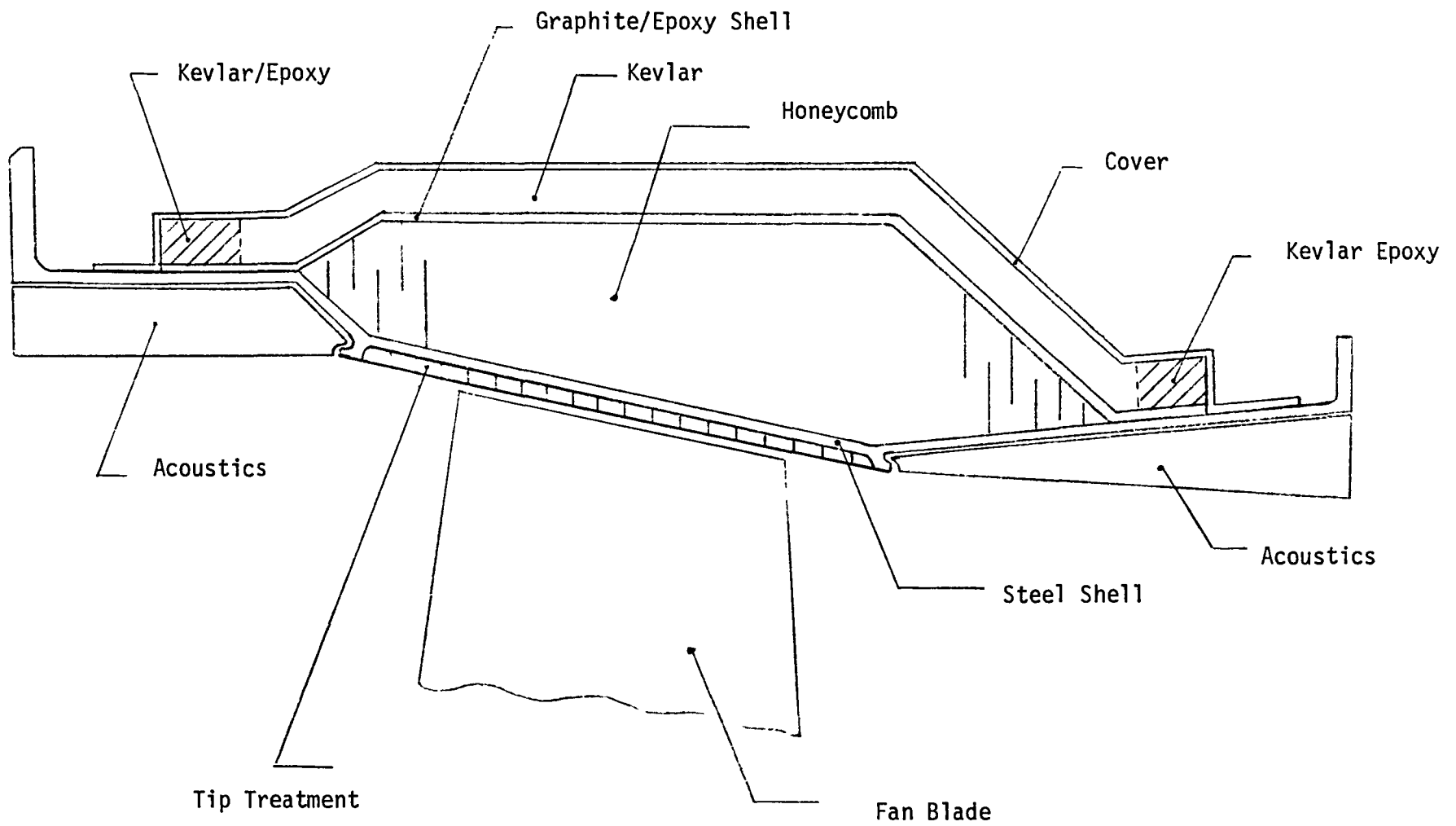


Figure 52. Lightweight Containment Design.

concept would change if these type blades were used, although the amount of Kevlar may vary depending on the impact energy.

A typical superhybrid blade that might be considered as a replacement for the titanium blade used in the state-of-the-art blade containment design is shown in Figure 53. This blade was designed under NASA Contract NAS3-20402 and is discussed in detail in Reference (2). The blade is 0.77 kg (1.7 lb) lighter than the titanium blade it replaces; and, due to the lighter airfoil portion of the blade, it has a somewhat lower center of gravity. Thus, if this blade were released under the same conditions as the baseline titanium blade, it would have a lower kinetic energy than the titanium blade. Under these conditions, the superhybrid blade would have a kinetic energy at blade release of 132,900 J (98,000 ft-lb) of Kevlar would be required to contain the superhybrid blade. Even though the composite portion of the superhybrid blade does break up on impact and some energy must be absorbed by this action, the testing done during this program did not indicate that this had any significant effect on the containment process or on the amount of material required to contain the blade. The primary reduction in containment weight that can be obtained through the use of superhybrid blades rather than titanium blades is therefore in the reduction in thickness of Kevlar required due to the lower blade energy that must be contained. The weight of a lightweight containment system made to contain a superhybrid blade designed for, and released under, the same conditions as the titanium blade previously discussed would result in a 7.7 kg (17 lb) weight savings over that required for the titanium blade.

A typical boron/aluminum blade, intended to perform the equivalent function as the baseline titanium blade, was designed under NASA Contract NAS3-21041 (Reference 3). This blade was completely redesigned based on the specific characteristics of the boron/aluminum material. This redesign resulted in a change in the number of blades in the rotor, removal of the midspan shrouds, and other minor configuration changes. Since the number of blades is reduced, the individual blade weight is slightly higher (2%) than the titanium blade and the blade center of gravity is slightly lower due to the removal of

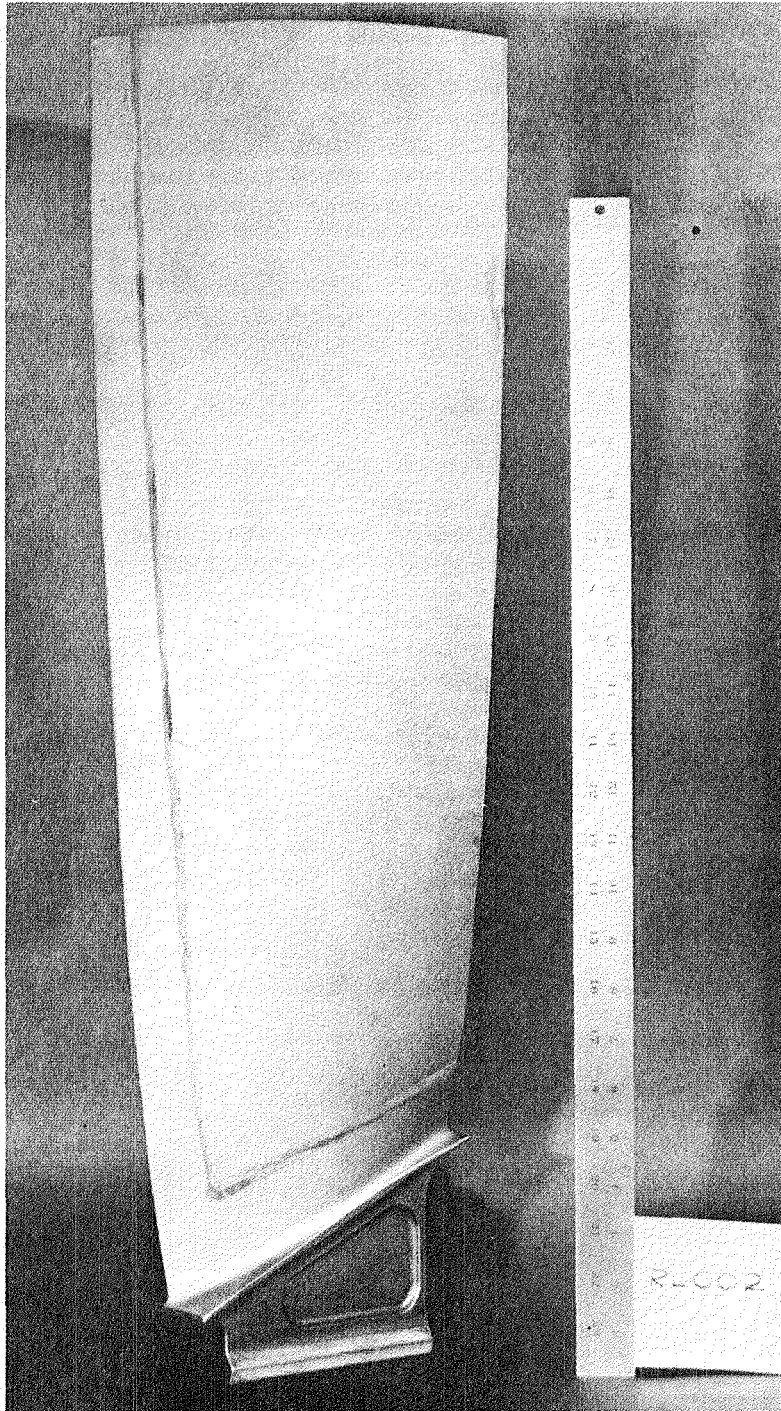


Figure 53. Superhybrid - CF6 TiCom Prototype Blade.

the midspan shrouds. The net result is that the kinetic energy to be contained is virtually the same as for the titanium blade. Since the breakup characteristics of large boron/aluminum blades are not known at this time, it is assumed that they will not affect the amount of containment required. Since the energies are equivalent between the titanium blade and the boron/aluminum blade, the containment weight would also be the same and the design shown in Figure 52 could be used for either type blade.

4.0 CONCLUSIONS

A summary of the conclusions drawn from the work done under this program is presented below:

1. The basic concept of a lightweight sandwich casing wrapped with dry Kevlar cloth was shown to be a viable fan blade containment system that can provide 20% to 25% weight savings over state-of-the-art steel designs.
2. The containment process is relatively insensitive (over the range of materials and thicknesses tested) to the type of material used for the flowpath surface. This material configuration will depend on design considerations other than pure containment such as strength, stiffness, rub resistance, etc.
3. A much better containment process was obtained when the forward and aft edges of the dry Kevlar cloth were restrained from significant axial movement.
4. The bidirectional weave (328 type) proved to be better than the unidirectional weave (143 type) from a containment standpoint. The unidirectional weave was subject to considerably more splitting apart due to a lack of transverse fibers. This splitting allowed the blade easier passage through the Kevlar. Since these were the only two weaves tested, there may be some intermediate weave that may be better but any improvement would probably be marginal and have little effect on the total system weight.
5. The Kevlar felt, in the densities and thicknesses used in the program, had little effect on the containment process.
6. Although threshold containment was defined and demonstrated during the program, it was felt that a design based on this parameter was not sufficiently conservative for commercial design. Based on the test results obtained during the program, a more realistic design parameter relating Kevlar thickness to energy level was defined.

5.0 REFERENCES

1. Stotler, C.L. and Coppa, A.P., "Containment of Composite Fan Blades-Final Report," NASA CR-159544, July 1979.
2. Salemm, C.T. and Murphy, G.C., "Metal Spar/Superhybrid Shell Composite Fan Blades," NASA CR-159594, August 1979.
3. Salemm, C.T. and Yokel, S.A., "Design of Impact-Resistant Boron/Aluminum Large Fan Blades," NASA CR-135417, July 1978.

CONTRACT NAS 3-21823

	Mail Stop	Copies
NASA-Lewis Research Center 21000 Brookpark Road Cleveland, OH 44135		
Attn: Contracting Officer	501-11	1
Technical Report Control	5-5	1
Technology Utilization Office	3-19	1
AFSC Liaison Office	501-3	1
SamT Div.Contract File	49-6	1
Library	60-3	1
R. H. Johns	49-6	1
G. T. Smith	49-6	10
C. C. Chamis	49-6	1
J. P. Barranger	77-1	1
C. L. Walker	302-2	1
National Aeronautics & Space Administration Washington DC 20546		
Attn: NHS-22/Library		2
RTM-6/L. A. Harris		2
RTM-6/W. Brainard		1
NASA-Ames Research Center Moffett Field, CA 94035		
Attn: Library	202-3	1
NASA-Goddard Space Flight Center Greenbelt, MD 20771		
Attn: 252/Library		1
NASA-John F. Kennedy Space Center Kennedy Space Center, FL 32931		
Attn: Library	AD-CSO-1	1
NASA-Langley Research Center Hampton, VA 23365		
Attn: Library	185	2
NASA-Lyndon B. Johnson Space Center Houston, TX 77001		
Attn: JM6/Library		1
NASA-George C. Marshall Space Flight Center Marshall Space Flight Center, AL 35812		
Attn: AS61/Library		1

Jet Propulsion Laboratory
 4800 Oak Grove Drive
 Pasadena, CA 91103
 Attn: Library

1

NASA S&T Info Facility
 P. O. Box 8757
 Baltimore-Washington Int. Airport
 MD 21240
 Attn: Acquisition Dept.

1

Air Force Systems Command
 Aeronautical Systems Division
 Wright-Patterson AFB, OH 45433
 Attn: Library
 C. W. Cowie

1

1

Air Force Wright Aeronautical Laboratories
 Wright-Patterson AFB, OH 45433
 Attn: I. Gershon

1

Aerospace Corp.
 2400 E. El Segundo Blvd.
 Los Angeles, CA 90045
 Attn: Library-Documents

1

Air Force Office of Scientific Research
 Washington DC 20333
 Attn: Library

1

Department of The Army
 U. S. Army Material Command
 Washington DC 20315
 Attn: AMCRD-RC

1

U. S. Army Ballistics Research Lab.
 Aberdeen Proving Ground, MD 21005
 Attn: Dr. Donald F. Haskell
 DRXBR-BM

1

Mechanics Research Lab.
 Army Materials and Mechanics Research Center
 Watertown, MA 02172
 Attn: Dr. Donald W. Oplinger

1

U. S. Army Missile Command
 Redstone Scientific Information Center
 Redstone Arsenal, AL 35808
 Attn: Document Section

1

Plastics Tech. Evaluation Center
 ARRADCOM
 Dover, NJ 07801
 Attn: A. M. Anzalone, Bldg. 3401

1

Commanding Officer U. S. Army Research Office (Durham) Box CM, Duke Station Durham, NC 27706 Attn: Library	1
Bureau of Naval Weapons Department of the Navy Washington DC 20360 Attn: RRRE-6	1
Commander U. S. Naval Ordnance Laboratory White Oak Silver Springs, MD 20910 Attn: Library	1
Director, Code 6180 U. S. Naval Research Laboratory Washington DC 20390 Attn: Library	1
Denver Federal Center U. S. Bureau of Reclamation P. O. Box 25007 Denver, CO 80225 Attn: P. M. Lorenz	1
National Technical Information Service Springfield, VA 22151	4
Naval Air Propulsion Test Center Aeronautical Engine Department Trenton, NJ 08628 Attn: Mr. James Salvino	1
Naval Air Propulsion Test Center Aeronautical Engine Dept. Trenton, NJ 08628 Attn: Mr. Robert DeLucia	1
Naval Air Propulsion Test Center Aeronautical Engine Department Trenton, NJ 08628 Attn: Mr. G. J. Mangano	1
Federal Aviation Administration Code ANE-214, Propulsion Section 12 New England Executive Park Burlington, MA 01803 Attn: Mr. Robert Berman	1

Federal Aviation Administration DOT Office of Aviation Safety, FOB 10A 800 Independence Ave., S.W. Washington DC 20591 Attn: Mr. John H. Enders	1
Federal Aviation Administration AFS-140 Washington DC 20591 Attn: Mr. A. K. Forney	1
FAA, AFS-140 800 Independence Ave., SW Washington DC 20591 Attn: Dr. Thomas G. Horeff	1
FAA, ARD-520 2100 Second Street, SW Washington DC 20591 Attn: Cdr. John J. Shea	1
National Transportation Safety Board 800 Independence Ave., SW Washington DC 20594 Attn: Mr. Edward P. Wizniak, TE-20 MIT, Room 33-313 Cambridge, MA 02139 Attn: Professor John Dugundji Professor James Mar	1 1 1
Rockwell International Corp. Los Angeles International Airport Los Angeles, CA 90009 Attn: Mr. Joseph Gaussein D 422/402 AB71	1
MIT, Room 33-207 Cambridge, MA 02139 Attn: Professor Rene H. Miller	1
MIT, Room 41-219 Cambridge, MA 02139 Attn: Professor Emmett A. Witmer	1
MIT, Room 6-202 Cambridge, MA 02139 Attn: Dr. David Roylance	1
University of Illinois at Chicago Circle Dept. of Materials Engineering Box 4348 Chicago, IL 60680 Attn: Dr. Robert L. Spilker	1

Detroit Diesel Allison General Motors Corp. Speed Code T3, Box 894 Indianapolis, IN 46206 Attn: Mr. William Springer	1
Detroit Diesel Allison General Motors Corp. Indianapolis, IN 46206 Attn: Mr. Joseph Berg Library N. Provenzano	1 1 1
AVCO, Lycoming Division 550 South Main Street Stratford, CT 06497 Attn: Mr. Herbert Kaehler	1
AVCO, Lycoming Division 550 South Main Street Stratford, CT 06497 Attn: Mr. John Veneri	1
Beech Aircraft Corp., Plant 1 Wichita, KA 67201 Attn: Mr. M. K. O'Connor	1
Albany International Research Co. 1000 Providence Highway Dedham, MA 02026 Attn: James Blout	1
Boeing Commercial Airplane Co. Seattle, WA 98111 Attn: C. Lewis	1
Boeing Aerospace Co. Impact Mechanics Lab. P. O. Box 3999 Seattle, WA 98124 Attn: Dr. R. J. Bristow	1
Boeing Commercial Airplane Co. P. O. Box 3707 Seattle, WA 98124 Attn: Dr. Ralph B. McCormick Dr. Dirk Bower	1 1
Boeing Commercial Airplane Co. P. O. Box 3707 M/S 73-01 Seattle, WA 98124 Attn: Mr. David T. Powell	1

Boeing Commercial Airplane Co. P. O. Box 3707 Seattle, WA 98124 Attn: Dr. John H. Gerstle	1
Boeing Company Wichita, KA Attn: Mr. C. F. Tiffany	1
McDonnell Douglas Aircraft Corp. P. O. Box 516 Lambert Field, MO 63166 Attn: Library	1
Douglas Aircraft Co. 3855 Lakewood Blvd. Mail Code 36-41 Long Beach, CA 90846 Attn: Ron Kawai	1
General Dynamics P. O. Box 748 Fort Worth, TX 76101 Attn: Library	1
General Dynamics/Convair Aerospace P. O. Box 1128 San Diego, CA 92112 Attn: Library J. Jensen	1 1
Garrett Airesearch Mfg. Co. Box 5217 Phoenix, AZ 85010 Attn: E. Nelson	1
General Electric Company Aircraft Engine Group Lynn, MA 01902 Attn: Mr. Herbert Garten	1
Grumman Aircraft Engineering Corp. Bethpage, Long Island, NY 11714 Attn: Library	1
IIT Research Institute Technology Center Chicago, IL 60616 Attn: Library I. M. Daniel	1 1

Lockheed California Co. P. O. Box 551 Dept. 73-31, Bldg. 90, PL. A-1 Burbank, CA 91520 Attn: Mr. D. T. Pland	1
Lockheed California Co. P. O. Box 551 Dept. 75-71, Bldg. 63, PL. A-1 Burbank, CA 91520 Attn: Mr. Jack E. Wignot	1
Northrop Space Laboratories 3401 West Bradway Hawthorne, CA 90250 Attn: Library	1
North American Rockwell, Inc. Rocketdyne Division 6633 Canoga Ave. Canoga Park, CA 91304 Attn: Library, Dept. 596-306	1
North American Rockwell, Inc. Space and Information Systems Div. 12214 Lakewood Blvd. Dowey, CA 90241 Attn: Library	1
Norton Company Industrial Ceramics Div. Armor and Spectramic Products Worcester, MA 01606 Attn: Mr. George E. Buron	1
Norton Company 1 New Bond Street Industrial Ceramics Div. Worcester, MA 01606 Attn: Mr. Paul B. Gardner	1
United Aircraft Corporation Pratt & Whitney Group Government Products Division P. O. B2691 West Palm Beach, FL 33402 Attn: Library Mr. J. T. Dixon	1 1

United Aircraft Corporation	
Pratt & Whitney Aircraft Group	
400 Main Street	
East Hartford, CT 06108	
Attn: Library	1
Dr. J. E. Doherty	1
Dr. S. A. Sattar	1
Dr. A. T. Weaver	1
J. Woodward	1
United Aircraft Corporation	
Hamilton Standard Division	
Windsor Locks, CT 06096	
Attn: Dr. G. P. Townsend	1
Library	1
Aeronautical Research Association	
of Princeton, Inc.	
P. O. Box 2229	
Princeton, NJ 08540	
Attn: Dr. Thomas McDonough	1
Teledyne CAE	
Box 6971	
Toledo, OH 43612	
Attn: T. Moyer	1
Rensselaer Polytechnic Institute	
Troy, NY 12181	
Attn: Prof. R. Loewy	1
Republic Aviation	
Fairchild Hiller Corp.	
Farmington, L.I., NY	
Attn: Library	1
Rohr Industries	
Foot of H Street	
Chula Vista, CA 92010	
Attn: Mr. John Meaney	1
TWA, Inc.	
Kansas City International Airport	
P. O. Box 20126	
Kansas City, MO 64195	
Attn: Mr. John J. Morelli	1
TRW Systems, Inc.	
One Space Park	
Redondo Beach, CA 90278	
Attn: Technical Library	1

	9
Mr. Herbert J. Rubel 1451 Holly Lane, N.E. Atlanta, GA 30329	1
Canadair, Ltd. P. O. Box 6087 Montreal, CANADA H3C 3G9 Attn: Mr. E. G. Carrington	1
Civil Aviation Authority Airworthiness Division Brabazon House Redhill Surrey RH 1 1 SQ ENGLAND Attn: Mr. G. L. Gunstone	1
British Aircraft Corp., Ltd. Commercial Aircraft Division Filton House, Bristol BS 99 7AR ENGLAND Attn: Mr. J. C. Wallin British Aircraft Corp., Ltd.	1
Rolls-Royce (1971) Limited Moor Lane, P. O. Box 31 Derby DEX 8 BJ UNITED KINGDOM Attn: Mr. Denis M. McCarthy Chief Engineer, Staff Engineering	1

End of Document